DEBRE BERHAN UNIVERITY

COLLEGE OF ENGINEERING

Removal of Hexavalent Chromium from Synthetic and Armament Engineering Industry Waste Water by Using Activated Carbon-Graphene Oxide Composite

A Thesis submitted to the Department of chemical Engineering Collage of Engineering Debre Berhan University

In partial fulfillment of the Requiems for the Degree of Masters of

Science in Chemical Engineering (Process Engineering)

By: Yohana Tadiwos

Advisor: Dr. Feleke Bayu

Co-Advisor: Dr. Asfaw Negash

: Dr. Minbale Gashu

December, 2022

Debre Berhan, Ethiopia

APPROVAL SHEET-1

This is to certify that the thesis entitled: **Removal of Hexavalent Chromium from Synthetic and Armament Engineering Industry Waste Water by Using Activated Carbon-Graphene Oxide Composite** submitted in parietal fulfillment of the requirements for the degree of <u>Masters of science</u> with specialization in process Engineering of the Graduate program of the Chemical Engineering , Collage of Engineering, Debe Berhan University and is record of original research carried out by Yohana Tadiwos PGR(SP)/029/13, under my supervision, and no part of the thesis has been submitted for any other degree or diploma. The assistance and help received during the course of this investigation have been duly acknowledged, therefore, I recommend that it to be accepted as fulfilling the thesis requirements.

_____ _____ _____

Name of Advisor   Signature   Date

_____ _____ _____

Name of co-Advisor   Signature   Date

APPROVAL SHEET-2

The undersigned members of the boarded of the examiners of final open defense by Yohana Tadiwos have read and evaluated his thesis entitled **Removal of Hexavalent Chromium from Synthetic and Armament Industry Waste Water by Using Activated Carbon-Graphene Oxide Composite** and examined the candidate. This is therefore to certify that the thesis has been accepted in partial fulfillment of the requirement for the degree of Master of Science in Process Engineering.

_____ _____ _____

Name of chairperson   Signature   Date

_____ _____ _____

Name of internal Examiner   Signature   Date

_____ _____ _____

Name of External Examiner   Signature   Date

DECLARTION

I declare that this thesis is my genuine work. And that all sources of materials used for this thesis have been profoundly acknowledged. This thesis has been submitted in partial fulfillment of requirements for masters of Science Msc of Process Engineering at Debre Berhan University and it is deposited at University of library to be made available for users under the rule of the library. I declare that this thesis is not submitted to any other institution anywhere for the award of any academic degree, diploma or certificate.

Brief quotations from this thesis are allowable without special permission, permission, provided that accurate acknowledgement of source is made. Requests for permission for extended quotation from or reproduction of this manuscript in whole or in part may be granted by the head of the department or the Dean of College of Post Graduate when in his/her judgment the proposed use of the material is in the interest of scholarship. In all other instances, however, permission must be obtained from the author and advisors of this thesis.

Name: Yohana Tadiwos Estifanos   Signature:_____

Date of submission:_____

ACKNOWLEDGMENTS

Above all, I would like to honour and give to God, my lord and savior, who had been my strength throughout my studies.

Table of Contents

LIST OF TABLES

LIST OF FIGURES

ACRONYMS AND NOTATIONS

AC   Activated carbon

GO   Graphene Oxide

ANOVA   Analysis of Variance

BBD   Box- Behnken Design

C_e Equilibrium Concentration

C_o Initial Concentration of Chromium (VI)

DOE   Design of Expert

FTIR   Fourier Transform Infrared Spectroscopy

K_1 Pseudo-first-order Kinetics Constant

K_2 Pseudo-second-order Kinetics Constant

K_f Freundlich Constant

K_L Langmuir Constant

PZC   Point of Zero Charge

IEP   Individual Education Program

q_e Adsorptive Uptake of chromium (VI) at Equilibrium

q_m Langmuir Constant

q_t Adsorptive Uptake of chromium (VI) at any time

EPA   Environmental Protection Agency

RPM   Revolution per Minute

SEM   Scanning Electron Microscope

XRD   X-Ray Diffraction

TGA   Thermo Gravimetric Analysis

BET   Brunner-Emmett-Teller

DLS   Dynamic light scattering

BAC   Bamboo Activated Carbon

SAC   Sawdust Activated Carbon

CAC   Corncob Activated Carbon

Cr (VI)   Hexavalent Chromium

EDTA   Ethylene Diaminetetra Acetic Acid

Abstract

Nowadays, developing cost effective, and non-hazardous materials for the removal of toxic heavy metals discharged from industrial wastewater is one of the major challenging problem of the world particularly, developing countries. Among the different toxic heavy metals, Hexavalent chromium (Cr (VI)) is one of the most known toxic heavy metal and serious environmental concerns due to its long persistence in the environment and highly deadly nature in living organisms discharged from electroplating process, painting, tannery, and metal work industries. Hence, this study mainly focuses on the synthesis of activated carbon from corncob, sawdust and bamboo, and activated carbon-graphene oxide composite (BAC/GO) for the application of Cr (VI) adsorption. The most effective AC was synthesized from bamboo. Furthermore, the bamboo activated carbon combined with electrochemically exfoliated graphene oxide was synthesized to increase the adsorption efficiency of activated carbon prepared from bamboo. The synthesized materials were characterized using different techniques i.e. UV-Vis spectrophotometer, FTIR, XRD, TGA, DLS, BET, and SEM-EDX. The results confirmed that the developed activated carbon and composite successfully synthesized. From the single effect study the highest adsorption efficiency of bamboo activated carbon was 99.18% at the optimum process conditions of adsorption factors. Additionally, the kinetics of the adsorption was well-fitted to pseudo-second order ($R^2 =0.9998$) and the corresponding rate constants were obtained. The isotherm of adsorption of corncob activated carbon, sawdust activated carbon, bamboo activated carbon, and BAC/GO composite was well-fitted to freundlich isotherm ($R^2 = 0.9835, 0.9733, 0.9634$, and 0.9755, respectively) than Langmuir isotherm. The developed model's validation and interaction effects between process parameters were investigated by Box Behnken Design and the maximum Cr (VI) adsorption efficiency (99.34%) was attained at PH (2), adsorbent dose (2.5mg/L), initial Cr (VI) ion concentration (12.5mg/L), and contact time (90 min). Also at this optimum operating conditions the adsorption efficiency of corncob activated carbon, sawdust activated carbon and bamboo activated carbon were examined and the obtained result was (90.5%, 94.8%, and 98.95%), respectively. Moreover, the Cr (VI) adsorption efficiency of BAC/GO composite was investigated using real Armament engineering industrial wastewater and the obtained adsorption efficiency was (99.85 %). Generally, this study demonstrates that the developed BAC/GO composite was synthesized from waste and it has excellent adsorption capacity, easy to prepare and use, cost effective and non-hazardous than corncob activated carbon, sawdust activated carbon and bamboo activated carbon.

Key words: *Adsorption, hexavalent chromium, adsorption kinetics, adsorption isotherm*

CHAPTER ONE

1 INTRODUCTION

1.1 Background

Industrial effluents containing heavy metals pollute the aquatic environment. (Kerur et al., 2020) Toxic heavy metals are considered one of the pollutants that have direct effect on human and animals. Heavy metals are released from industries such as metal plating, mining, batteries; manufacturing etc (Kadirvelu et al., 2001). Heavy metals are contained with high concentration in the effluent of many industries such as metal processing, landfill leachate, mining, pulp and paper; and pesticides (Guo et al., 2020).The environmental issues due to globalization and rapid industrialization are becoming more and more sensitive for human being (Gunatilake, 2015). The industries likely to contribute to heavy metals discharge are leather industries, tanning industries, the textile industry and armament industry(Kerur et al., 2020). Heavy metals in industrial wastewater include lead, chromium, mercury, uranium, selenium, zinc, arsenic, cadmium (Ahalya et al., 2003). These metals have been extensively studied and their effects on human health regularly reviewed by international bodies WHO. Acute heavy metal intoxications may damage central nervous function, the cardiovascular and gastrointestinal (GI) systems, lungs, kidneys, liver, endocrine glands, and bones. Chronic heavy metal exposure has been implicated in several degenerative diseases of these same systems and may increase risk of some cancers.(Arora, 2019)

Nowadays, numerous methods have been proposed for efficient heavy metal removal from waste waters, including but not limited to chemical precipitation, ion exchange, adsorption, membrane filtration and electrochemical technologies. After reviewing different wastewater treatment techniques, it is observed that adsorption is a technologically simple, efficient, cost effective, and non-destructive technique. It has an excellent ability to remove various pollutants, including dyes, metal ions, minerals, and other contaminants from water and wastewater (Crini & Lichtfouse, 2019) . adsorption offers flexibility in design and operation and, in many cases it will generate high-quality treated effluent (Hua et al., 2012) adsorption is Physical method usually considered a cost-effective and reliable method for wastewater treatment (Q. Liu et al., 2020). The removal efficiency of adsorption can range up to 99.9%. The United States

Environmental Protection Agency (USEPA) declared the adsorption process as one of the most excellent and best waste water treatment techniques, among others (Rashid et al., 2021)

Among the different industries armament engineering industry was design to manufacture different types of Armaments and civilian products. Such as small, medium, heavy armaments and different types of spare parts which are used for vehicles & machineries. Electroplating is one of the processes of depositing a coating having a desirable form by means of electrolysis using electricity in armament engineering industry. Electroplating industry consumes and discharge large volumes of wastewater. Use of various chemicals and metal salt creates pollution problems (Sivasangari et al., 2007).

Figure 1-1: Armament engineering industry waste water in Ethiopia

Chromium is released into the environment from electroplating, anodizing, metal finishing, tannery, dying and fertilizer industries (Dermentzis et al., 2011). Hexavalent chromium Cr (VI) is a major problem when it comes to environmental pollution prevention efforts and worker safety. Cr (VI), in the aqueous liquid and misting forms, is a known carcinogen which is extremely expensive to dispose of because of its toxic nature (Audino and Laboratories, 2006). Cr (VI) has been considered a toxic metal for many years, perhaps because of the poisonous effects of high exposures to industrial dichromate's (Group, 2019). Cr (VI) is produced industrially when Trivalent chromium Cr(III) is heated in the presence of mineral bases and atmospheric oxygen (for instance, during metal finishing processes)(Nadler, 2004).In recent years, many attempts have been made to analyze and to reduce the presence of Cr (VI) in water.

In order to minimize the pollution towards the environment, many technologies have been developed to treat the wastewater such as membrane separation process, flocculation,

coagulation and adsorption (Koo et al., 2015). Adsorption is method compared to other methods appears to be a simple attractive process and becomes a veritable choice. Moreover, light of its high efficiency, ease of handling and availability of different bio sorbents (Menkiti et al., 2015). Adsorption process is improved by in limited renewal affected by biological growth on the surface of the carbon. Activated carbon is the most widely used adsorbent. It is a highly porous, amorphous solid consisting of micro crystallites with a graphite lattice, usually prepared in small pellets or a powder. It can remove a wide variety of toxic metals (Arora, 2019). Activated carbons have been found to be an effective means of recovering Cr(VI) from wastewater (Barbusinski et al., 2017)(Álvarez et al., 2007)

Therefor there's requirement to look for low cost adsorbent for Cr (VI) removal from cheaper and readily available materials which will be used economically on a large scale. Adsorption on to low cost adsorbent, like corncob sawdust, and bamboo residues activated carbons also as a support grapheme oxide offers a cheap and fantastic option for removal for Cr (VI).The abundance and accessibility of residue of bamboo, corncob, saw dust and as a support to form composite of graphene oxide and activated carbon make it economically achievable. In this research deals with the examination of Cr (VI) removal from Armament Engineering industry by abundantly available activated carbon and graphene oxide adsorbent, however activated carbon is now prepared from wood work shop waste like sawdust and bamboo, also from waste of corncob and then graphene oxide from waste of dry battery cell and form composite to increase the adsorption efficiency. This process will be helped out through adjustment of various factors like pH, adsorption amount (dosage), contact time and initial Cr (VI) concentration, and there for the adsorption kinetics and isotherms are examined.

1.2 Statement of the Problem

Nowadays industries are becoming a key for economic development. Ethiopian government also has given a high priority for industrial development. However, generation of industrial waste, including hazardous waste has become a great challenge. Heavy metals such as Cadmium, Chromium, Copper, Mercury, Nickel and Zinc are some of these chronic industrial wastes discharged to environment which are causing a lot of damage to human and animal health, plants. Electroplating is one of the sources for these heavy metals.

Electroplating of metal by chrome involves discharging chrome remnant with wastewater. Chromium is a mobile in the environment and is highly toxic. According to the World Health Organization (WHO) drinking water guidelines, the maximum allowable limit for total chromium ion in water is 0.05 mg /L. However, as research shows, in electroplating wastewater like that of armament electroplating, the concentration of chromium ion is too much. Therefore, it needs treatment to control the associated risks. Commercially as well as in research level, there are different treatment techniques. Comparatively, adsorption method offers significant advantages such as low cost and better availability, profitability and efficiency, over the conventional methods. In this research, adsorption using low cost activated carbon embedded with Graphene Oxide is employed to eliminate the toxic Hexavalent chromium from armament electroplating wastewater.

1.3 Objective

1.3.1 General objective

The main objective of this study is to remove hexavalent chromium from Armament Engineering industry using activated carbon/graphene oxide composite material as adsorbent.

1.3.2 Specific objectives

The specific objective of this study:

- To characterize the developed activated carbons-graphene oxide using UV-Vis, FTIR, XRD, SEM-EDXS, DLS and BET.
- To study the effect of pH, adsorption dosage, contact time and initial concentration of chromium on adsorption efficiency of bamboo residue, corncob, sawdust and the composite of activated carbon with grapheme oxide.

- To study the performance of the prepared composite adsorbent by treating wastewater from Armament electroplating industry.

1.4 Significance of the Research

Electroplating industry is one such industry that generates large amounts of metal rich wastewater heavy metals can damage the environment and consequently may result in health risk due to their toxicity even at very low concentrations the solubility of heavy metals in wastewater is low so they cannot be degraded. The research tended to solve this problem after it was completed. It will use generally in two ways for whole environment. In one way it will use for armament industry to remove Cr (VI) from waste effluents and as a result, it will save the aquatic ecosystem as well as other living organisms. This will contribute to keeping the countries ecosystem safer. In second way, it will use for industry to reduce the cost of waste effluent treatment since Bamboo activated carbon/graphene oxide composite effective and cheaper. Similarly in our country production of activated carbon increasing to industrial scale, it will able to fulfill its demand of activated carbon so adding some ratio of graphnene oxide to increase its efficiency. And also to prevent the Cr (VI) ion concentration release to the environment which can cause toxicity that can be hazard to human health, the study will provide an opportunity to clean environment and it gives a great priority for cleaner technology and also it has health benefits Furthermore, the university will help to promote its mission and build up the link with the industries which have Cr (VI) in their waste water.

CHAPTER TWO

1 LITERATURE REVIEW

2.1 Electroplating

Electroplating wastewater industry is one of the major industries which generate a large portion of wastewater containing heavy metals (Khorasgani, 2013). It is an industry, involving the deposition of the protective and decorative layers on the metal or non-metal surfaces. It is also one of the most hazardous sources of environmental pollution due to a large amount of the formed wastewaters, containing the high concentrations of the heavy metals (copper, iron, nickel, cadmium, chromium, aluminum, lead, zinc and others), acids, alkalis, organic compounds and surfactants The presence of one or another heavy metal ion depends on kind of technological process on the manufactory as well as function of galvanic coating (Belova et al., 2020).

The technological processes of electroplating wastewater treatment are classified according to the reactions and chemical composition of the electrolytes, which are the source of wastewater forming. Consequently, the operations on the electroplating manufactories can be divided into four groups according to four wastewater types (Belova et al., 2020).

> ➢ The operations, forming the solutions or rinse waters, which include the cyanide compounds the main processes of galvanizing and washing after these solutions
>
> ➢ The operations, forming the solutions or rinse waters, which include the chromium compounds the main processes of chrome plating, chromium passivation and washing after these solutions
>
> ➢ The operations, forming the solutions or rinse waters, which include the heavy metal ions the main processes of electrochemical metal reduction and washing after these solutions
>
> ➢ The operations, forming the solutions or rinse waters, which do not include the above mentioned compounds the minor works.

2.2 Classification of Electroplating Industry

Electroplating industries have generated a large quantity of wastewater containing mostly various toxic heavy metals. According to the technology employed at electroplating process, wastewater can be classified into acidic and alkaline wastewater. And acidic wastewater can be turned into sludge's by precipitation using pH adjustment and coagulation. alkaline wastewater contains complex agents such as citric acid, Ethylene diaminetetra acetic acid (EDTA) or tartaric

acid, which prompt a metal organic complex formation whereby heavy metals cannot be hydrolyzed, even after adjusting higher pH values (>12) (M. L. Rahman et al., 2021).

2.3 Electroplating Wastewater and Heavy Metals

Electroplating wastewater has more heavy metal which has more carcinogenic effects which causes various health problems and also causes difficult for the survival of plants and aquatic organisms and collected the wastewaters near electroplating industry (Sivasangari et al., 2007). The chemical treatment was planned to be replaced by physicochemical process like adsorption. The wastewater emanated from bronze and chrome plating units were mixed together to prepare a composite wastewater sample (Mazumder et al., 2011).

2.4 Chrome Plating Process in Armament Industry

Chrome plating, or chromium electroplating, electrochemically coats a layer of chromium onto another metal object (Mohan & Pittman, 2006).In general the main objective of Chrome plating is for both internal and external surface which is used to Material corrosion protection, cracking protection, to have the material shiny and attractive appearance, Resistance heat, erosion, low and also for coefficient of friction. There are two commercial purposes for chromium electroplating decorative and functional. Decorative chrome plating is performed primarily for aesthetics while functional chrome plating imparts corrosion resistance and increased surface hardness. Many automotive components are functionally chrome plated. Chrome plating is achieved with a "reverse Galvanic cell". An electrical potential is applied to two electrodes the anode and the cathode immersed in an electrically conductive solution (Sessarego, 2017).A simplified chrome plating process where the material to be plated in chromium is immersed in a series of baths, progressing from left to right the material begins in the activation bath where chromic acid etches the surface and prepares the material. The material is then immersed in the electroplating bath and is electroplated. Upon finishing the plating operation, the chromium-coated material must have its surfaces rinsed because they are covered in acid, unreacted chromium compounds, and any other compounds contaminating the electroplating bath (Sessarego, 2017).

2.5 Chemical Procedure of Electroplating in Armament Industry

Step-1: De-oiling: is the removal of oils, grease and other dusts and dirty by using of chemicals.

Step-2: Neutralize: is the deactivation of material work pieces by chemicals using soap and Na_2CO_3 in order to prevent rust. The parts to be immerged in the solution completely

Step-3: Chrome plating: There are variations of Chromium plating – ordinary chrome, hard chrome and bright chrome.
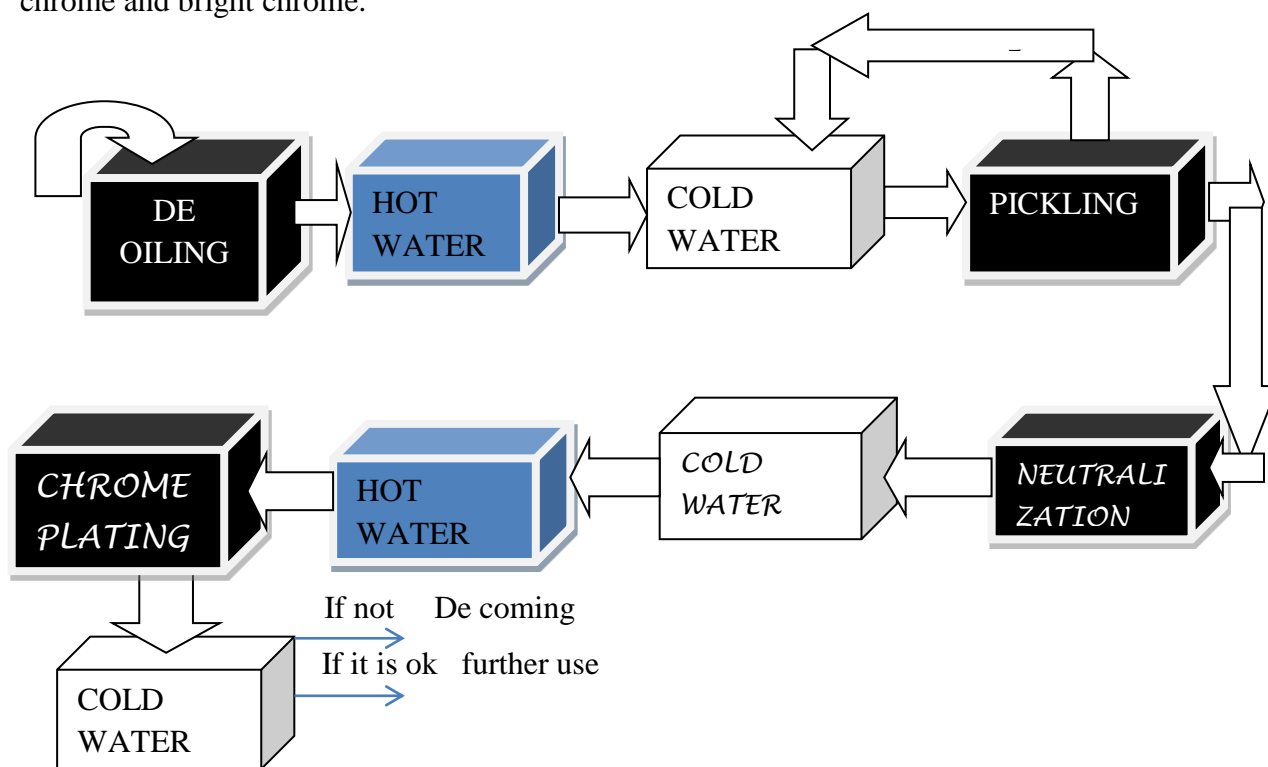
Figure 1-1: Schematic diagram of electroplating process

2.6 Heavy Metal Toxicity

Environmental pollution by a various types of heavy metal sources is prevalent in water and wastewater and has become an increasingly serious problem in recent years .Heavy metal ions are frequently existed in the effluents of municipal wastewaters and wastewaters of multiple industries such as battery manufacturing, electroplating, leather tanning, metal finishing, paint manufacturing, steel fabrication (Abbas, 2014), Even though the electroplating industry uses less water in comparison to the other industries, their effluents are far more toxic. Electroplating wastewaters contain heavy metals, like chromium, nickel, lead (Seyoum & Asso, 2015). The removal of poisonous heavy metals from wastewaters is considered one of the most important

fields of water treatment since many industries generate a lot of hazardous contamination issues to the environment(Ayub et al., 2020).

Table 1-1: The use and health effects of some heavy metal on human being

Heave metals	Use	Health effect	Reference
Cadmium	Electroplating, fertilizers, mineral processing and Battery manufacturing	Cancer, lung insufficiency, Disturbances in cardiovascular system, liver and kidney damage	Sharma, 1995 Copper
Copper	Copper and brass plating, mining, metal industries and copper-ammonium rayon industries	Normocytic, hypochromic anemia, leucopenia and osteoporosis Ulcer,	Aksu and Kutsal, 1997
Chromium	Metal plating, electroplating, leather, mining, galvanometric, dye production	Ulcer, skin irritation, liver and kidney damage	LandisandYo,2003; Kumar et al.,2007
Lead	Metal plating, textile, battery manufacturer, automotive and petroleum industries	Spontaneous abortion, damage nervous system, kidney and brain damage Memory	Tunali et al., 2006
Mercury	Metallurgy industries, chemical manufacturing and metal finishing	Memory problems, increased heart rate, tremors, kidney and brain damage	Abia.,2005, Abia., 2006

Source: (WHO, 2008

2.7 Chromium

Chromium is an essential nutrient for plant and animal metabolism. However, the increasing accumulation of chromium in the environment from industrial outputs has caused great concern. Chromium contaminated wastewaters can originate from dyes and pigment manufacturing, wood preserving, electroplating and leather tanning (Ahalya et al., 2010).

Chromium is one of the most frequently used metal contaminants and is considered to be one of the top 20 contaminants on the Superfund priority list of hazardous substances (Dhal et al.,

2013). Chromium can exist in several oxidation states, ranging from Cr^{2+} to Cr^{6+}, but in soils the most stable and common forms are trivalent (Cr (III)) and Hexavalent (Cr (VI)) species which display quite different chemical properties and affect organisms in different ways. Cr (VI) is more hazardous to health because of its high toxicity. The stricter environmental regulations to the discharge of heavy metal cations make it necessary to develop processes for its removal from waste water(Wagner & Jula, 2018).

Hexavalent chromium which is primarily present in the form of chromate (CrO_4^{2-}) and dichromate ($Cr_2O_7^{2-}$) poses significantly higher levels of toxicity than the other valiancy states(Ahalya et al., 2010). Cr (VI) is water soluble in the full pH range, while Cr (III) tends to be adsorbed on soil surface or precipitate as chromium hydroxide in a slightly acidic and alkaline environment. Therefore, Cr (III) has the high potential for environmental contamination, especially of aquifers and surface water. In its hexavalent form, the U.S. Environmental Protection Agency (EPA) has classified chromium as a Group 'A' human carcinogen and is one of the main pollutants. In both of its prevalent forms, trivalent and hexavalent chromium it can cause allergic contact. As regards the chromium chemicals the largest amount is consumed to manufacture pigments for use in paints and inks. Other applications include Leather tanning, Metal corrosion inhibition, Drilling mud, Textile dyes, Catalysts, wood (Dhal et al., 2013).

Chromite is used in the refractory industry to make bricks, mortar, and ramming and gunning mixes. Chromite enhances their thermal shock and slag resistance, volume stability and strength. Chromium is widely distributed in rocks, fresh water and sea water. The distribution and concentration of Chromium in various environmental samples (soils/solid waste) are given in 'Supplementary material'(Dhal et al., 2013). The maximum allowed concentration of chromium ions in drinking water is 0.05 mg/L (Nourbakhsh et al., 1994).

2.8 Adsorption

The term adsorption was first used by Heinrich Kayser in the year 1881. Adsorption is the physical adherence or bonding of ions and molecules onto the surface of another phase. It is a surface phenomenon which increases in concentration of one particular component at the surface or interface between two phases. Adsorption processes differ from absorption processes; adsorption is a surface based process in which atoms, ions or molecules from a substance adhere

to the surface of the adsorbent. Absorption is the process which involves the entire volume of the absorbing substance into the solid material body (Villabona-ortíz et al., 2021).
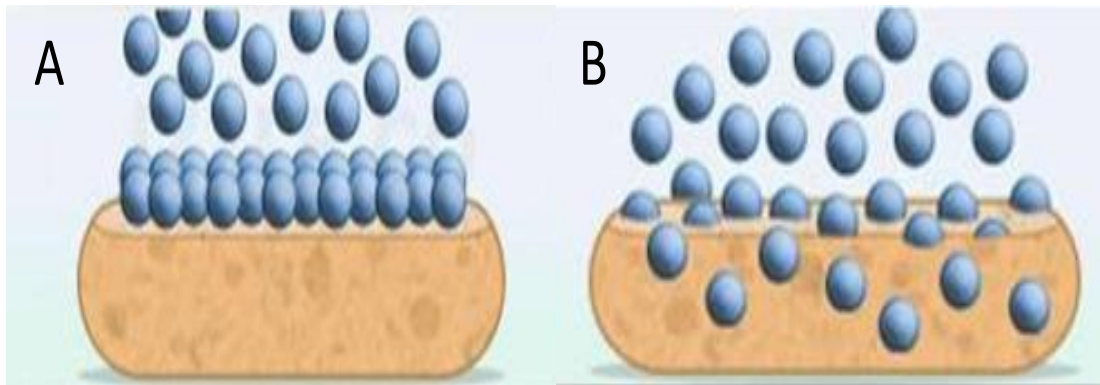
Figure 1-2: Adsorption process

Figure 2-2 A) Shows the adsorption process in which atoms, ions or molecules are adhering to the surface of the adsorbent, and B) shows the absorption process, in which atoms, ions or molecules entering the volume of the absorbing substance.

According to the type of adsorbent and adsorbate bonds formed, adsorption can be classified into:

➢ **Physical adsorption**: achieved when the adsorbate adheres on to the surface of the adsorbent through Van der Waals interactions. Physical adsorption is usually fast and reversible since the process involves the formation of week bonds between the adsorbate and adsorbent, thus the adsorption bonds are easily formed and broken (Ben-Mansour et al., 2016).

➢ **Chemical adsorption:** occurs as a result of a chemical interaction between the adsorbate molecules and the adsorbent surface. A chemisorption process is usually slow and irreversible this is because the chemisorption's process involves the formation of strong bonds between the adsorbate and adsorbent and can change both the surface and adsorbate chemical character(Webb, 2003).

2.8.1   Adsorption Mechanisms

The main principles of adsorption are the mass transfer of a molecule from a gas or a liquid onto a solid surface. Since adsorbents have porous structure they have a capacity to holds up an adsorbate molecule onto their surfaces. Generally, adsorption of adsorbate onto the surface of adsorbent can be described as follows: Adsorbate is transferred from the liquid to adsorbents boundary layer , External diffusion occurs, where by the solute is transferred to the surface of the adsorbent through the boundary layer, The adsorbate is diffused from the surface to active sites, termed intra particle diffusion.
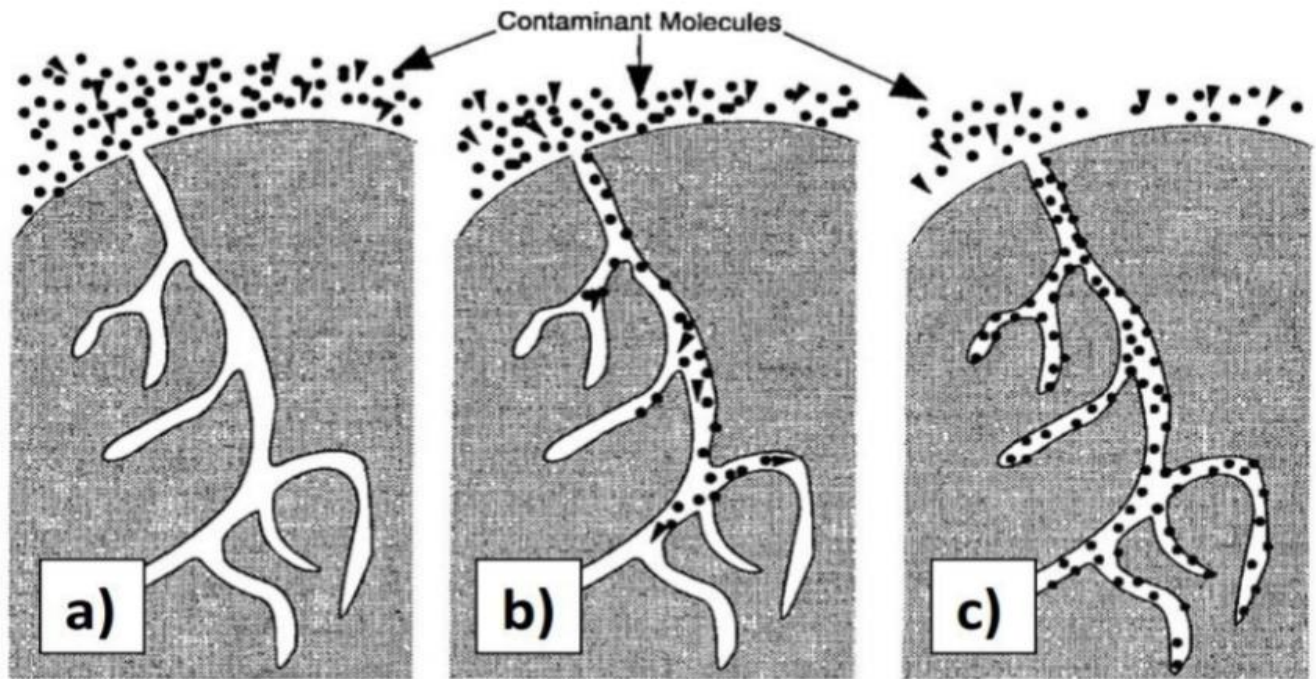
Figure 1-3: Steps of adsorption mechanism

Three steps of adsorption mechanism in Figure 2-3: a) diffusion of adsorbate onto adsorbent surface, b) migration of adsorbate into porous surface of adsorbent, and c) mono layer buildup of adsorbate onto adsorbent.

2.8.2 Types of Adsorbents

Adsorbents can be classified as natural adsorbents and synthetic adsorbents (Ćosović et al., 2010).

1. **Natural Adsorbents:** Natural sorbents are increasingly widely used in water purification processes due to their frequent occurrence in nature, low cost as compared with synthetic materials, remarkable properties with respect to adsorption, ion exchange and filtration, and also due to the fact that efficient methods are developed to regulate the geometric structure or these materials and chemical nature of their surface.

2. **Synthetic Adsorbent:** Synthetic adsorbents are widely used as polymeric media for recovery and separation of pharmaceuticals or their intermediates, foods, nutraceuticals, etc. Therefore, both pore and chemical characteristics of the synthetic adsorbents will affect the separation and adsorption capacity of target compounds.

Adsorbents also categorized on the basis of their matrix composition, polarity, chemical and physical resistance, by their particle size distribution, their inner and specific surface areas, density, and porosity as well as their pore radius distribution .Most commonly used types of adsorbents are: activated carbon (Wagner & Jula, 2018), Silica Gel (Ads- et al., 2000), Clays(Edi et al., 2015), and Graphene oxide (Peng et al., 2017).

2.8.3 Factors Affecting Adsorption Process

The adsorption of solute on solid/liquid interface depends on many factors such as physicochemical properties of the solid surface porosity, surface area, presence or absence of charged or polarity of solution, the nature of the solute properties of the liquid phase (pH, salt concentration, temperature, presence of the competitive solute); complication in the liquid phase (Simate et al., 2012). Some of the factors are:

A. Effect of pH on Adsorption

The pH of the solution has a complex effect on the process adsorption involving the electrostatic interaction, since the pH can affect the electrical properties of the solid surface and solute. The pH at which a substance has equal numbers of negatively and positively charged sites is called the isoelectric point (IEP). At pH values lower than the IEP, the net surface charge is positive and anion adsorption is dominant whereas at pH values higher than the IEP the net charge is

negative and acation adsorption occurs. Some substances may consist of a combination of nonpolar and ionzable functional groups (Aldegs et al., 2008).

B. Effect of Adsorbent Dosage on Adsorption

Adsorption increases with increase in adsorbent dose due to increase of available surface area and functional groups for adsorbate interaction and uptake. The increase in adsorbate adsorption with increasing dose of adsorbent may be due to the increase in availability of surface active sites resulting from the increased dose of the adsorbents so when increase adsorbent dose also increase adsorption efficiency (Battas et al., 2019).

C. Effect of Contact Time

The rate of adsorption increases with an increase in contact time to a certain extent. Further increase in contact time does not increase the uptake due to deposition of adsorbate on the available adsorption site on adsorbent material. At this point, the amount of the adsorbate desorbing from the adsorbent is in a state of dynamic equilibrium with the amount of the adsorbate being adsorbed onto the adsorbent. Variation of contact time results into change in the optimum sorption efficiency of adsorbate from wastewaters. However, the equilibration time for adsorption of adsorbate onto different adsorbents also depends on a number of factors such as: the electrostatic attraction of adsorbate adsorbent, complication reaction on the outside surfaces of adsorbents, distribution of pores on adsorbents, availability of sorption sites or pores or composition of the adsorbents, inter particle diffusion of adsorbate on the pores of the adsorbents and other environmental conditions(Olatunji et al., 2015).

D. Effect of Initial Concentration

The equilibrium adsorption increases with increase in the initial adsorbate concentration. This variation of the initial concentration generates an increase in the initial rate of adsorption. This is because the diffusion of adsorbate molecules from the solution to the adsorbent surface is accelerated by increasing the adsorbate concentration. The increase in uptake capacity of the sorbent with increasing adsorbent concentration may be due to the increase of sorbate quantity. The amount of the adsorbate adsorbed at equilibrium on adsorbent increased with an increase in the initial adsorbate concentration of solution to a value which corresponds to the maximum capacity of adsorption. This can be explained by the fact that adsorbent had a limited number of active sites, which would have become saturated above a certain concentration (M. M. Rahman et al., 2019).

2.9 Adsorption Process Modeling

Adsorption modeling helps to identify the removal efficiency of an adsorbent. Adsorption modeling is applied to describe the experimental data by using kinetic and adsorption isotherm.

2.9.1 Adsorption Kinetics

The kinetic equation of the chemical reaction shows the dependence of the reaction rate on the concentrations of the reactants. The kinetic equation of chemical reaction is decided experimentally by using the gathering data from the experiment. The study of adsorption kinetics is vital because it provides valuable information on reaction pathways and describes the mechanism of the reaction (Kortlever et al., 2015).

Adsorption kinetics helps to determine the general rate of the adsorption process. Contact time from experimental results can be used to study the rate-limiting step in the adsorption process in terms of kinetic energy. The kinetic experiment is doing by employing a batch technique to review the effect of contact time and also the uptake concentration of Cr (VI) adsorption. The aqueous samples are taking at different time intervals, and also the concentrations of Cr (VI) are similarly measuring (Theydan, 2018). The genera adsorption process is often controlled either by one or more seeps such as pore diffusion, surface diffusion, or a combination of more than one step. Lagergrens first order equation and Hos second-order equation are example of kinetic models commonly used to describe these adsorption kinetic model(Abas et al., 2015).

2.9.1.1 Pseudo-First-Order Model

The first-order model which is supposed to be the earliest was established by Lagragren in 1898 (Qiu et al., 2009). A first-order rate equation to explain the kinetic process of liquid-solid phase adsorption processes is usually expressed as:

2.9.1.2 Pseudo-Second-Order Model

The pseudo-first order rate equation of Lagergren developed a rate equation which considered rates of ion-exchange adsorption in the exchange adsorption of ions from aqueous solutions(Aurich et al., 2017). The kinetics of sorption also defined by a pseudo-second-order model (Aurich et al., 2017). The reaction rate is dependent on the quantity lute on the surface of

the adsorbent the driving force (q_{e} _ q_{t}) is proportional to the number of active sites available on the adsorbent (Kajjumba et al., 2018), The differential equation for this reaction:

2.9.2   Adsorption Isotherm Models

An adsorption isotherm is the presentation of the amount of solute adsorbed per unit weight of adsorbent as a function of the equilibrium concentration in the bulk solution at constant temperature. The adsorption isotherm describes an equilibrium state so that it does not describe time dependent factors. It is obtained by determining the amount of molecules attached to the adsorbing material after establishment of equilibrium in a static gas atmosphere(De Gisi et al., 2016). The adsorption isotherm is the equilibrium relationship between the concentration in the fluid phase and the concentration in the adsorbent particles at a given temperature. The quantity adsorbed is nearly always normalized by the mass of the adsorbent to allow comparison of different materials. (X. Chen, 2015)

Equilibrium isotherm is described by adsorption isotherm, characterized by certain constants whose values express the surface properties and affinity of the adsorbent adsorption equilibrium is established when the concentration of adsorbate in the bulk solution is in dynamic balance with that at the adsorbent interface. The analysis of equilibrium adsorption data by fitting them to different isotherm models is an important step to find the suitable model that can be used for design purposes (X. Chen, 2015). The adsorption isotherm is important for the description of how the adsorbate will interact with the adsorbent and gives an idea of the adsorption capacity of the adsorbent. The surface phase may be considered as a monolayer or multilayer (Ayawei et al., 2017).The distribution pattern of metal ions between the phases (solid and liquid) is usually explained by adsorption isotherms, like Langmuir and Freundlich adsorption isotherms are commonly used for the description of adsorption data (Ayawei et al., 2017).

2.9.2.1   Langmuir Adsorption Isotherm

Langmuir isotherm interpretations for the surface coverage by balancing the relative rates of adsorption and desorption (dynamic equilibrium). Adsorption is proportional to the fraction of the surface of the adsorbent that is open while desorption is proportional to the fraction of the adsorbent surface that is covered (Ayawei et al., 2017). This model was originally developed to explain gas-solid-phase adsorption onto AC. Later on, it was adapted to liquid systems simply by

replacing the partial pressure of the adsorbate with its equivalent value in concentration. The Langmuir isotherm model is based on the assumptions that adoption is limited to one monolayer, the energy of sorption is the same for all sites and is independent of the degree of surface coverage, and adsorption to one site is independent of the occupancy condition of the adjacent site with no interaction between adjoining sorbed molecules(Yoro et al., 2020).

2.9.2.2   Freundlich Adsorption Isotherm

Freundlich adsorption isotherm is an empirical equation and it assume that the adsorption processes take place on a heterogeneous adsorbent surface and can be useful to multilayer adsorption (Labied et al., 2018). This isotherm provides an expression that defines the surface heterogeneity and the exponential distribution of active sites and their energies (Ayawei et al., 2017). This model describes the relationship between the numbers of metals adsorbed per unit mass of adsorbent (q_e) and the concentration of similar metals at equilibrium (C_e). for adsorption from solution (Ghorbani-Khosrowshahi & Behnajady, 2016).

Freundlich constant indicate adsorption capacity (l/mg) and adsorption intensity, respectively; n depicts the extent of non-linearity between solution concentration and adsorption. $n = 1$ depicts the adsorption to be linear, $n > 1$ depicts adsorption to be a chemical process, and $n < 0$ indicates the adsorption process to be a physical process(Albadarin et al., 2012). Freundlich isotherm model is presented by plotting a graph of log C_e versus log q_e . The constant k_f and n are calculated from slope and intercept.

2.10   Activated Carbon

Activated carbon (AC) is the most widely used for waste water treatment by its high adsorption capacity, due to its high porosity and large surface area. The adsorbent properties of activated carbons are essentially due to their surface area, universal adsorption effect, highly micro porous structure, and a high degree of surface reactivity. The availability of favorable pore size makes the internal surface accessible and enhances the adsorption rate. The most widely used activated carbons have a specific surface area of 800 to1500 m2/g. adsorption capacity of active carbons is determined by their physical or porous structure, it is strongly influenced by the chemical structure of their surface(Wagner & Jula, 2018).

AC have a highly developed porosity and an extended interparticulate surface area. Their preparation involves two main steps: the carbonization and the activation of the carbonized product. Thus, all carbonaceous materials can be converted into AC, although the properties of the final product will be different, depending on the nature of the raw material used, the nature of the activating agent, and the conditions of the carbonization and activation processes. During the carbonization processmost of the noncarbon elements such as oxygen, hydrogen, and nitrogen are eliminated as volatile gaseous species by the pyrolytic decomposition of the starting material. Activated carbons have a microcrystalline structure. But this microcrystalline structure differs from that of graphite with respect to interlayer spacing, which is 0.335 nm in the case of graphite and ranges between 0.34 and 0.35 nm in AC. The orientation of the stacks of aromatic sheets is also different, being less ordered in ACs(Wagner & Jula, 2018).

2.11   Graphene Oxide

Graphene, defined as a single layer of carbon atoms densely packed in a benzene ring structure, has a large specific surface area, high adsorption capacity and electrical conductivity(Gadipelli & Guo, 2015). Due to its unique properties, graphene and its derivatives can act as a conductive carrier, adsorbent, photosensitizer, photostabilizer, photocatalyst and co-catalyst in nanocomposites(Olak-Kucharczyk et al., 2020).

Graphene oxide (GO) has found prominence after discovery of graphene. GO has attracted much attention as a potential originator for the large scale production of graphene based materials leading to low cost of synthesis; and the tunability of the electronic properties as a semimetal, a semiconductor, or an insulator. GO is prepared by top-down and bottom-up approaches. The top-down approach is mechanical exfoliations and chemical exfoliations. Reliability of large area and homogeneity is larger issues in this technique (M. Gopala Krishnamurthy, D. Dinakar, I. M. Chhabra, P. Kishore, 2019). Of battery electrodes (graphite electrodes) for the synthesis of GO.

GO can be effectively deoxygenated through chemical reduction, resulting in restoration of much conjugation, as apparent by the recovery of electrical conductivity. A systematic investigation on the chemical reduction of exfoliated GO, by treatment with various reducing agents (Feng , 2013). Commonly used graphite electrodes in electrochemical exfoliation are either natural graphite in forms of foils, rods, sheets etc. The electrochemical exfoliation of graphite relies on

efficient ion intercalations among graphene layers to expand their interlayer spacing. Ion intercalations are expected to be influenced by graphite electrodes microstructures, such as graphite particulate sizes, defects, layer arrangements, and thickness, composition, and suitable pretreatment. Several recent studies have explored how these parameters affect graphene synthesis thick graphite rods or sheets are usually exfoliated at considerably lower rates than thin graphite foils or flakes. The slower exfoliation rate fosters graphite oxidation, resulting in more hydrophilic graphene materials (F. Liu et al., 2019).

2.12   Over views of bamboo, saw dust and corn cob

2.12.1   Bamboo

Bamboo is very common natural resources that can be found in Asia especially China, Thailand and Vietnam(Koo et al., 2015). Bamboo can be used as building materials; decoration and slope maintenance work because it is strong, light, flexible and handy to build. Bamboo is used as the base of production for activated carbon because it is considered as the renewable source due to the rapid growth in short period of time. Not only this, price of production is lower when using bamboo to produce AC because the price of bamboo is about 1/3 to 1/5 compare to commercial activated carbon. There was a study on the bamboo used as the absorbent for the application of gas pollutants such as benzene, ammonia and some other volatile organic particles that can be found in the air. Chemical compositions of bamboo are alcohol-toluene extraction, alpha-cellulose and lignin; different part have different percentage of chemical composition(X. Li, 2004). Bamboo can be converted into charcoal and AC carbonization followed by activation bamboo is considered as one of the possible solutions since it does not only reduce the quantity of waste in landfill but also converts these materials to an adsorbent for wastewater treatment or other applications (Mahanim et al., 2011).

2.12.2 Eucalyptus Sawdust

One of these plant wastes is sawdust, sourced from wood. This large scale production of saw dust and its lack of proper disposal management may result in several environmental problems. Therefore, the conversion of saw dust into activated carbon production for the removal of toxic pollutants from aqueous solutions is a right step in the right direction and of great importance from the environment (Aworanti & Agarry, 2017). When the AC production process is complete, steam is introduced immediately to reduce costs and processing time. The effect of steam

activation temperature of 500 °C, 600 °C, and 700 °C on the properties of the AC from eucalyptus wood chips was investigated (Mopoung & Dejang, 2021)

2.12.3 Corncob

Among these carbon sources, corncob is a good precursor for preparing carbon with ultra-high specific surface area. The carbons prepared from corncob AC have been used in wastewater treatment such as removal of organic pollutants However, a comprehensive study of activating corncob with different chemical activation strategies to prepare carbon with high specific surface area and pore volumes, and their subsequent performance in gas storage such as the hydrogen adsorption(Sun & Webley, 2010).corncob AC was prepared by chemical activation with H3PO4. The adsorption potential and applicability of corncob AC in the removal of 2,4-D from aqueous solution. The effects of contact time, initial concentration of 2,4-D, temperature and pH were investigated(Njoku & Hameed, 2011).

2.12.4 Composite of AC and GO

GO-AC has been prepared by a simple one step mixing route to be used as an effective composite. For a two component composite adsorbent system composites of activated charbon and reduced graphene oxide. It was demonstrated to be effective as highly electrocatalytically active counter electrode material adsorbent for removal of harmful dyes. This material is attractive for its cheapness, easy availability, as well as its effectiveness. Thus, composites of AC, especially with GO, have been established as an important and interesting material to be studied and examined. AC-GO nanocomposite does act as a selective adsorbent, for positive cationic dyes like mitilenblue .The GO was synthesized by modified Hummer's Method and then mixed with AC the nanocomposite, which was characterized and used as an adsorbent to remove the hexavalent chromium adsorption.Graphene-based materials, AC as such, and their composites are also important in many other applications besides adsorption, such as supercapacitors, batteries, etc. Though both graphene oxide and activated caron are very common and has been tested as a very good adsorbent individually, together as a composite, will act as a more powerful adsorbent(Bhattacharyyae et al., 2021).

2.12.5 Gaps in Litrature review

In this study the assessed literature indicates only focused on synthesis of activated carbons and graphene oxide. Also applied it to different waste water of different industries for the application of adsorption (Natrayan et al., 2022). But few studies or all most no studies has been done on the waste treatment of electroplating with activated carbon emended with graphene oxide composite to treat heavy metal such as Chromium, Copper, Mercury, Nickel and Zinc etc. Some of these chronic industrial wastes discharged to environments which are causing a lot of damage and major challenges of the world. Hexavalent chromium is present in the effluents produced from electroplating, leather tanning, cement, mining, dyeing, fertilizer, and photography industries and can result in environmental and public health problems (Demirbas et al., 2004). It is well known that heavy metals can damage nerves, liver and bones, and they also block functional groups of essential enzymes. Also, acute systemic poisoning can result from high exposure to hexavalent chromium(J. Chen et al., 2014).

Review of litrature related to electroplating waste water havey metals (Gin et al., 2014),(S. Li et al., 2018),(Elystia et al., 2020),(Yahya et al., 2020),(Konstantinos et al., 2011) indicated that electroplating contains some heavy metals that pollute natural water and its very difficult to treat it by conventional treatment processes due to its high cost and difficult operating conditions. Adsorption in one of the alternatives(Nagar, 2019). This study mainly focused on electroplating wast water treatemnt which have high amount of Cr(VI) amount. There are different treatment techniques. Comparatively, adsorption method offers significant advantages because of low cost and better availability, profitability and efficiency. Therefore adsorption using low cost activated carbon with Graphene Oxide is used to eliminate the toxic Hexavalent chromium from armament electroplating wastewater.

CHAPTER THREE

3 MATERIALS AND METHODS

3.1 Materials

3.1.1   Reagents and chemicals

Table 3-1: Reagents and chemicals

Materials /chemicals	Function
Bamboo, sawdust and corncob	As adsorbent
Electroplating wastewater	As adsorbate
Distilled water	Washing, preparation and diluting.
HCl	pH adjustment
NaOH	
NaCl	For zero point of charge analysis
H_3PO_4	For formation of cross linked structure
HNO_3	Oxidizing
$k_2Cr_2O_7$	As Source of Cr(VI)
Waste dry battery cell	GO source
Equipment	**Functions**
Analytical balance	Weighing of sample
Mill	Size reduction
Sieves with mechanical shaker	Sieving analysis
pH meter	Measuring of P^H solution
magnetic stirrer	Mixing /agitation
crucible, furnace ,oven	Drying and characterization
volumetric flasks, test tubes, conical flask and , Erlenmeyer flasks	Measuring
Centrifuge	For separation
Furnace	Carbonization
whatman number 42 filter paper	Filtration

3.2 Experimental Methods

3.2.1   Raw Material Collection and Pretreatment

Bamboo residues was collected from an area of furniture houses (Addis Ababa, the sawdust was collected from an area of sawmill (Debre Berhan sawmill factory), and the corncob was collected

from local market of Debre Berehan and the graphite rod was obtained from waste dry battery cell. The collected raw material corncob, sawdust and bamboo were washed and dried in the shade until most of moisture content was evaporated, then dried at oven 105 ^{o}C for 24 hours. The dried materials were crashed with grinder and sieved with 60mesh. Then after the raw material were pretreated to use for further processes.

3.2.2 Activated Carbon Preparation from Bamboo

A 100 mg was used to impregnated with phosphoric acid with the ratio of 1:1 by Wight (Q. S. Liu et al., 2010) for 24 hours mixed until to form a pest to permit the impregnating reagent to be fully adsorbed on the raw material. The mixture ware dried in oven at 105 ^{0}C for 12 hours. The dried sample transferred to crucible for carbonization shown in Figure 3-1. Then activation was done in muffle furnace at 800 ^{0}C for 2 hours. Then after it kept at room temperature until the product was cooled. The prepared activated carbon was washed continuously and repeatedly by using deionized water until the pH reaches 6-7 to eliminate acid and lastly, the product dried in an oven at 105 ^{0}C for 3 hours. The prepared sample were cooled in dissector and Finally, the activated carbon was ground by pestle and mortar the particles having an average size range of 0.5 mm (20–50 mesh) then stored in air tight plastics for further studies or characterization.

Figure 3-1: processes of bamboo activated carbon preparation

3.2.3 Activated Carbon Prepared from Sawdust

The raw material was collected from Deber Berhan saw mill factory and washed with tap water and rising by deionized water to remove unwanted residues then drying at 105 ^{0}C for 4 hours, the drying sample sieved to the required uniform particle size of 60 meshes. The pretreated sieved saw dust was impregnated with phosphoric acid (50% by weight) at the weight ratio of 1:1(Patnukao et al., 2008). Then mixed it until form homogenized mixture was obtained for 24 hours at room temperature for activation process shown in Figure 3-2. Then it was keep at105 ^{0}C

an oven for 12 hours to remove moisture content and ready for carbonization process. After oven drying the sample with crucible were ready for carbonization by muffle furnace at 500 ^{0}C(Mohan & Pittman, 2006) for 1 hour. The prepared activated carbon was washed continuously using deionized water until the pH reaches to 6-7 to remove the acid and then the product dried in an oven at 105 ^{0}C for 3 hours. Finally the granular activated carbon was grounded and converted to powdered form. The particles having an average diameter of 0.5 mm (20–50 mesh) the prepared sample stored in air tight plastics for further studies.
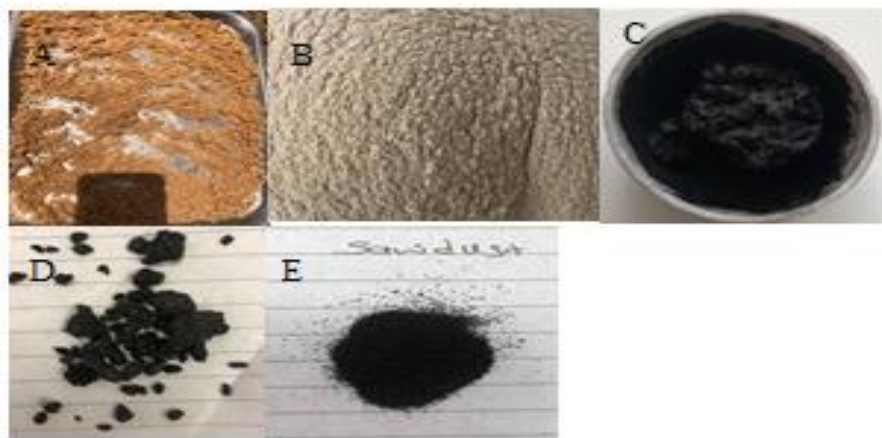
Figure 3-2: processes of sawdust activated carbon preparation

3.2.4   Activated Carbon Prepared from Corncob

The raw material was collected from and showarobit local farmers (household). Then the raw material was crashed with continuous hammering on the small pieces of corncob. The corncob was washed with deionized water and dries it under oven for 105 ^{0}C for 6 hours. Then for reduced the size grinder was used, and sieved with 60mesh. powder form of the sample was soaked (impregnated) with phosphoric acid (50% by weight) and the impregnation ratio 1:1 (w/w) for 24 hours at room temperature (Njoku & Hameed, 2011). The mixture were dried in an oven at 105 ^{0}C for 12 hours to dehydrate the sample then, and then transferred to a crucible, then the crucible put to muffle furnace at 500 ^{0}C to for 2 hours and cooled at room temperature (Sun & Webley, 2010).The activated carbon washed repeatedly with hot deionized water until the pH reaches 6-7 the granular activated carbon was dried in an oven at 105 ^{0}C for 24 hours, and grounded and sieved with 60 mesh to form uniform size and to increase surface area of adsorbent the process shows in Figure 3-3 and finally kept in an airtight container for further use.

Figure 3-3: processes of sawdust activated carbon preparation
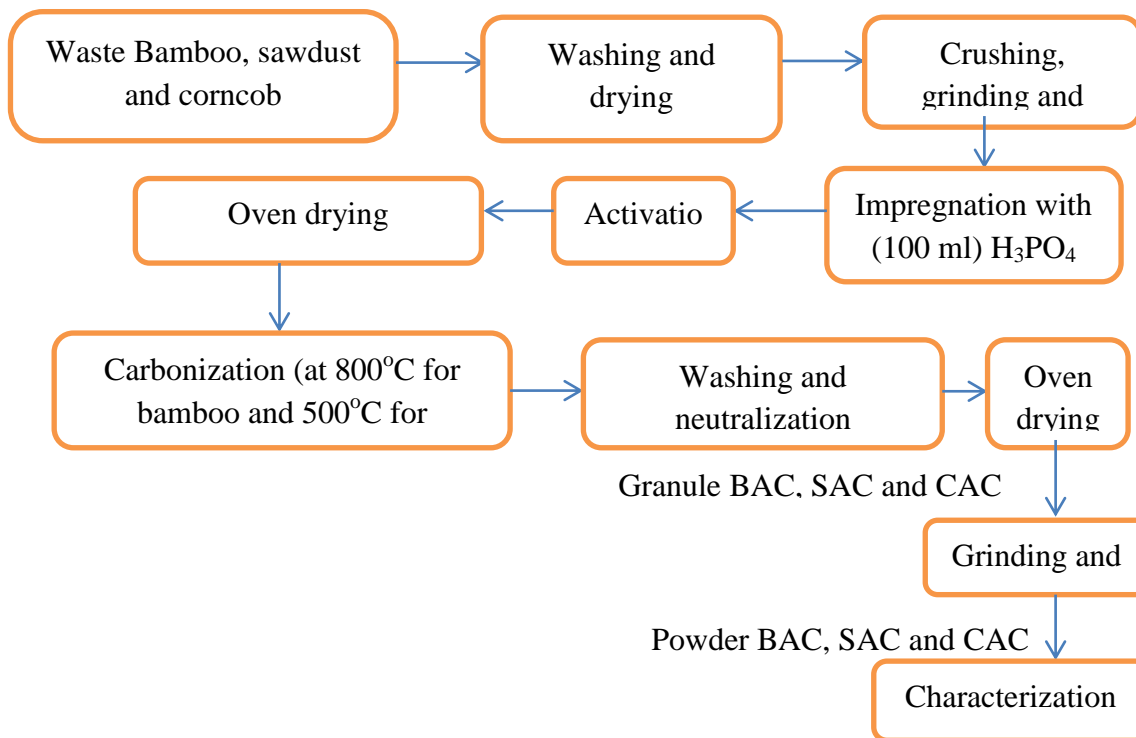
Figure 3-4: General schematic diagram for preparation of Bamboo, sawdust and corncob activated carbon

3.2.5 Preparation of Graphite

Graphite powder prepared from dry dry cell batteries. First the electrodes separated from the batteries. To remove all kinds of impurities like MnO_2, metal particles and carbon, the electrodes were rubbed and washed several times with water. After drying, the electrodes were grinded and

crushed to produce a fine graphite powder. However, there were still some inorganic materials present in the graphite powder, containing aquaregia (HCl and HNO3) (3:1) and heated for 2 hours. Finally, this was centrifuged and washed three times in distilled water to bring to normal pH. Recovered graphite powder was dried at 100 ^{0}Cfor 2 hours.

3.2.6 Synthesis of Graphene Oxide

Electrochemical exfoliation experiments were started with two electrodes system. Electrodes which obtained from waste dry cell batteries used as anode electrode and source of graphene and platinum wire electrode used as cathode electrode, then the two electrodes placed parallel with separation distance of 5.0 cm. The voltage supply used at low tension variable 10 V was applied to the electrodes the experiment was carried out at room temperature. For the efficient electrochemical exfoliation of graphite a NaOH/H_2O solution was used, then GO layers were gradually exfoliated from the expanded graphite electrodes and dispersed in to aqueous solution. The precipitation was subsequently collected and centrifuge then washed repeatedly with deionized water and ethanol to remove unexfoliated GO. Finally the powder dried in to an oven at 60 ^{0}C for 24 hours shown in Figure 3.5.
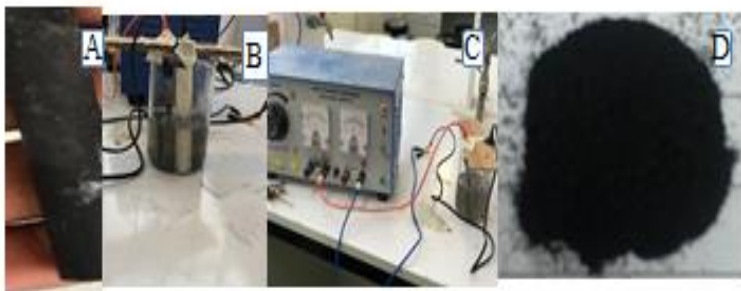
Figure 3-5: Electrochemical exfoliation of Graphene Oxide from waste dry cell batrry A) Graphite rod from new battry cell B) graphite rod immeresed NaOH/H_2O solution C) exfolation of geraphene oxide D) GO powder
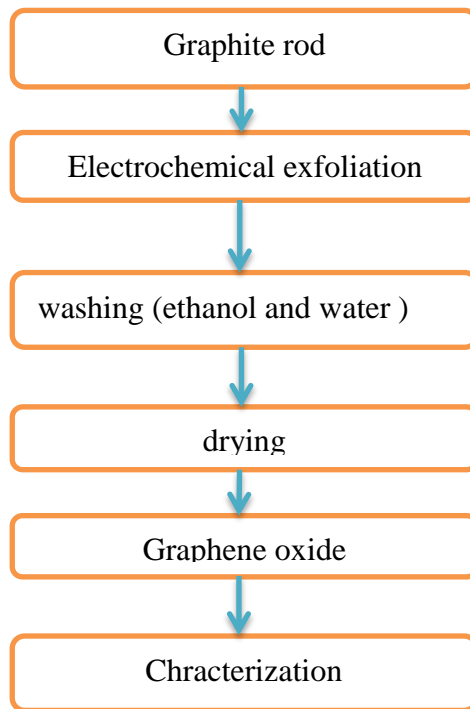
Figure 3-6: Schematic diagram for preparation Graphene oxide

3.2.7 Preparation of Composite AC/GO Composite

In this section composite of activated carbon and graphene oxide was prepared. 0.9 gr AC from bamboo was dispersed well in 250 ml of distilled water and adds 100 ml ethanol was prepared and stirred in a magnetic stirrer for 3 hours. 0.1 gr graphene oxide and the result mixture of were stirred for 12hours. Then dried in an oven at 105 ^{0}C for 4 hours and finally prepared sample (BAC/GO composite stored in air tight plastics for further studies and characterizations. The preparation step was shown in Figure 3-7.
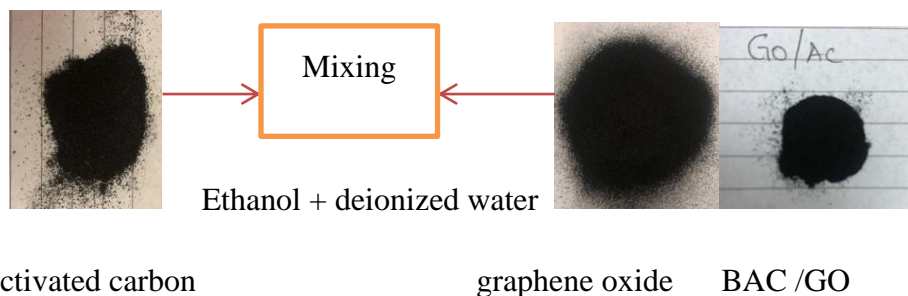
Figure 3-7: BAC /GO preparation

3.2.8 Characterization of Activated Carbon

3.2.8.1 Proximate Analysis

Proximate analysis is a simple means of determining the distribution of products obtained when the coal sample is heated under specified conditions. It was performed to work out the amount of moisture content, volatile matter, fixed carbon and ash content often used analysis for characterizing a material in connection with their utilization(Aragaw, 2016).

❖ **Moisture Content Determination**

This method is used to determine the percentage of water in a sample by drying the sample to a constant weight .A sample of (1 gram) was placed into a dry crucible (of known weight) and weighed accurately. The crucible was placed in an electrical hot air oven maintained at about 105 ^{0}C. After 4 hours the crucible was taken out, cooled in desiccators, and weighed again. The percentage difference in weight was expressed because of the moisture content of the sample (bamboo, sawdust, corncob and BAC/GO composite).

$$\text{Moisture content (\%)} = \frac{M_2 - M_3}{M_2 - M_1} \times 100 \ldots\ldots\ldots\ldots\ldots\ldots\ldots\ldots\ldots\ldots\ldots\ldots \quad (3.1)$$

Where $=M_1$ crucible was weighed empty

$= M_2$ crucible was weighed with original activated carbons (bamboo, sawdust and corncob)

$=M_3$ crucible was weighed with dried activated carbons (bamboo, sawdust and corncob)

❖ **Ash Content Determination**

A known weight of sample (1 gram) was measured and then placed in the dry and know the weight of the crucible. Then the crucible was placed in the muffle furnace and it was then ignited at 600 for 3hrs. After igniting the required temperature and time, the crucible was removed out from the furnace and cooled to room temperature and then reweighed. The weight of the ash content was expressed as a percentage of the weight of the activated carbon sample. The percentage of ash was calculated by:

$$\text{Ash content (\%)} = \frac{M_3 - M_1}{M_2 - M_1} \times 100 \ldots\ldots\ldots\ldots\ldots\ldots\ldots\ldots\ldots\ldots\ldots\ldots\ldots \quad (3.2)$$

Where $=M_1$ crucible was weighed empty

= M_2 crucible was weighed with original activated carbons (bamboo, sawdust and corncob)

=M_3 crucible was weighed with dried activated carbons (bamboo, sawdust and corncob)

❖ **Volatile Matter Determination**

A 1.0 gr of each sample was heated at a temperature of 800 ^{0}C for 8 minutes. Then the crucible with the sample was cooled at room temperature .The volatile matter was calculated using the formula

Volatile matter (%) = *E-F*

$$\text{Where } E \ (\%) = \frac{M_2 - M_3}{M_2 - M_1} \times 100 \text{..} \quad (3.3)$$

Where = M_1 crucible was weighed empty

= M_2 crucible was weighed with original activated carbons (bamboo, sawdust and corncob)

=M_3 crucible was weighed with dried activated carbons (bamboo, sawdust and corncob)

= E weight loss in %

=F moister content in % as defined in above equation (mc)

❖ **Fixed Carbon Determination**

Fixed carbon was calculated as the summation of the percentage of all proximate analysis (moister content, ash content and volatile content) and subtract from 100. Fixed carbon determined by the formula

Weight % fixed carbon = 100 – weight % moisture+ weight % ash+ weight % volatile matter

3.2.8.2 Yield

Carbonization temperature plays an important role on the yield of activated carbon. Yield is defined as the ratio of weight activated carbon produced to the dry weight of precursor. The yield of activated carbons was calculated because the percentage weight of the activated carbons was divided by the weight of dried bamboo, saw dust and corncob.

Yield was calculated by using the following formula

Yield (%) $= \frac{M_C}{M_O} \times 100$ .... (3.4)

Where MC= the dry Wight (g) prepared activated carbons (bamboo, sawdust and corncob)

   MO= the dry Wight of precursors

3.2.8.3 Bulk Density

It can be determined by measuring dried cylinder and the dry activated carbons packed inside the measuring graduated cylinder, and weighed. The weight of activated carbons packed in measuring cylinder determined from the difference in weight of empty and adsorbent filled measuring cylinder. The bulk density computed using Equation 3.5(Malik et al., 2015).

$$\text{Bulk density} = \frac{M_2 - M_1}{V} .... (3.5)$$

Where $= M_2 =$ Weight of measuring cylinder and sample (gram)

   $M_{1=}$ Weight of measuring cylinder

   $V =$ volume of measuring cylinder (mL)

3.2.8.4 Determination of Zero Point Charge (pH$_{pzc}$)

The ACs and BAC/GO composite pH point of zero charge (pH$_{pzc}$) is defined as the pH of aqueous solution in which the solid exist under neutral electrical potential, and this was identifying using the experimental procedure on the characterization of acidic and basic surface sites on carbon using different techniques(Labied et al., 2018). In order to determine the surface of AC acidic or basic the pH of point of zero charge 0.1g of adsorbent is added to 200mL solution of 0.1MNaCl whose initial pH has been measured and adjusted with NaOH or HCl. The containers are sealed and placed on a shaker for 24 hours after which the pH was measured.

3.2.8.5 UV-Vis Spectrophotometer

UV-Vis spectrophotometer analyzers use ion selective electrodes, UV-Vis absorption, as an analytical technique in one integrated machine (Amendola & Meneghetti, 2009).The fast analytical technique that measures the absorbance or transmittance of light that transmittance represents how much light is absorbed at each wavelength and most interested in the highest peak Λ_{max} the practical range for UV-Vis spectrophotometer varies from 200–800 nm; above 800 nm is infrared, while below 200 nm is known as vacuum UV. Here UV-VIS SMART

SPECTROPHOTOME -TER was used for determining the concentration variation analysis of ACs and BAC/GO composite and waste. The spectrum has an operation range (UV 3600 Shimadzu, Japan) of 250 to 1200 nm

3.2.8.6 Fourier Transform Infrared Spectroscopy

The Fourier Transform Infrared Spectroscopy (FTIR) studies were performed to determine the various functional groups on the surface of the material and differentiate unknown material in a non-destructive way. This instrument is using infrared spectrum to categorize solid, liquid, or gas surface by adsorption. The spectra performed 399-4000 cm^{-1} and measured at $4cm^{-1}$ resolution with $0.964233cm^{-1}$ data interval. The background spectrum of air subtracted from the spectra of the samples was recorded at the beginning of analysis. The FTIR analysis was carried out using perkin Elmer FTIR spectrometer (perkin Elmer, 65, USA) at Bahirdar Institute of Technology (Bahirdar, Ethiopia).

3.2.8.7 X-Ray Diffraction

X-Ray Diffraction (XRD) analysis X-ray was used to characterize adsorbent (ACs and BAC/GO composite) was achieved by XRD using in order to identify the main adsorbent minerals (Khenblouche et al., 2019). XRD has long been used as a definitive technique for identifying minerals and other crystalline phases in a wide range of materials. The simple was dried sample for 24 hours at 100 ^{0}C by using oven drier. Then the sample scanned in 2Θ using XRD -7000 X-ray diffractometer ranging from 5 to 85 ^{0}C and the operated at a voltage of 40kv.

3.2.8.8 Thermo Gravimetric Analysis

Thermo gravimetric analysis (TGA) is a quantitative analytical technique that monitors the mass of a sample is measured as a function of temperature or time. The sample is subjected to a controlled temperature program in a controlled atmosphere (Rodrigo, et al., 2021). In addition, it measure thermal stability, isothermal mass loss, and material composition. The thermal stability of the samples was examined using TGA-5500 Model with a temperature range 10-900 at heating rate of 10 ^{0}C /min under the inert atmosphere of nitrogen with a flow rate of 100ml/min.

3.2.8.9 Brunner-Emmett-Teller

Brunner-Emmett-Teller (BET) used to determine the physical adsorption of a gas particle on a solid surface and provides essential chemical analysis method for the measurement of the Specific surface area (Sharma et al., 2004). The BET method usually utilizes gas as Nitrogen which does not interact with the material surface as adsorbate to quantify specific surface area(Thommes et al., 2015). The sample was degassed at 200 ^{0}C in a vacuum condition for a period of at least 24 hours. The adsorption of Nitrogen gas by the sample was carried out using Quantachrome Novawin BET model to determine surface area, Pore volume and, Pore size of a given simple at 89.62 kPa.

3.2.8.10   Dynamic Light Scattering

Dynamic light scattering (DLS) is a spectroscopic measurement technique, which relies on a numerical transformation of spectral measurement signals of representative samples into size distributions (Babick, 2019). The particle size of ACs and BAC/GO composite was analyzed using Zeta sizer nano series (ZE3600) at Addis Ababa science and Technology University (AASTU)

3.2.8.11   Scanning Electron Microscopy with Energy Dispersive X-Ray Analysis

 Scanning electron microscopy (SEM) is an instrument that produces sample images by scanning the surface of the sample with a focused beam of an electron. SEM-EDX used to analyze the surface morphology of the sample by interacts with an electron beam and creating signal that comprises information about the morphology of the surface and composition. In this study the adsorbent (i.e. ACs, GO, and BAC/GO composite) morphology was analyzed using FEI INSPECT F50 model with 10 kv operating voltage.

3.2.8.12   Study of various effects on adsorption

Literature suggests that removal of Cr (VI) from wastewater over activated carbon with GO composite using adsorption depends very much on the factors such as pH, contact time, initial concentration and adsorbent time. Therefore, the influences of these parameters were investigated by varying any one of the process parameters and holding the other parameters constant.

3.2.9 Effects of pH of Solution

To determine the effect of pH on Cr (VI) metal ion using ACs as an adsorbent was conducted using 100mL of 10 mg/L of Cr (VI) solution. The pH values of the solution were adjusted pH range 2 to 12 in separated flasks.by adding 0.1 M HCl or 1M NaOH Solution. The same adsorbent dosage 3 mg/L was added separately to the flasks. The samples were shaken on V.D.R.L shaker (180 rpm) at room temperature for 120 min contact time to make sure equilibrium is reached the sample were filtered separately with watman filter papers and analyzed in the UV-Vis spectrophotometer at λ_{max}=350 nm to obtain final concentration of Cr (VI).

3.2.9.1 Effect of Adsorbent Dosage

The effect of adsorbent dose was studied by conducting the experiment from 1 to 4 g / 100mL of ACs with 400 ml conical flask. The adsorption efficiency for different dose pH and contact time was kept constant with metal ion concentration of 5 mg/L. The experiment was conducted at room temperate on V.D.R.L shaker (180rpm) for 120 min. the mixture was filtered with watman filter papers and analyzed in the UV-Vis spectrophotometer at 350 nm to obtain final concentration of Cr (VI).

3.2.9.2 Effect of Initial Cr (VI) Concentration

The effect of initial Cr (VI) concentration were determined by using different concentration ranges from 5 to 20mg/L. 100mL of aqueous solution containing 10 mg/L Cr (VI) was taken in 400mL conical flasks and known quality adsorbent 40mg/L was added the sample was shaken for 120 min by shaking V.D.R.L shaker at room temperature. The sample was filtered with watman filter papers and analyzed in the UV-Vis spectrophotometer at 350 nm to get final concentration of Cr (VI).

3.2.9.3 Effect of Contact Time

For the determination of the optimum time in the adsorption of Cr (VI) process by the activated carbon (i.e. bamboo, sawdust and corncob). In this study 2.5 mg/L of adsorbent was conducted with 100mL solution of 20mg/L Cr (VI) ion adjusted to pH = 2. The solution was transferred to 400 mL conical flask was analyzed for residual Cr (VI) at different time intervals (30-180 min).

Other parameters were kept constant and shaking speed 180 rpm in at room temperature. The mixture was filtered with watman filter papers and analyzed in the UV-Vis spectrophotometer at 350 nm to get final concentration of hexavalent chromium.

3.2.10 Determination of Adsorption Kinetics

The kinetics of the adsorption rate were analyzed using two kinetic models, pseudo-first-order and pseudo-second-order a significant contribution of intra particle diffusion (Macedo et al., 2006) Adsorption kinetics describes the solute adsorption rate and is important characteristic in evaluating the efficiency of adsorption of ACs. To analysis the kinetic models of experiment data and the model predicted values were conducted by using coefficients of correlation R^2. Then the data was obtained from the kinetics were analyzed using origin 2021. Therefor the one which have high R^2 value was selected as a general equation for kinetics of Cr (VI) adsorption.

3.2.11 Determination of Adsorption Isotherm

Batch equilibrium adsorption experiments were used for adsorbent assessment through plots of adsorption isotherms. Adsorption isotherms can also be mathematically expressed. The adsorption isotherm is the equilibrium relationship between the concentration in the fluid phase and the concentration in the adsorbent particles at a given temperature. The quantity adsorbed is nearly always normalized by the mass of the adsorbent to allow comparison of different materials(X. Chen, 2015). Adsorption isotherms are mathematical models that describe the distribution of the adsorbate species among liquid and solid phases, based on a set of assumptions that are related to the heterogeneity/homogeneity of the solid surface, the type of coverage, and the possibility of interaction between the adsorbate species. In order to construct adsorption isotherm for ACs and BAC/GO composite, experiment was carried out by varying adsorbent dose from 0.1 gr to 4 gr in 100 ml solution of the metal ions with initial concentration of 40 mg/L(Seyoum & Asso, 2015). The data obtained from isotherm were analyzed using origin 2021, the one which have high R^2 value was selected as a general equation for kinetics of Cr (VI) adsorption.

Table 3-2: Adsorption kinetics and equilibrium isotherm model used to compare adsorption of hexavalent chromium on bamboo activated carbon composite with Graphene oxide.

Kinetic models	Equation
Pseudo-first order	$\log (q_e - q_t) = \log q_e - (K_1 / 0.2303) \times t$
Pseudo-second order	$\dfrac{t}{q_t} = \dfrac{1}{K_2 q_e 2} + \dfrac{1}{q_t} t$

Equilibrium isotherm models	Equation
Langmuir	$\dfrac{1}{q_e} = \dfrac{1}{q_m} + \dfrac{1}{q_m K_L} \left(\dfrac{1}{C_e}\right)$
Freundlich	$\log q_e = \log K_f + \dfrac{1}{n} \log C_e$

3.2.12 Statistical Design of Experiment

Design of experiment (DOE) refers to the process planning, designing, and analyzing the experiments to conclude the objective values efficiently. The principal steps of statistically designed experiments are the determination of response variables, factors and factor levels, choice the experimental design, and finally statistical analysis of the data (Antony et al., 2003). To develop an adsorption design on the percentage removal of hexavalent chromium some actors affect the process such as PH, adsorption dosage, initial Cr (VI) concentration, and contact time was studied. Modeling of the adsorption of hexavalent chromium on prepared BAC/GO composite was carried out by using Box-Behnken design (BBD) by using the software design expert -13. This technique is appropriate Response surface and contour plots were developed using the fitted quadratic equation obtained from the regression analysis and BBD is more economical in practice, more universe and efficiency (Montgomery, 2013).

Box - Behnken design consists of 2^k factorials with incomplete block designs. These designs are useful in avoiding experiments performed under extreme conditions, for which unsatisfactory results might occur. The center points are used to determine the experimental error of the data. The model used correlate the response with hexavalent chromium adoption from aqueous

solution was used to develop an empirical model using a second degree polynomial equation (Lazic et al., 2004).

$$Y = b_o + \sum b_i X_i + \sum b_{ii} X_i^2 + \sum \sum b_{ij} X_i X_j \dots \dots \dots \dots \dots \dots \dots \dots (3.6)$$

Where Y is the predated response, b_0 the constant coefficient, b_i the linear coefficients, b_{ij} the interaction coefficient, b_{ii} the quadratic coefficient and $X_i X_j$ are the coded factors of the adsorption of hexavalent chromium on BAC/GO composite variables. The entire number of tests (*N*) required for the four independent variables is:

$$N = 2^k + 2k + x_o = 2^4 + 2 \times 4 + 5 = 2 \dots \dots \dots \dots \dots \dots \dots \dots (3.7)$$

Where N is that the total number of experimental runs required, K is that the number of variables and X_o is that number of central points. Thus for this design total number of experimental runs will be 29 (K=4, X_o =5).The range of factors and levels, which were varied consistent with the experimental design, are given in Table 3.3.

Table 3-3: Experimental range and levels for adsorption of Cr (VI)

	Name of process parameter	Unit	Lower value	Higher value
A	pH		2	7
B	BAC /GO dosage	mg/L	1	4
C	Cr(VI) concentration	mg/L	5	30
D	Contact time	min	30	150

3.2.13 Electroplating Effluent Sample Collection and Analysis

3.2.13.1   Description of Study Area

In this study, electroplating effluent sample was collected from Gafat Armament Engineering industry established in January 1980 E.C in Debrezeit Beshftu Ethiopia. It was design to manufacture different types of Armaments and civilian products. Such as small medium heavy armaments & different types of spare parts which are used for vehicles and machineries. Newly again the factory was modernized to product additional Up graded weapons such as 7.62×39mm, AK-47, 40mm Launchers and other weapons which are used for commercial purposes. Gafat has 408 hector areas and it has ten different factories facilities such as small armament production

factory, Medium caliber production factory, Rocket Launcher, Mortars production factory, Heavy armament and Howitzer factory, Material treatment factory, Barrel manufacturing factory, Receiver body manufacturing factory, Accessory and equipment manufacturing factory, Shooting parts manufacturing factory & Precision Casting factory.

3.2.13.2 Sample Collection and Treatment

The sample was collected manually from Gafat Armament Engineering industry when it leaves from electroplating after chrome plating process. The sample was collected using a 500mL polyethylene plastic sampling bottle which was prepared for sample collection first by washing with concentrated HNO_3 then washed with distilled water to protect contamination. The collected sample was immediately transferred to Digestion process to separate the Cr (VI) from other heavy metals. To conduct this study a 100 mL of concentrated HNO_3 and 5 mL of concentrated HCl. The sample is covered covers and heated on a steam bath source at 90 to 95 ^{0}c until volume has been reduced to 15-20mL. The beaker allowed cooling and filtering the sample with filter pepper then adjusting the final volume to 100 mL with reagent water and the sample preserved in refrigerator at 4 ± 2 ^{0}C to protect the contamination of sample until the analysis instrument to be ready.

Figure 3-8: Sample preparation

3.2.13.3 Effluent Analysis

For UV- visible spectrophotometer analysis, evaluated the section of chromium without a pervious separation step because this reaction is selective for hexavalent chromium. The treated electroplating waste water from Armament engineering industry hexavalent chromium was analyzed using the UV- visible spectrophotometer at a wavelength of 540 nm.

3.2.13.4 Preparation of Chromium Ion Solution

The synthetic effluent prepared within the laboratory was prepared actual electroplating waste water. Potassium dichromate ($k_2Cr_2O_7$) was used because of the source of Cr (VI) stock solution. The Cr (VI) ion stock solution of 1000 mg/l was prepared by 2.829 g of 99% $k_2Cr_2O_7$ dissolved in 1.0L distilled water in volumetric flask. Potassium dichromate was properly mixed with distilled water in volumetric flask just after 2-3 min of shaking by hand and also the stock solution was changed in to yellow color. The working solutions desired concentrations of Cr (VI) ion were prepared from this stock solution by appropriate dilution. For instance, 10 mg/L chromium stock solution was prepared by diluting 10 mL to 1000 mL chromium stock solution with distilled water in a 1000 mL volumetric flask up to the mark. The desired amount of distilled water is decided by the entire volume of the solution minus the required volume Of Cr (VI) diluted solution. Similarly, solutions with different metal concentrations such as (2-10 mg/L) were prepared. The pH of the solution was adjusted by either 0.1M HNO_3 or 0.1M NaOH solution using pH meter before the adsorption process, to control the pH at the specified value.

3.2.13.5 Batch Adsorption Experiment

The experiments were carried out within the batch model adsorption process to investigate the removal efficiencies of prepared BAC/GO composite at room temperature. Batch adsorption experiments for adsorption of Cr (VI) on BAC/GO composite were conducted using synthetic solutions of the metal. A batch mode adsorption study for Cr (VI) metal ion was carried out to analyze the effect of various parameters like pH of the solution, adsorbent dosage, initial concentration of chromium, and contact time. The solution containing adsorbate of 100 mL and added the desired quality of adsorbent was taken in 250 mL capacity conical flasks and agitated in V.D.R.L shaker at the desired contact time. All adsorbate samples were filtered using filter paper (whatman No-1) before analysis to reduce interference of carbon fines with the analysis. All the experiments have performed in duplicate and therefore the mean values were reported by

the instrument. Finally, the performance of BAC/GO composite analyzed detailed description of the experimental procedure of batch adsorption studies.

3.2.13.6   Analysis of Chromium Metal Ion

For quality control purpose, the final residual concentration of Cr (VI) after adsorption was also determined spectrophotometric in the absence of diphenylcarbazide at a wavelength of 350 nm. The direct method (absence of diphenylcarbazide) is usually recommended to determine the concentration of Cr (VI) greater than 1 mg/L (Sanchez-Hachair & Hofmann, 2018). The various standard concentrations $K_2Cr_2O_7$ solutions were prepared and their absorbance was recorded by using a UV- spectrophotometer. After recording absorbance values of the standard solutions construct a calibration curve. A linear plot was obtained indicating adherence to Beer Lamberts law within the concentration range studied. Because the calibration curve was used in the reading of the unknown concentrations, their accuracy was of absolute importance. The general equation to determine the percentage removal of Cr (VI) for aqueous solution was the following.

$$\text{Percentage removal of Cr (VI)} = \frac{C_o - C_e}{C_o} \times 100 \text{.......................... (3.8)}$$

Where C_o and C_e are the concentration of Cr (VI) at the beginning and the end of the adsorption capacities of adsorbents used in this study were determined by using the equation:

$$q_e = \frac{(C_o - C_e)V}{1000W} \text{.. (3.9)}$$

Where q_e (mg/g) is the amount of chromium adsorbed per unit weight of adsorbent, V is the volume of aqueous solution (mL), and W is the adsorbent weight

CHAPTER FOUR

4 RESULTS AND DISSCUSSION

4.2 Characterizations of Prepared Activated Carbons

4.2.1 Evaluation of Proximate Analysis

The preliminary investigation of proximate analysis for activated carbons prepared from Bamboo, *Eucalyptus* sawdust and corncob was done to know the performance of AC for further studies. The proximate analysis Bamboo, *Eucalyptus* sawdust and corncob ACs was done according to standard methods and given by percentage by weight. The obtained values are presented in the below Table 4.1. The detailed calculation part is additionally also include under appendix A.

Table 4-1: The proximate analysis of activated carbon prepared from Bamboo, *Eucalyptus* sawdust, corncob and BAC/GO composite

Parameter	Bamboo AC	*Eucalyptus* sawdust AC	Corncob AC	BAC/GO composite
Moisture content (%)	15.98	19.98	22.98	9.98
Ash content (%)	2.2	6.27	11.2	2.05
Volatile content (%)	47.82	49.98	52.46	47.15
Fixed carbon (%)	34.09	23.77	21.36	40.82

❖ **Moister content**

Measuring the moisture content of the adsorbent was one of the important features to understand the adsorbent quality. The laboratory result of moisture content of ACs from bamboo, sawdust, corncob and BAC/GO composite with was low determined to be 15.98%, 19.98%, 22.98% and 9.98%, respectively. The moisture content ACs refers to the percentage of the water content of the sample. The BAC/GO composite moisture content was lower than the pure bamboo AC so it may give a good opportunity for the higher adsorption efficiency of Cr (VI) from waste water.

❖ **Ash content**

The ash content was main property of activated carbons because the more the ash content, the ACs become soft and more compacted, and therefore the chance of porous decrease but the AC with less amount of ash content would have more strength and more porous. Therefore, acid

activation is the best technique used to reduce the ash content during the activation. The percentage of ash content for bamboo, sawdust, corncob and BAC/GO composite samples were found to be 2.2%, 6.27%, 11.2% and 2.05% respectively. The low ash content in the sample indicates that the precursor contains low inorganic matter (Shrestha et al., 2018). The obtained value for BAC/GO composite was favorable because the ash content serves as interference during the adsorption.

❖ Volatile content

The percentage of volatile content for bamboo, sawdust, corncob and BAC/GO composite samples was 47.82%, 49.98%, 52.46% and 47.15% respectively as shown in Table 4-1. The lower volatile content of composite of BAC/GO showed that some organic molecule of the material were attacked and it is stable for the adsorption experiment of Cr (VI) ion from the aqueous solution to raise the quality of fixed carbon. The optimum volatile matter and ash content give a higher percentage of fixed carbon.

4.2.2   The yield

As generally recognized, the transformation from lignocellulose materials in to carbon involved releasing of O and H atoms as H_2O, CO, CO_2, CH_4, aldehydes or distillation of tar the carbonization yield depends on the amount of carbon removed by binding with O and H atoms.(Gottipati, 2012).The yield of bamboo, sawdust, corncob, and BAC/GO composite is respectively 59.87%, 52.97%, 34.4% and 62.67%, so those value of maximum yield was an indicator of the high efficiency of the process using H_3PO_4 activation process and in GO controlling the synthesis conditions to achieving the optimum yield expand. Higher yield are desirable in AC and graphene oxide production and it helps to reduce production cost. The detailed calculation part is included under appendix B.1.

4.2.3   Evaluation of bulk density

Bulk density is an important parameter especially when adsorbent is to be investigated for its filterability. The bulk density contents of bamboo, sawdust, corncob and BAC/GO composite obtained was found, 0.52g/ml, 0.328g/ml, 0.311g/ml and 0.96g/ml respectively. The higher bulk density (BAC/GO composite = 0.96g/ml) was provides greater volume activity and normally indicates high-quality adsorbent. It suggests that BAC/GO composite is added to water it will

sink and that with result in better contact with the adsorbate thereby leading to an effective adsorption process. That is, it would be able to filter more liquid volume before available cake space filled and it can be stabled or without adsorbed with the solution (Jamiu Mosebolatan Jabar, 2016). The detail callculation part is also included under Appendix B.2.

4.2.4 Determination of Point of Zero Charge

The adsorption on solid-liquid systems is influenced by the appearance of surface electric charges in the adsorbent and the adsorbate (Bernal et al., 2018). When AC is placed in contact with an electrolytic solution, the surface ionizes depending on the developed AC of the functional groups present in the surface, and the charged particle is surrounded by ions of the opposite charge since it is apparently electrically neutral (Wu & Pendleton, 2001). The pH value required for the net surface charge of AC is zero and is known as the point of zero charge (pHpzc) (Alvarez-galvan & Minofar, 2022). The AC pH point of zero charge (pHpzc) is defined as the pH of aqueous solution, in which the solid exists under neutral electrical potential(Labied et al., 2018). The obtained pHpzc of CAC, SAC and BAC were shown below in Figure 4-1.
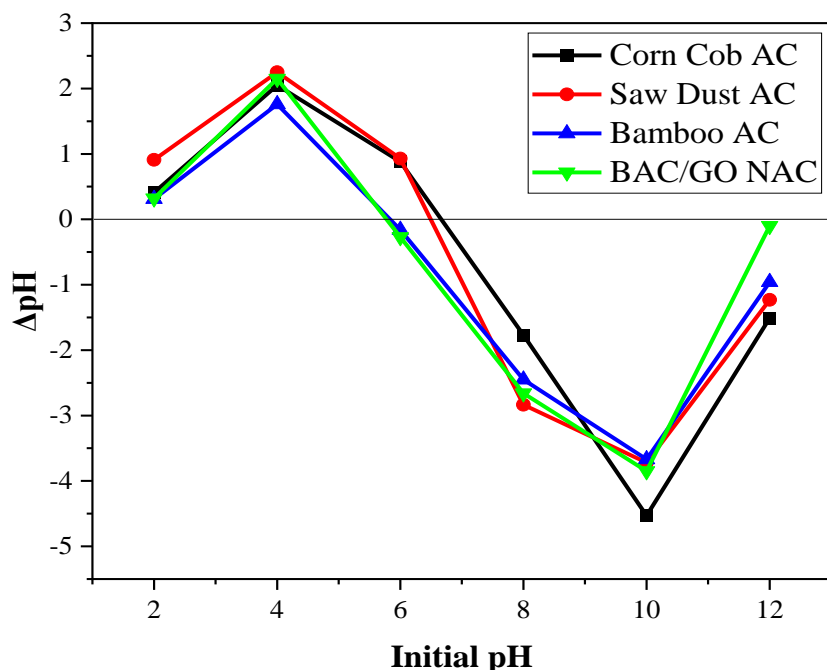
Figure 4-1: Point of zero charge for Corn Cob, Saw Dust Bamboo AC and BAC/GO

The pH of points of zero charge for bamboo, sawdust corncob, and BAC/GO composite were 6.7, 6.5, 5.8 and 5.7 respectively as shown in Figure 4-1. According to pHpzc result, all samples

exhibited cationic (positive) surface charge. If the pH of the solution is less than pHpzc, the surface of the AC going to be protonated by the competition of H^+. In contrary when the pHpzc is greater than the pH of the solution which results the surface of the AC is deprotonated by OH^- ions present in a given solution(Buckner et al., 2016). Therefore, all synthesized materials have perfect charge balance in the acidic region and the surfaces of ACs are positively charged which enable to attract anions materials. Based on this result it can be concluded that the developed AC material have better performance and efficient for the removal of Cr (VI) heavy metal from wastewater in acidic solution.

4.2.5   UV-Vis Spectrophotometer analysis

The UV–visible absorption spectrum of the synthesized, graphite and GO, ACs and BAC/GO composite has been recorded and is represented as shown in Figure 4-2 and 4-3. The UV-Visible spectra graphite to GO exhibited absorption peak at 237 nm which was attributed to transition of aromatic C=C bonds and a weak shoulder at 307 nm due to the C=O bonds present in GO. The absorption spectra at 264 nm in graphite spectrum is red shifted to 237 in GO, which confirms the reduction of graphite and the partial restoration of GO as shown in Figure 4-2. The UV-visible spectra graphite to corncob, sawdust, and bamboo possess a characteristics adsorption peak 234.9 nm, 228.8 nm, and 263.3 nm respectively as shown in Figure 4-3 due to the presence of C and O in the AC. In addition BAC/GO composite exhibits a peak at 236 nm and 279 nm so it confirms the composite have both AC and GO properties. It indicates that BAC/GO composite was successfully forms combination.
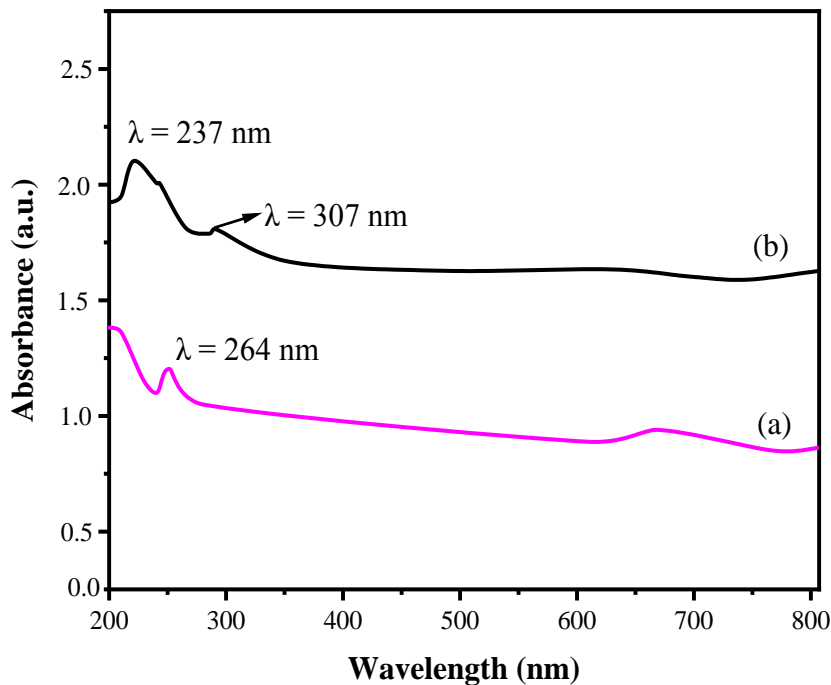
Figure 4-2: UV-Vis spectrometry of A) Graphite b) GO
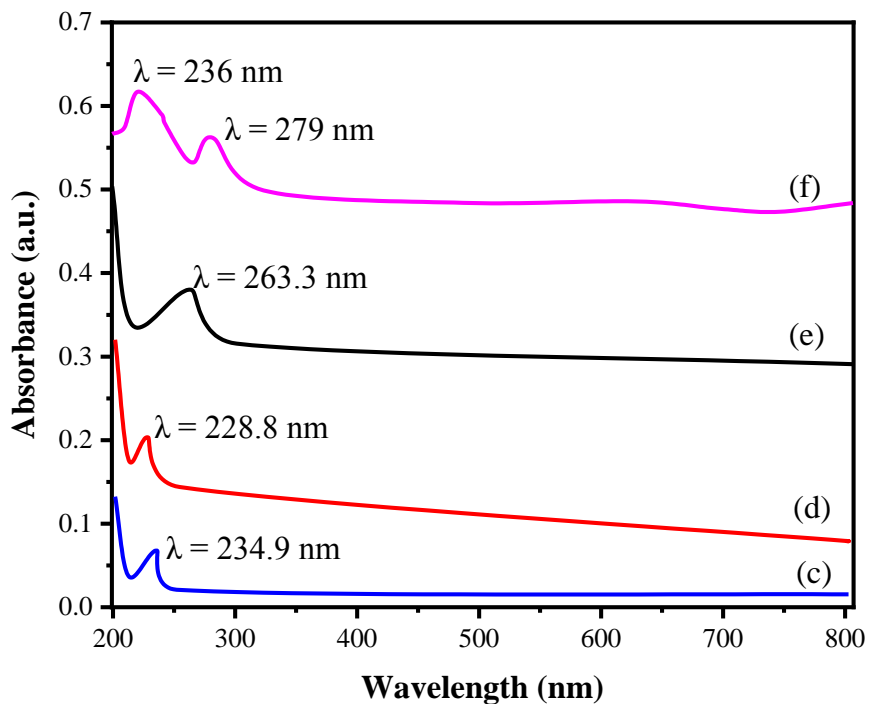
Figure 4-3: UV-Vis spectrophotometer analysis of c) corncob ac, d) sawdust ac, e) bamboo ac, f) composite

4.2.6 Fourier Transform Infrared Spectroscopy

The Fourier Transform Infrared Spectroscopy (FT-IR) spectra of the three adsorbents corncob, sawdust and bamboo AC were performed in order to explore the surface characteristics of the bio-sorbents as shown in Figure 4-4 a) corncob, b) sawdust and c) bamboo. The spectra display a number of absorption peaks, indicating the possible functional groups present on these bio-sorbents that may be responsible for the removal of heavy metal ions from aqueous solutions. The bands at 3383.5, 3442.3 and 3376.7 cm^{-1} as shown in Figure 4-4 a), b) and c) respectively are due to the hydroxyl group (O-H) and N-H stretch (mainly primary and secondary amines) present on the adsorbents. The stretching of OH groups bound to methyl radicals presented at band 2353.7, 2358.5 and 2373.5 cm^{-1} of corncob, sawdust and bamboo AC as shown in figure 4-2. Moreover, as shown in Figure 4-4 a) the band observed at 1642.1 cm^{-1} is assigned to C = C bond (from alkenes), the bands at 1303.6 and 1098.5 cm^{-1} are assigned to C-O stretch (alcohols, ethers, acids, esters). The peak at 1053.9 cm-1as shown in Figure 4-4 a) indicates the presence of methylene C = H bend. As shown in Figure 4-4 c) the peak at 1568.8 cm^{-1} was corresponds to N-H bend of amines and amides.

Furthermore, the peak at 1038.7 cm^{-1} was due to C–H bend of $CH_2=CH_2$- from vinyl groups. These peaks which correspond to different functional groups are possible sites for adsorption of metal ions by the adsorbents(Jia et al., 2002). The peaks were observed at 920.8 and 966.2 cm^{-1}[a] as shown in Figure 4-4 b) and c) due to vinyl C-H out of plane bend. There was a peak at 542.6 because of C-H groups were out of plane deformation. Generally the presence of surface functional groups like amine (N-H) and carboxylic (C-O and C=O), hydroxyl (O-H) groups are important sorption sites in the adsorption process removal of Cr (VI) ions from aqueous solution and wastewater.
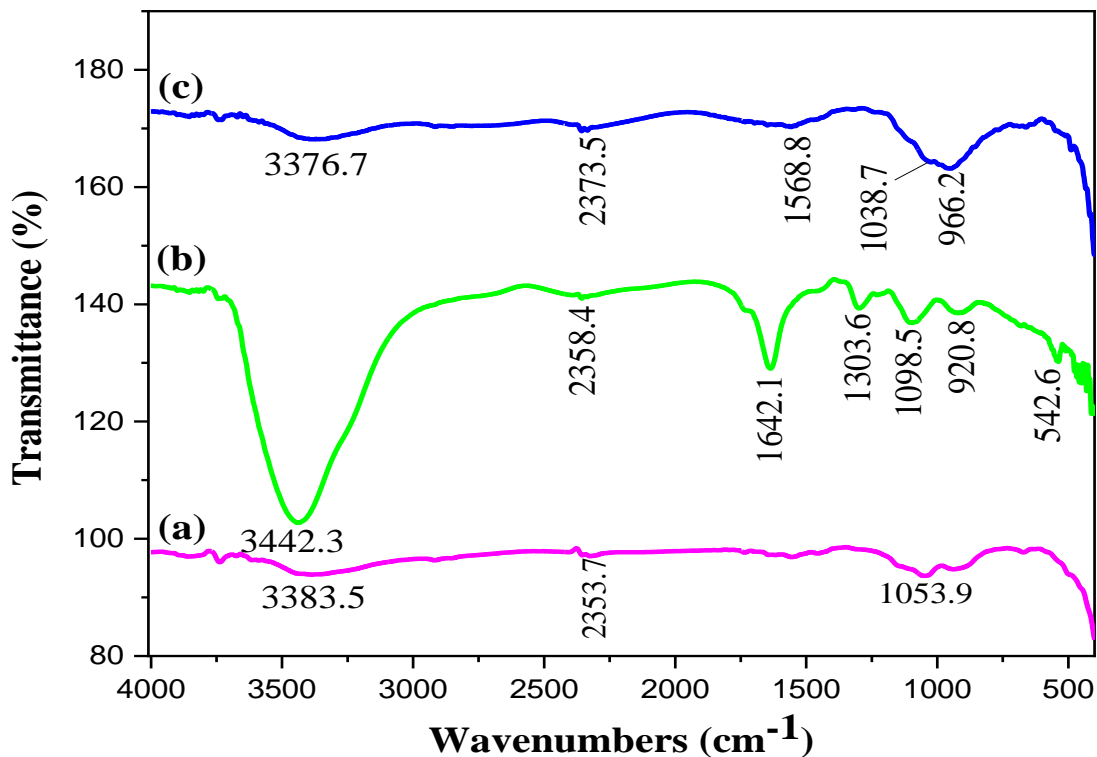
Figure 4-4: FTIR of a) Corncob, b) Sawdust and c) Bamboo

In addition, the FTIR spectra of graphite and GO were shown in Figure 4-5 the weak band located at 3673 and 3676 cm^{-1} were related to O-H stretching vibrations existed in graphite and GO respectively. The peaks located at 2991 and 2993 cm^{-1} as shown in Figure 4-5 a) and b) were due to symmetric and asymmetric stretching vibration of C–H bond respectively. The peak at 1698 cm^{-1} as shown in Figure 4-5 b) indicates the Carbonyl C =C stretching vibration of oxidized graphitic domain. The peak observed at 1400 cm^{-1} in as shown in Figure 4-5 a) can be attributed to the deformation O-H groups. Various oxygen configurations in the structure include the vibration modes of epoxide (C–O–C) (1230–1420 cm^{-1}) in both samples. The peak at 1068 and 1065 cm^{-1} as shown in Figure 4-5 a) and (b) indicate the C–O stretching vibration of alkoxy group. Thus the result obtained from FTIR affirmed the presence of various oxygen containing functional groups like hydroxyl, epoxy, carboxyl, carbonyl within the GO structure which indicate the developed GO was successfully synthesized from waste dry cell using electrochemical exfoliation method.
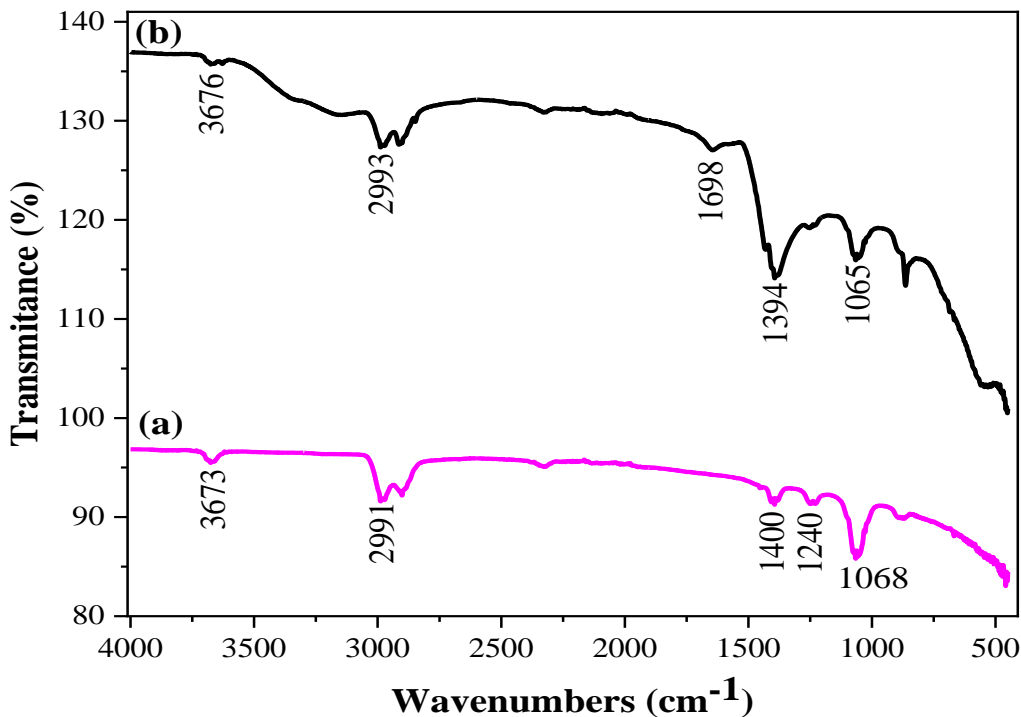
Figure 4-5: FTIR of a) graphite and b) GO

Moreover, the infrared spectra of the BAC/GO composite were exhibited as shown in Figure 4-6. The broad band at 3434.6 cm^{-1} in Figure 4-6 b) was the O-H stretching vibration peaks due to the presence of adsorbed moisture by BAC/GO composite. The peaks at 1635.3 cm^{-1} as shown in Figure 4-6 indicates C=C stretching vibration peaks of the aromatic rings. After adding of GO in to BAC matrix, the vibration peaks of 1038 cm^{-1} become weak. This indicated that after forming of BAC/GO composite a large number of oxygen-containing functional groups of the material were removed. It also indicates that the porous carbon surface retained a small number of oxygen-containing functional groups.
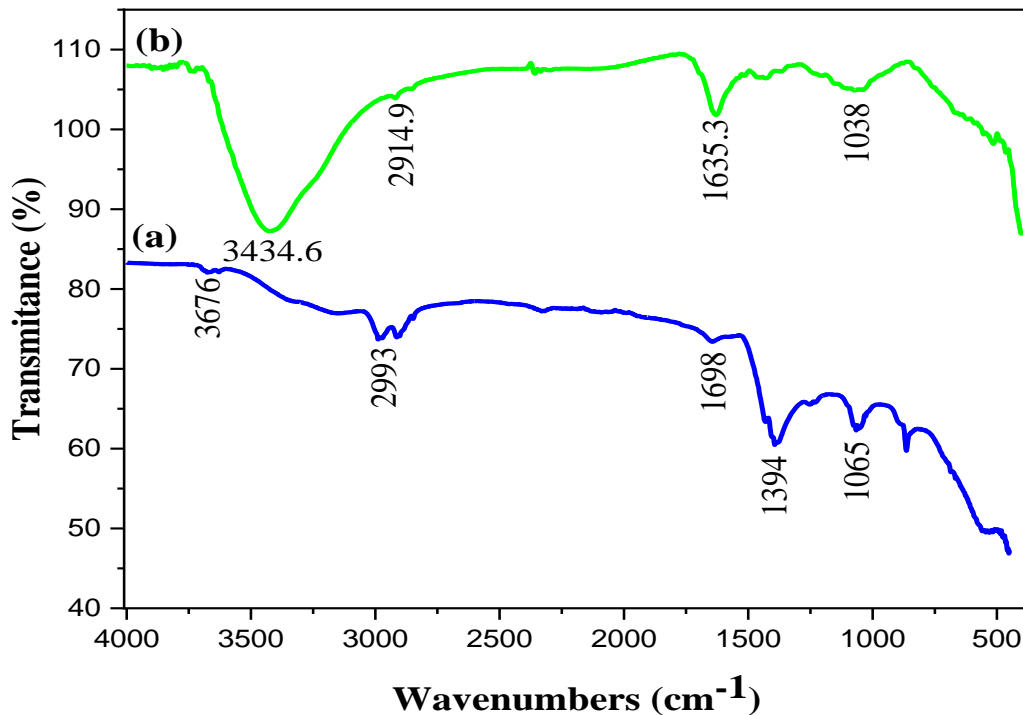
Figure 4-6: BAC/GO FTIR graph a) GO and b) BAC/GO composite

4.2.7 X-Ray Diffraction

X-Ray diffraction (XRD) analysis were carried out to examined the amorphous and crystallinity nature of the synthesized ACs (Gupta et al., 2013). The obtained XRD spectra of each developed AC were exhibited in Figure 4-7. The peaks at $2\theta = 20.3^0$, 25.6^0, and 37.7^0 as shown in Figure 4-7 a) and $2\theta = 20.5^0$, 24.2^0, and 37.7^0 as shown in Figure 4-7 b) were indicates the development of fragmented crystallites (graphitized) carbonaceous structure in both corncob and sawdust AC respectively. On the other hand, as shown in Figure 4-7 c) the narrow and sharp peaks were not exhibited in the XRD patterns of BAC, which indicates the surface of the synthesized BAC has pure amorphous region with well-developed micro-pores. The amorphous region of a given AC increased, when adsorption efficiency also increases. Generally, an amorphous material normally has high specific surface area to volume ratio and higher surface acidity (Zheng et al., 2014). These properties increase the force of the interaction between adsorbent and substrate material, which normally lead to a higher adsorbed amount (Iram et al., 2010). In addition, as shown in Figure 4-7 c) the broad and weak peak in range of $2\theta= 14.96^0 - 35.66^0$ was exhibited in all

samples which indicates the synthesized AC is not composed of well crystalline graphite's, but ill crystalline micro graphite's.
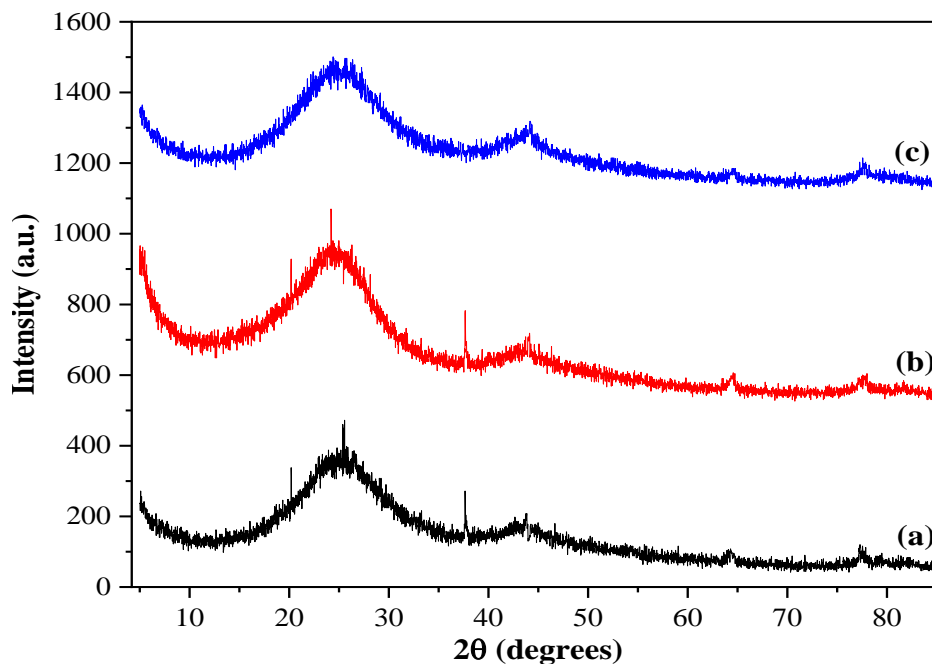
Figure 4-7: XRD patterns of a) corncob, b) sawdust and c) bamboo

The XRD patterns of graphite and graphene oxide were shown in Figure 4-8. In the case of pure graphite as shown in Figure 4-8 a), a strong XRD peak at 2θ = 26.5° and a slight peak at 2θ = 54.5° were observed specific to the (002) and (004) planes with d-spacing of 0.35 nm and 0.19 nm, respectively which indicates the presence of carbon components in the sample structure. In addition, the XRD patterns of graphite shows the crystal structure. The small peak at $2\theta = 53.84^{0}$ as shown in Figure 4-8 a) indicates the presence of water molecule in the sample. The graphene oxide as shown in Figure 4-8 b) shows a wide diffraction peak that is at 2θ = 11.6° with the spacing between plane d) is 0.75 nm, confirming the successful GO synthesis from waste dry cell battery using electrochemical exfoliation method. Increasing the distance between fields in the graphene oxide is due to the presence of oxygen-functional groups and water molecules into the carbon layer structure. The same peak appeared at $2\theta = 26.5^{0}$ as shown in Figure 4-8 b) which indicates the reappearance of the carbon composition with diffraction line (002) which looks wider and the intensity is lower than the peak obtained in the graphite powder.
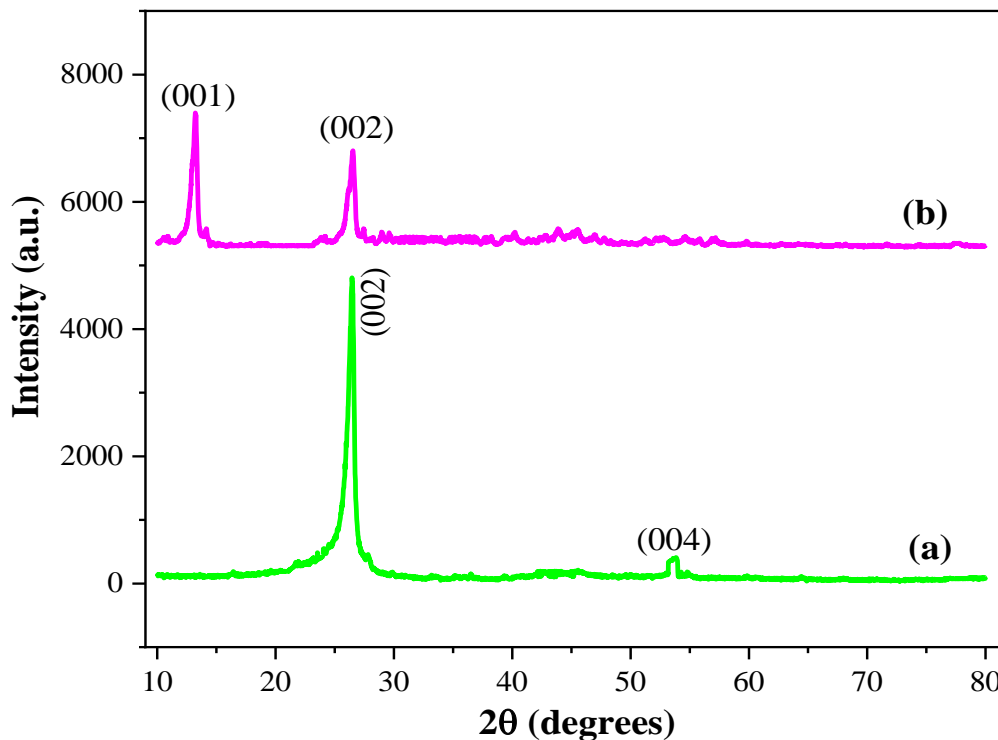
Figure 4-8: XRD patterns of a) graphite b) GO

The XRD patterns of bamboo AC, GO, and BAC/GO composite were exhibited in as shown in Figure 4-9. In the BAC/GO composite XRD patterns exhibited the same peaks with GO and from a good composites at the same peak position, which indicates the two samples are well mixed and the AC was successfully synthesized. The mixing of the two materials reduces the degree of interlayer aggregation that results the synthesized BAC/GO composites have more pores. The developed BAC/GO composite have an ultra-high specific surface area and a narrow pore size distribution, which are favorable for heavy metals (i.e. hexavalent chromium (Cr (VI)), lead (Pb), vanadium (Vd), etc.) adsorption(Technological trends in heavy metals removal from industrial wastewater: A reviewShrestha et al., 2021).The prepared adsorbent expected having an excellent performance and low cost.
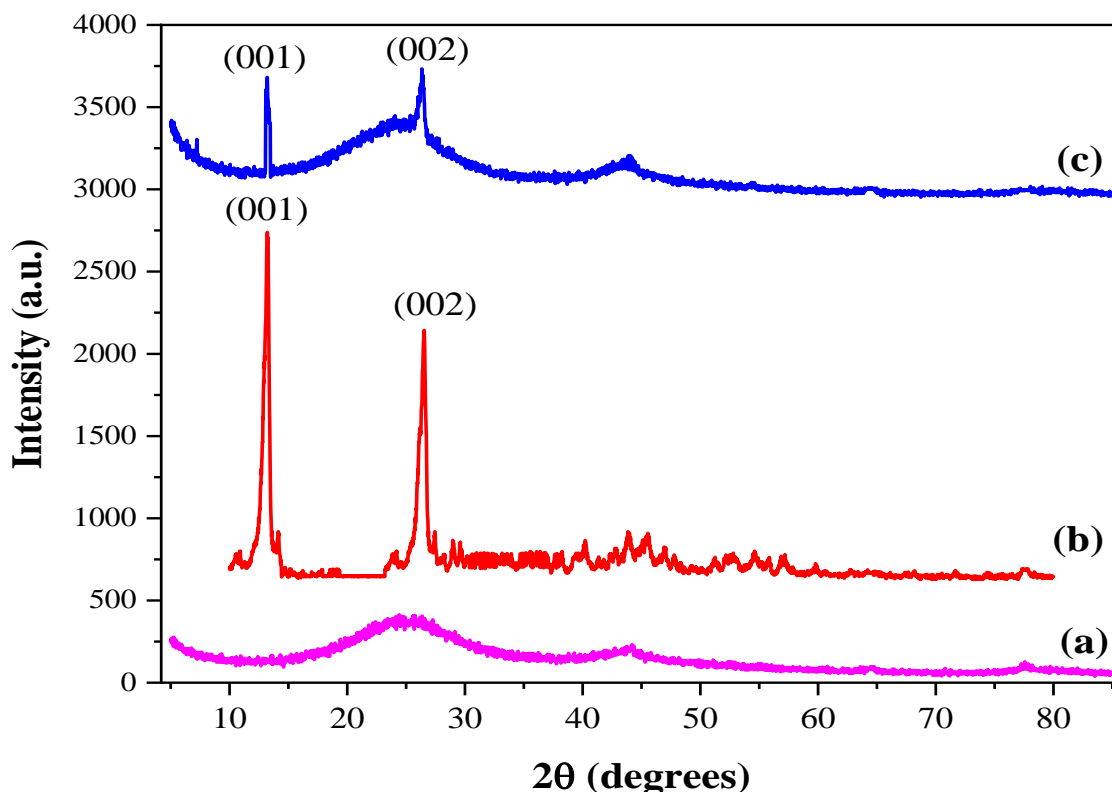
Figure 4-9: XRD patterns of a) BAC b) GO c) BAC/GO composite

4.2.8   Thermo Gravimetric Analysis

Thermo gravimetric analysis TGA analysis was conducted to test the thermal stability of BAC, GO and BAC/GO composite. According to TGA results three stages were observed in the quality loss curve of all samples as shown in Figure 4-10. Firstly, a roughly 4.6%, 5.43% and 6.9% weight loss occurred in BAC, GO and BAC/GO composite, respectively, at the temperature range of 13 ^{0}C - 200 ^{0}C. This is primarily due to the loss of H_2O molecules and some organic compounds from each sample. The main weight loss in the second stage from 200 ^{0}C-700 ^{0}C may be associated with the thermal decomposition reaction of hemicellulose, cellulose and lignin from BAC and thermal decomposition of instable oxygen-containing functional groups from GO. In the same temperature range, the weight loss of BAC/GO composite was smaller than pure BAC, which indicate the thermal stability of the synthesized BAC/GO composite was increases due to the presence of GO in the AC matrix. Graphene oxide was very stable substance in the normal state. The weight loss of BAC, GO and BAC/GO composite at this temperature

range was 60.4%, 47.7% and 49.6% respectively. The final weight loss in the range of 800 ^{0}C – 900 ^{0}C was insignificant in GO, implying that the decomposition reactions were almost completed. Therefore, the suitable temperature for preparation of GO should be at least 800 ^{0}C. On the other hand, small thermal decomposition was occurred in both BAC and BAC/GO composite which mainly due to the combustion of the carbon skeleton. The weight loss in the third stage of BAC, GO and BAC/GO composite were 16.1%, 2.6% and 12.65%. The total weight loss of BAC, GO, and BAC/GO composite were 81.15%, 55.73% and 69.15% respectively. As a conclusion, the TGA analysis results indicated that BAC/GO composite has excellent thermal stability than BAC.
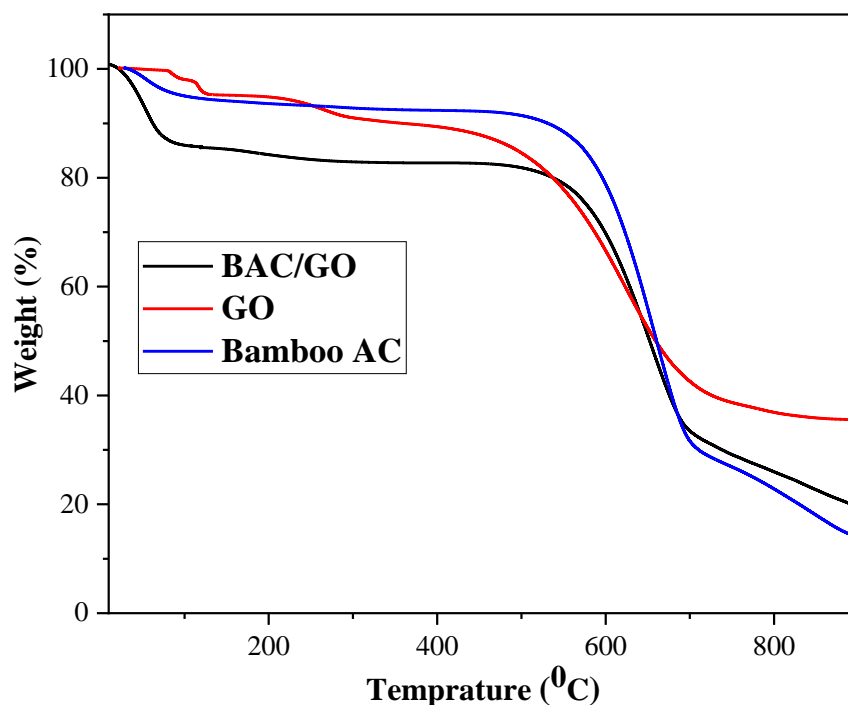
Figure 4-10: TGA analysis a) BAC/GO, b) GO, and c) Bamboo

4.2.9 Brunner-Emmett-Teller

The surface area, pore size and volume of BAC and BAC/GO composite were measured using the Brunauer-Emmett-Teller isotherm (BET) method. The obtained results were shown in Table 4-5. According to BET analysis the result showed that the addition of GO in BAC matrix efficiently increases the surface area and Pore volume of BAC. This will give a good opportunity to increase the efficiency of the adsorbent in the adsorption process of toxic metal ions like

Cr(VI) this is due to its high degree of micro porosity forms more adsorbing sites(Kyotani, 2003).

In addition, the presence of GO on the carbon surface of BAC can increase the hydrophilicity of the carbon which supports the adsorption of heavy metal ions into the pores of the carbon and can give effective adsorption performance (Yang et al., 2019). On the other hand the pore size of BAC/GO composite was reduced after addition of GO, which indicates GO successfully incorporated with BAC. If the pore size of AC is small, it will reduce the diffusion of adsorbate, due to that the particles which found in adsorbate was easily captured and stacked by the pores of BAC/GO composite. Therefore, the synthesized BAC/GO composite has high adsorption performance than pure BAC Appendix D.1.

Table 4-2: BET result

Sample	Surface area (m^2/g)	Pore volume (cc/g)	Pore size (nm)
BAC	1200.1	0.3958	0.1838
BAC/GO	1633.7	0.5978	0.1538

4.2.10 Dynamic Light Scattering

The particle size distribution profile of chemically AC and BAC/GO composite were studied using the Dynamic light scattering (DLS) pattern to detect the intensity, particle size, Z-Average, poly dispersity index (PDI) and standard deviation of the sample. The DLS spectra of BAC and BAC/GO composite were shown in Appendix D.2. According to the above DLS result, initially the particle size of pure BAC was 164.5 nm. But the limited specific surface area and particle size of BAC was modified. However the BAC/GO composite particle size was 128.3 nm which is around to the nano size range. This confirms the BAC/GO composite, the adsorption kinetics rate will faster than the AC. Generally if the surface area and pore volume of the AC increase, the size of the particle decrease, that result the faster rate of adsorption kinetics during adsorption process. The summarized DLS result of BAC and BAC/GO composite were shown below in Table 4-3.

Table: 4-3: DLS result of BAC and BAC/GO

Sample Name	Z-Average (nm)	PDI	Particle Size (nm)	% intensity	St. Dev (nm)
BAC	131.3	0.292	164.5	94.2	± 31.73
BAC/GO	119.4	0.328	128.3	91.7	± 30.1

4.2.11 Scanning Electron Microscopy with Energy Dispersive X-Ray Analysis

Scanning electron microscopy (SEM) technique was used to observe the surface physical morphology of BAC and BAC/GO composite. SEM micrographs of the produced BAC and BAC/GO compsite were given in Figure 4-11 a) and b). From Figure 4-11 a), the surface heterogeneity of the AC was significantly reduced due to the improvement in the surface area and pore development of the sample through H_3PO_4 activation process. In addition, Figure 4-11 a) shows cavities on their external surface that improve the porosity. Different pore sizes and shapes were observed on the BAC surface because of depolymerization and subsequent release of volatile organic substances from carbonization (Tomczyk et al., 2020). In Figure 4-11 b) it can be seen that the surface of the GO was slightly rough. The SEM image of BAC/GO composite was highly porous, which can realize that after the addition of GO on the surface of bamboo. These findings suggested that the prepared BAC/GO composite was potentially high performance with better surface modification than pure bamboo AC. Therefore BAC/GO composite used as a low cost adsorbent for various environmental applications such as removing of hazardous compounds from wastewater and in water purification purpose.
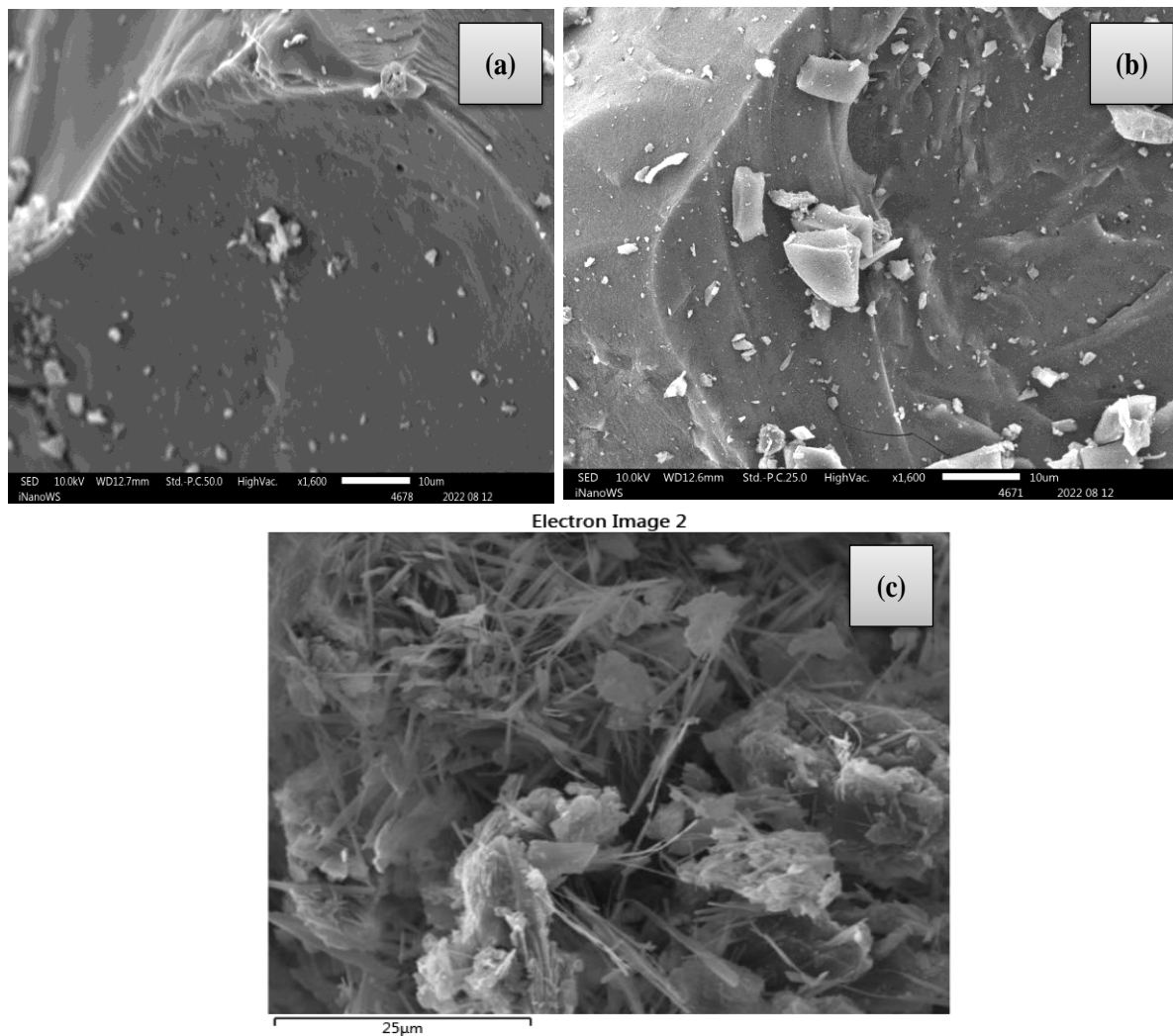
Figure 4-11: SEM image a) BAC, b) GO and c) BAC/GO composite

Furthermore, the elemental compositions of a given samples were analyzed using SEM-EDX and the obtained images were shown below in Figure 4-12. According to the results, the bamboo AC comprises C (69.6%), O (18%), P (9.7%) and Na (2.7%) in its structure as shown in Figure 4-12 a). In addition, Figure 4.12 b) confirms GO contains C (60.3%), O (31.5%) and Na (8.5%). Moreover, BAC/GO composite consist C (83.4%), O (11.4%), P (3.9%) and Na (1.2%) as sown in Figure 4-12 c) This confirms the AC and BAC/GO successfully synthesize with good purity.
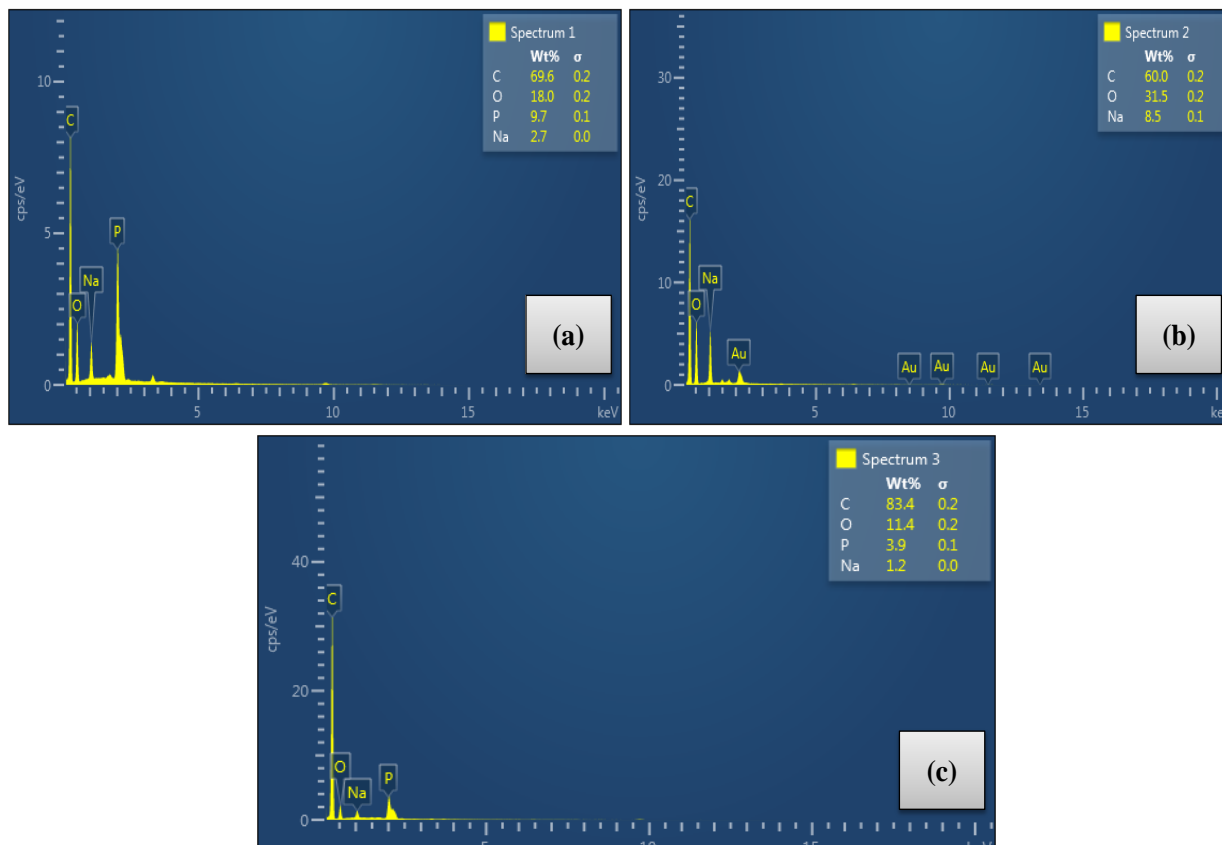
Figure 4-12: SEM-EDX image of a) BAC, b) GO and c) BAC/GO composite

4.3   Adsorption of Hexavalent Chromium

4.3.1   Effect of Process Parameter

4.3.1.1 The Effect of Initial pH of the Solution

In the adsorption process, the pH of a solution is one of the most important parameter which affects the performance of heavy metal ions adsorption by a given activated carbon and BAC/GO composite. The value of the pH strongly influences the properties of both adsorbate and adsorbents such as the ionic state of functional groups present on the adsorbent as well as the chemical properties of the studied metal ions in solution. For this reason, the pH affects not only the degree of ionization and specifications of the adsorbate, but also the surface charge of the adsorbent during reaction (Shojaeiarani et al., 2021). Therefore; the effect of pH directly impacts the electrostatic interactions between the adsorbate and adsorbent's surface due to that the rate adsorption decreased. The effect of initial pH of the Cr (VI) solution in the adsorption process

were examined by using corncob, sawdust, bamboo and BAC/GO composite at 5mg/L Cr (IV) concentration and the obtained results were illustrated in Figure 4-13.
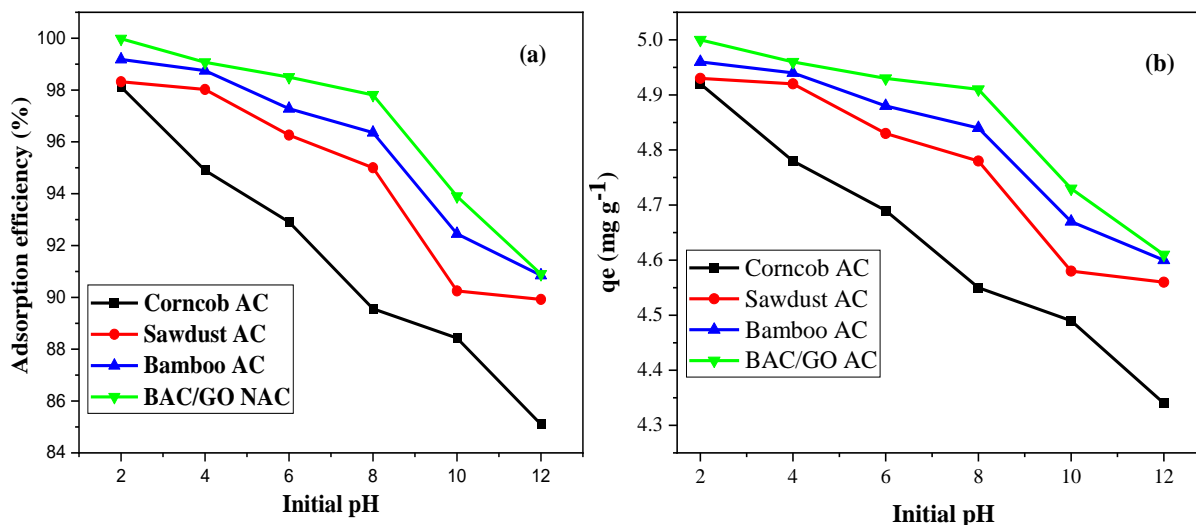
Figure 4-13: a) the effect of pH of the solution on adsorption efficiency and b) the effect of pH of the solution on adsorption capacity

According to Figure 4-13 a), the maximum removal percentage of Cr (VI) for all samples were observed at pH = 2. It shows that the adsorption of the cellulose adsorbent was highly pH dependent. Cr (VI) removal efficiency decreased with increasing the initial pH of the solution. At this optimum pH the obtained adsorption efficiency of corncob, sawdust, bamboo and BAC/GO composite were 98.12%, 98.32%, 99.18, and 99.98% respectively. At a lower pH (pH ≤ 3) value, Cr (VI) exists in the form of $HCrO_4^-$ and CrO_7^{2-}, which have negative charge. In addition, at low pH, there is presence of a large number of H^+ ions exists in the solution medium due to this the surface protonation of AC leads to the formation of positively charged sites (Mohan & Pittman, 2006). These protons interact with chromium atoms by an electrostatic attraction which leads the $HCrO_4^-$ ion adsorbed on the surface of activated carbon; thus causing an increase in chromium adsorption(Labied et al., 2018). It was found that at lower pH the system attain equilibrium faster and also the percentage of chromium adsorbed increased (Anah & Astrini, 2017). The increasing of pH from 2 to 12 the efficiency of adsorption also decrease due to the dual competition of both the ions (CrO_4^{2-} and OH^-) to be adsorbed on the surface of adsorbent. As a conclusion, pH= 2 is the optimum pH value for the highest removal efficiency or adsorption of chromium ions for all synthesized AC and BAC/GO composite. In addition, as shown in Figure 4-13 (b) exhibits the

adsorption capacity of each AC and BAC/GO composite were decreased when the pH value of the Cr (VI) solution increased.

4.3.1.2 Effect of Dosage

The effect of adsorbent dosage on Cr (VI) adsorption process was investigated by varying the amount of activated carbon from 1 to 4g/L.as shown in Figure 4-4 a) and b) illustrates the variation of removal percentage and adsorption capacity of Cr (VI) at different adsorbent doses. Generally, the all synthesized sample showed the removal percentage and capacity of Cr (VI) increased when the adsorbent dosage increases at an initial Cr (VI) concentration of 5 mg/L, while the adsorbent mass increased from 0.1 to 0.25 g/L with interval of 0.05 mg/L. This may be due to an increase in the availability of active sites when there is more amount of adsorbent dose (Labied et al., 2018). However, since there were no large differences observed between the adsorption percentages of Cr (VI) above adsorbent concentration of 0.25 g/L, we decided to take into account the most economical approach where it was considered that the adsorbent dose of 0.25 g/L is an optimum dose for this study. At the obtained optimum pH (pH=2) and dosage (0.25mg/L), the Cr (VI) adsorption percentage of corncob, sawdust, bamboo and BAC/GO composite were 98.72%, 99.25%, 99.48%, and 99.98% respectively. The synthesized BAC/GO composite has highest adsorption efficiency than pure BAC.
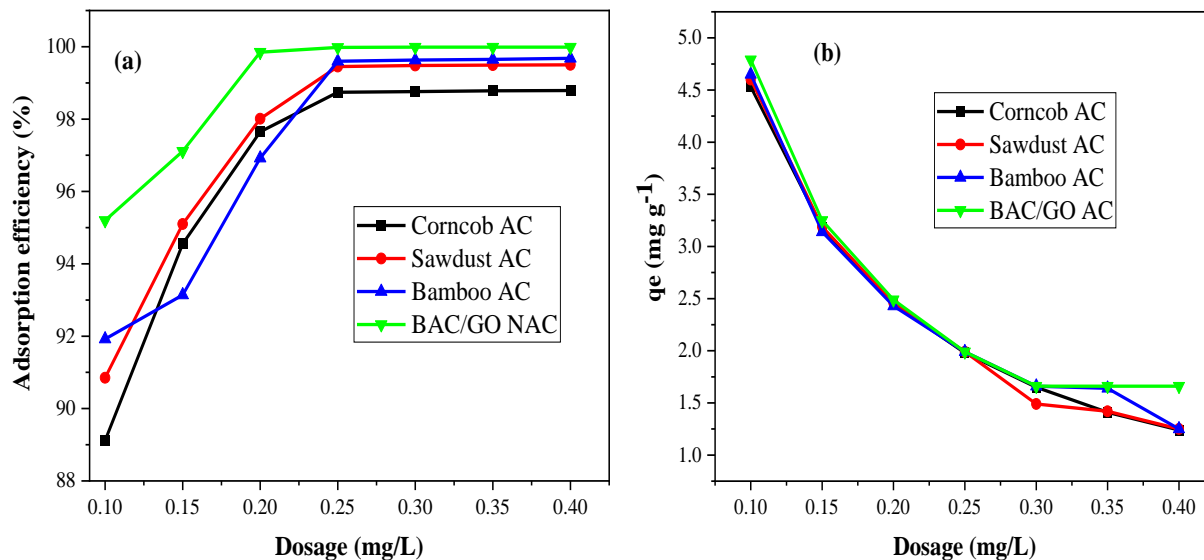
Figure 4-14: The effect of dosage a) adsorption efficiency and b) adsorption capacity

4.3.1.3 Effect of Initial Cr (VI) Concentration

The effect of initial hexavalent chromium concentration on the adsorption efficiency and adsorption capacity of the synthesized ACs and BAC/GO composite is shown in Figure 4-15. In all the samples, the adsorption efficiency and capacity as shown in Figure 4-15 a) and b) respectively, increased as the initial concentration of Cr (VI) ions increased from 5 to 12.5 mg/L. After 12.5 mg/L of Cr (VI) concentration, the adsorption rate and capacity were decreased due to a higher initial concentration enhanced the driving force between the aqueous and solid phases and increased the number of collisions between metal ions and adsorbents that resulted lower removal efficiency. In addition, at a certain high concentration the active vacant sites become saturated and create high competition for available bonding sites on the AC surface which reduce the adsorption efficiency of the adsorbent (Zhang et al., 2020). The optimum initial concentration of Cr (VI) was 12.5 mg/L. At this optimum concentration the obtained adsorption efficiency of corncob AC, sawdust AC, bamboo AC, and BAC/GO composite were 83.98%, 88.6%, 89.5%, and 94.6%, respectively.
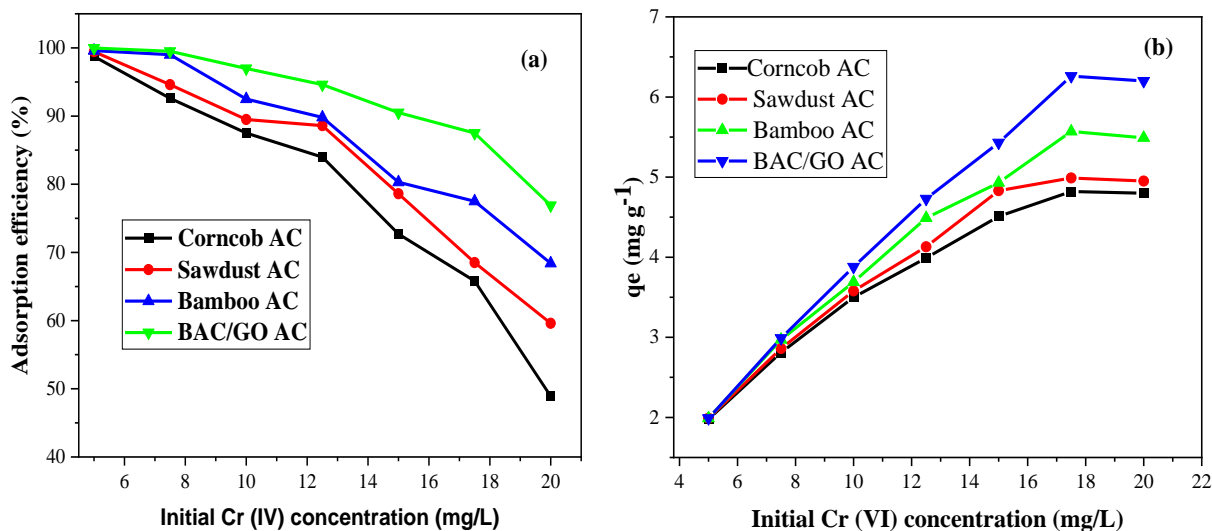
Figure 4-15: The effect of initial hexavalent chromium concentration of the solution a) adsorption efficiency and b) adsorption capacity

4.3.1.4 Effect of Contact Time

The adsorption of the Cr (VI) metal ions by using of corncob, sawdust, bamboo and BAC/GO composite were studied at various time intervals (30-180 min) and at optimal pH (pH=2), adsorbent dosage (0.25mg/L), and optimum concentration of Cr (VI) (12.5mg/L). The obtained

result was exhibited as shown in Figure 4-16. The obtained results were exhibited in the first time intervals ranging from 30-120 min the adsorption efficiency and capacity of Cr (VI) as shown in Figure 4-16 a) and b) respectively were high using the three synthesized AC. On the other hand, the adsorption efficiency was increased from 30 to 90min using BAC/GO composite. After optimums time, the adsorption process was proceeds at a slower rate and finally attains saturation. The initial fast reaction may be due to the increased number of vacant sites available on the surface of adsorbent; as a result the concentration gradient was increased between adsorbate in solution and adsorbate in the adsorbent. Then, as lower adsorption efficiency would follow as the available adsorption site decreased. This is due to the fact that a large number of vacant surface sites are available for adsorption during the initial stage, and after a lapse of time the remaining vacant surface sites are difficult to be occupied due to repulsive forces between the solute molecules on the solid and bulk phases (Tan et al., 2009). The maximum adsorption percentage of the three synthesized AC (corncob, sawdust and bamboo) and BAC/GO composite were occurs at 120 and 90min, respectively. The obtained adsorption efficiency of corncob, sawdust, bamboo, and BAC/GO composite were 83.98%, 88.42%, 90.5%, and 95.6% respectively. As a conclusion, the BAC/GO composite has lower contact time and high adsorption efficiency than pure BAC, which indicates the developed composite have large surface area to volume ratio and efficient for the removal of Cr (VI) from waste water.
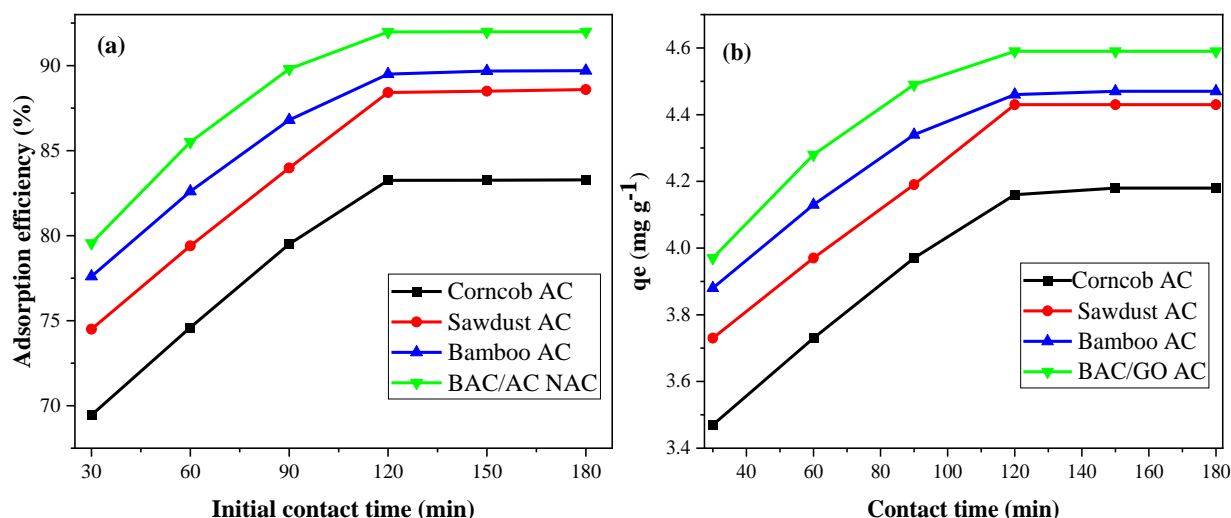
Figure 4-16: The effect initial contact time of the solution of chromium concentration of the solution a) adsorption efficiency and b) adsorption capacity

4.3.1.5 Adsorption Kinetics Model

Adsorption kinetic study is vital in determining the efficiency of adsorption. Kinetic and equilibrium data consideration are pertinent in the evaluation of adsorption dynamics significance, and by extension, the optimization of residence time.(Menkiti et al., 2015) To get the rate constants and therefor the order of adsorption reactions, pseudo-first-order, and pseudo-second-order kinetic model were applied to kinetic data obtained from optimum values of factors. The correlation coefficient (R^2) value ware used to express the conformity between experimental data and therefore the model predicted values. A comparatively high R^2 value indicated that the model successfully describes the kinetics of Cr (VI) adsorption. .

4.3.1.6 Pseudo-First Order Kinetic Model

Kinetic modeling of the removal of hexavalent chromium by BAC/GO composite was carried out using the well-known Lagrange model (Kalavathy et al., 2005).From the experimental data, a straight line was obtained by pitting Log ($q_e - q_t$) against t, as shown in Figure 4-14. The lower coefficients of correlation (R^2 =0.87032for corncob, R^2=0.8424 for sawdust, R^2=0.889 for bamboo) obtained suggest that the adsorption of Cr (VI) on prepared ACs does not follow the pseudo-first-order kinetics but R^2 =0.981 for BAC/GO composite follow the pseudo-first-order. The value of the rate constant k_1 and q_e were obtained from the slopes and intercepts of the plotted figures. The detailed callculation part is also included in Appendix E .1, E .2, E .3, E .4 (Table 7).

.
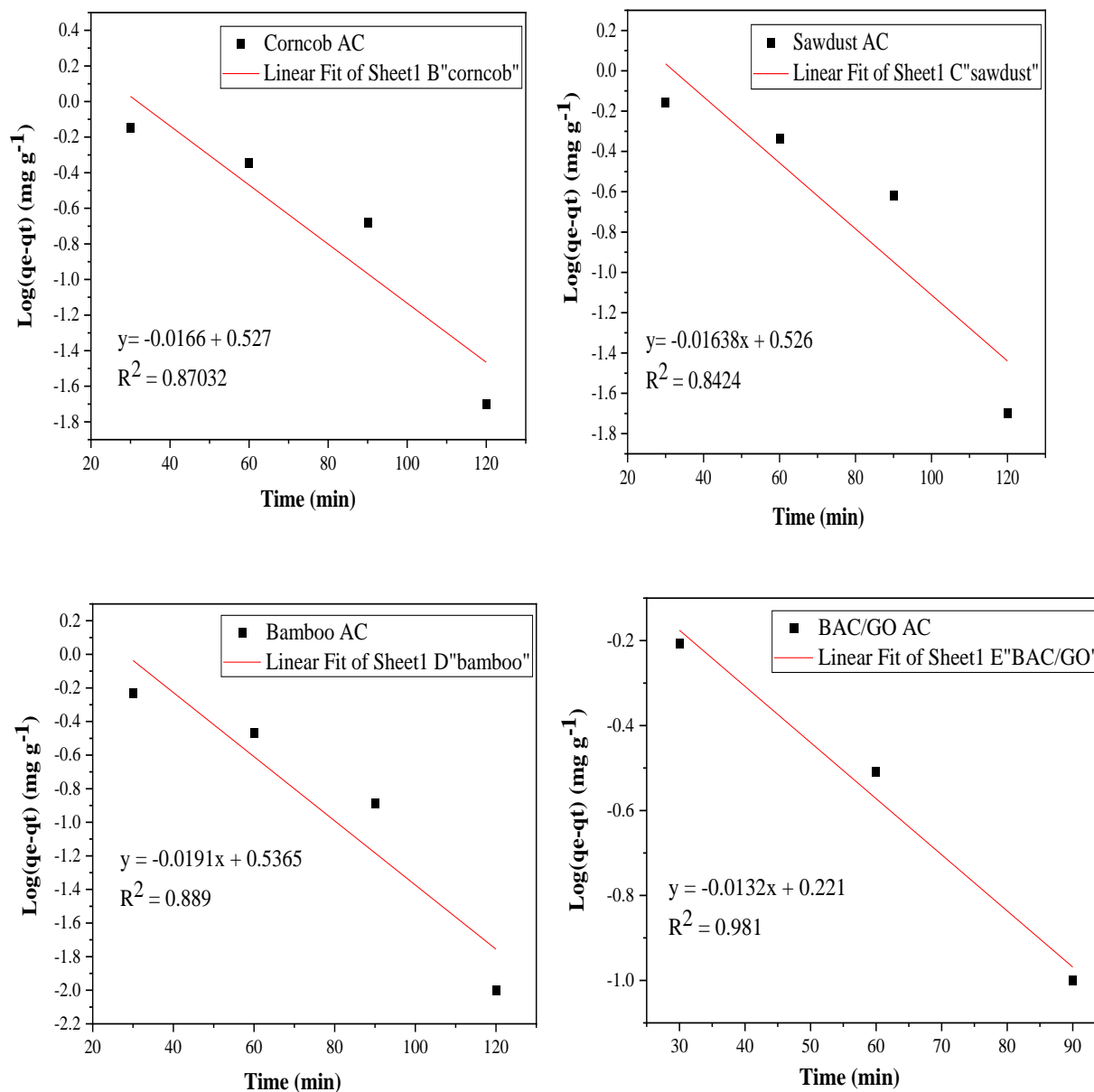
Figure 4-17:pseudo- first-order plots For adsorption of Cr(VI) on a) corncob   b) sawdust c) bamboo and d) BAC/GO composite

4.3.1.7 Pseudo-Second-Order Kinetic Model

From the experimental data, a straight line was obtained by plotting t/q_t versus t as shown in Figure 4-15. The regression (R^2= 0.9994 for corncob, R^2= 0.9993 for sawdust, R^2= 0.9997 for bamboo, R^2= 0.9998 for BAC/GO composite) value obtained is closed on the point of unity and therefore and the adequate fitting of plots confirmed that the adsorption of Cr (VI) by the

prepared ACs and composite followed pseudo-second-order kinetics(ALOthman et al., 2013). The value of q_e and K_2 where determined were determined from the slopes and intercepts of the plot. The detailed callculation part is additionally included in Appendix E .1, E .2, E .3, E .4 (Table 8).
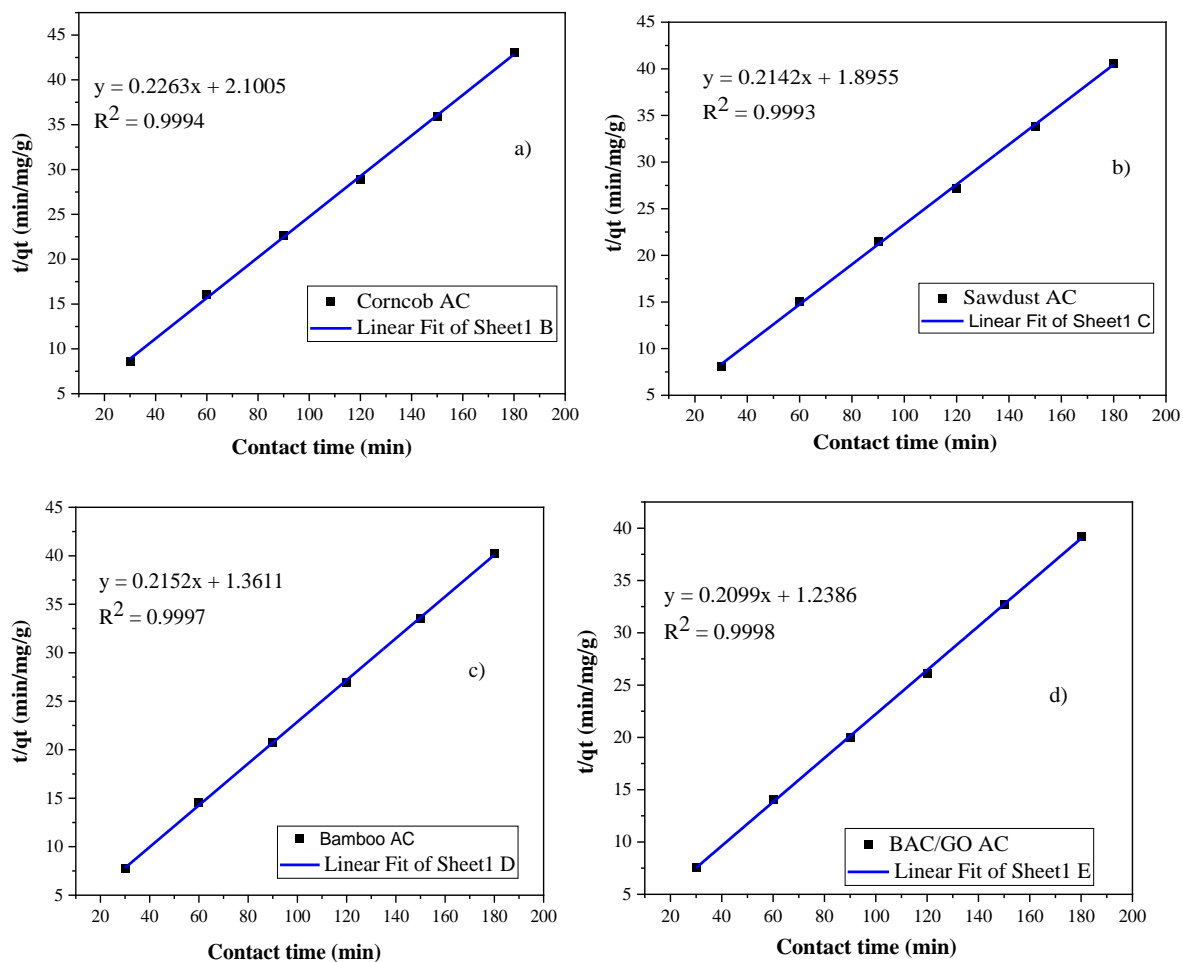
Figure 4-18: Pseudo-second-order plots for adsorption of Cr (VI) on a) corncob b) sawdust c) bamboo and d) BAC/GO composite

The values of the coefficient of correlation (R^2) and other kinetic parameters of pseudo first order and pseudo second order kinetic models as given in Table 4-7. The results demonstrated that among these two models, pseudo-second-order kinetic equation had high R^2 value, which implies the calculated (q_{ecal}) from graph (intercept) value was a very good approach with the experimental values ($q_{e\ exp}$). Therefore, the adsorption of Cr (VI) ions from aqueous solutions on to prepared ACs and composite was found to follow the pseudo-second-order kinetic equation. Therefore, it has been concluded that Cr (VI) adsorption on to corncob, sawdust, bamboo and

BAC/GO composite consists of chemical adsorption because the pseudo-second-order kinetic model suggests that the adsorption process involves a chemisorption mechanism (Theydan, 2018). Chemisorption involves the formation of a robust bond between the adsorbate and therefore the adsorbent that involves the transfer of electrons (Kajjumba et al., 2018).

Table 4-4: calculated values of various kinetic model constants and their correlation coefficients (R^2) for the adsorption of Cr (VI) on corncob, sawdust, bamboo and BAC/GO composite

Kinetic model	Parameters	Parameter value Corncob AC	Parameter value sawdust AC	Parameter value bamboo AC	Parameter value BAC/GO composite
Pseudo-first-order	$q_{e\,exp}$ (mg/g)	4.18	4.43	4.47	4.59
	$K1$(min^{-1})	0.038	0.038	0.044	0.029
	q_{ecal} (mg/g)	3.365	3.357	3.439	1.663
	R^2	0.8703	0.8424	0.889	0.981
Pseudo- second -order	$q_{e\,exp}$ (mg/g)	4.18	4.43	4.47	4.59
	$K2$(g/mg min)	0.0244	0.0242	0.0340	0.0356
	q_{ecal} (mg/g)	0.0218	0.0258	0.1274	0.0128
	R^2	0.9994	0.9993	0.9997	0.9998

4.3.2   Adsorption Isotherm Model

In the present study, adsorption isotherms have been used to describe adsorption behavior and to eliminate the adsorption capacity of corncob, sawdust, bamboo, and BAC/GO composite on the removal of Cr (VI) ions from synthetic electroplating effluents. To construct adsorption isotherms for the adsorbent, excrement were administered by varying the initial Cr (VI) ion concentrations from 5 to 20 mg/l and keeping other parameters at optimum values.

6.2.6.1   The Langmuir Isotherm

According to Langmuir isotherm, adsorption occurs at homogeneous sets and forms a monolayer (Mekonnen et al., 2015). The Langmuir model plots were shown in Figure 4-19 which demonstrates a linear correlation between $1/q_e$ and $1/C_{e.}$. The constant values were calculated from slope $1/q_m K_L$ and intercept $1/q_m R_L$ is dimensionless factor for the important characteristics

signifies the feasibility of the adsorption process for developed ACS and composite. The detailed calculation part is additionally included in Appendix E .1, E .2, E .3, E .4 (Table 9).
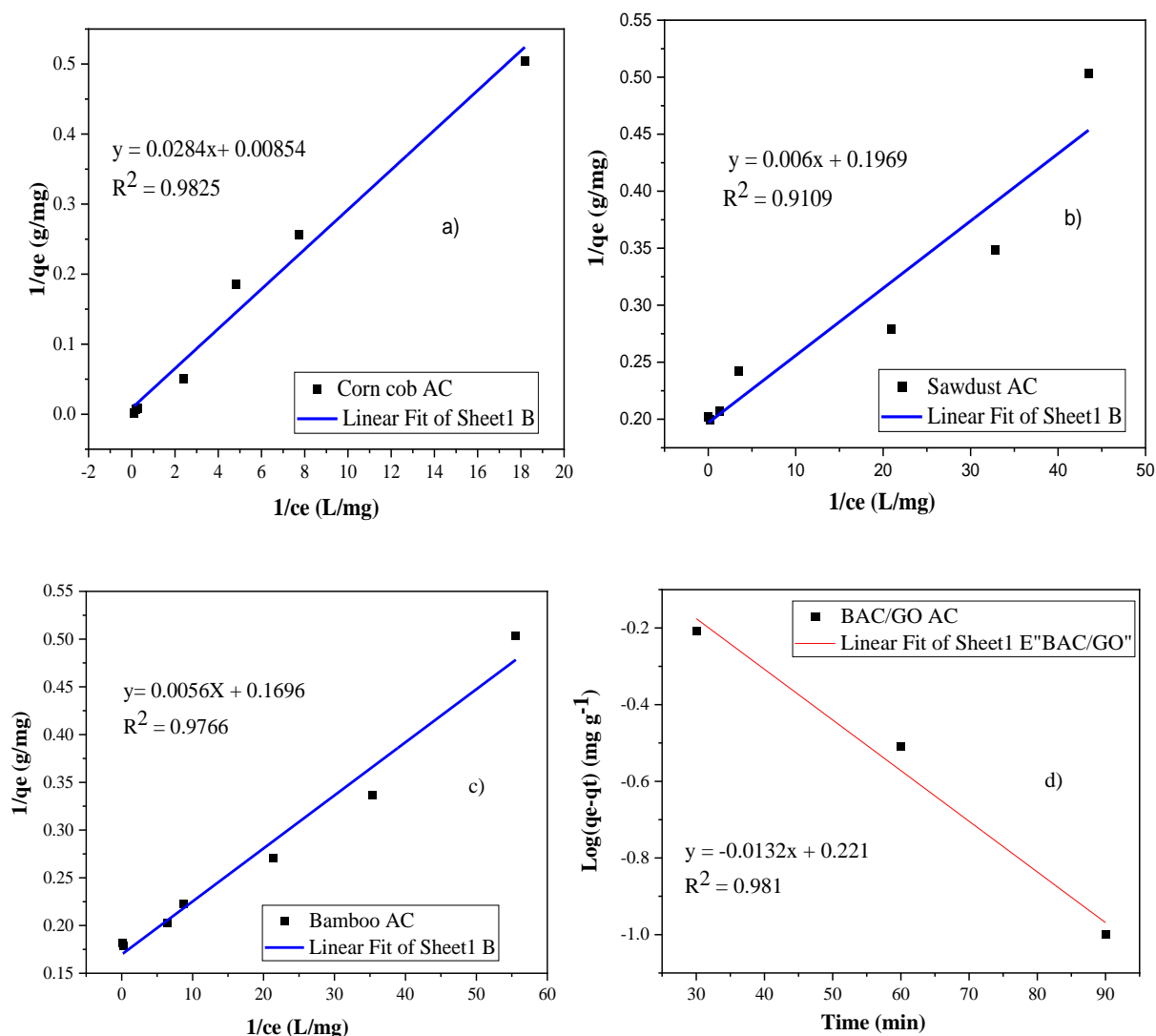
Figure 4-19: Langmuir isotherm Of a) corncob b) sawdust c) Bamboo and, d) BAC/GO composite adsorption at optimum values

As shown in Figure 4-19 the correlation coefficient obtained with the Langmuir equation was high (R^2= 0.9825 for corncob, R^2= 0.9101 for sawdust, R^2= 0.9766 for bamboo and, R^2= 0.981 for BAC/GO composite) which indicated a good fit between the parameters. The dimensionless parameter (R_L), which is measure of adsorption favorability, was found to be in range of 0.0605-0.0114 ($0 < R_L < 1$) and confirmed that Cr(VI) removal using corncob, sawdust, bamboo, and BAC/GO composite at optimum operating condition was favorable adsorption process.

4.3.2.1 Freundlich Isotherm

The relationship between equilibrium solid-liquid equilibrium phase capacity based on the multilayer adsorption properties consisting of heterogeneous surface of adsorbent was explained by Freundlich isotherm model (Mekonnen et al., 2015).

Where q_e is that the amount of Cr (VI) ion adsorbed (mg/g) at equilibrium, $k_{f\ and}$ n are Freundlich constant, $1/n$ is the heterogeneity factor which is related to the capacity and intensity of the adsorption, and C_e is the equilibrium concentration (mg/L). The slope values of isotherm between 0and 1 is measure of adsorption intensity of surface heterogeneity. The slope value gets closer to zero it becoming more heterogeneous, whereas, a value of $1/n$ below unity implies chemisorption process, $1/n$ above one is indicative of cooperative adsorption(Bayuo et al., 2019). The value of K_f (mg/g(L/mg)$^{1/n}$) and n were calculated from the intercept and slope of the plots log q_e against log C_e as show in Figure 4-20. The detailed calculation part also included in Appendix E .1, E .2, E .3, E .4 (Table 10).

The values of n (corncob =5.39, sawdust =1.77, bamboo = 5.11 and BAC/GO composite = 5.51) confirm that the BAC/GO composite has a heterogeneous surface than the ACs since the value satisfice the heterogeneity condition, $1 < n < 10$. Also a value of $1/n$ (corncob AC=0.1857, sawdust AC=0.5640, bamboo AC= 0.1957 and BAC/GO composite = 0.1816) below unity implies a chemisorption process the value of K_f where found to be (corncob AC=3.359, sawdust AC=3.664, bamboo AC= 4.211 and BAC/GO composite = 5.078) which implies that there was high uptake of Cr (VI) ions on to the adsorbent surface. It was found the coefficient of determination obtained from the Freundlich isotherm model for corncob 0.9835, for sawdust AC, 0.9733, for bamboo AC 0.9634, and for BAC/GO composite 0.9855 which is above that for the Langmuir isotherm model as given in the Table 4-8 However, the extent of conformity of Freundlich isotherm was high compared to the Langmuir adsorption isotherm, so it had been suggested heterogeneous nature.
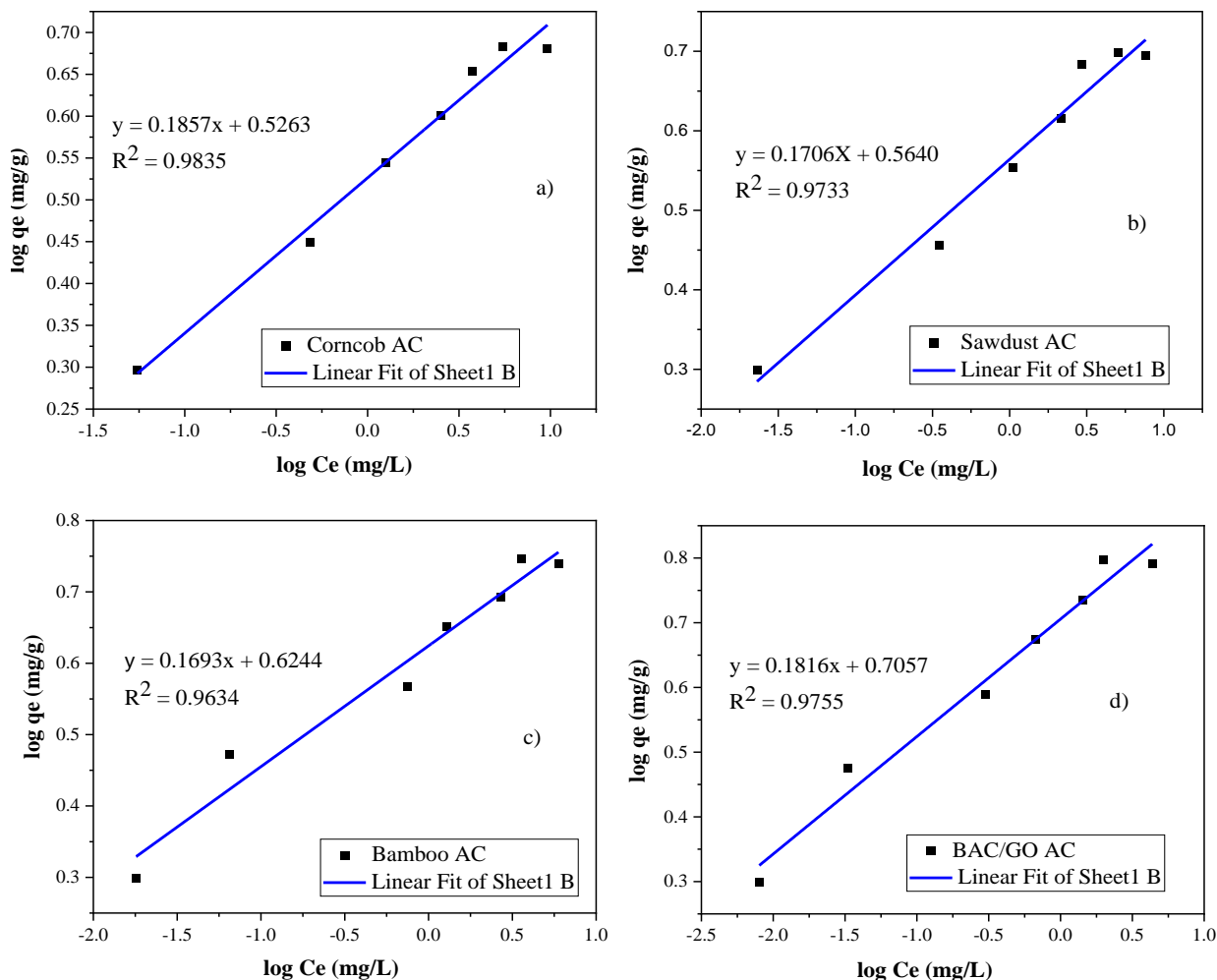
Figure 4-20: Freundlich isotherm Of a) corncob b) sawdust c) bamboo and d) BAC/GO composite for the Cr (VI) adsorption at optimum values

The higher value of coefficient of determination for Freundlich isotherm (R^2= corncob, R^2=0.9835, for sawdust, R^2= 0.9733, for bamboo, R2=0.9634, and for BAC/GO composite 0.9855) obtained indicates a good agreement between the experimental value and isotherm parameters and also confirm the multilayer adsorption Cr (VI) on to the activated carbons and composite surface.

Table 4-5: Calculated values of the various isotherm models constants and their correlation coefficient (R^2) for the adsorption of Cr (VI) on corncob, sawdust, bamboo and BAC/GO composite

Kinetic model	Parameters	Parameter value Corncob AC	Parameter value sawdust AC	Parameter value bamboo AC	Parameter value BAC/GO composite
Langmuir	q_m	117.09	5.08	5.89	6.14
	K_L	0.0301	32.817	30.318	45.250
	R^2	0.9825	0.9109	0.9766	0.981
Freundlich	q_m	0.5263	0.5640	4.211	5.078
	n	5.39	1.77	5.11	5.51
	$1/n$	0.1857	0.5640	0.1957	0.1816
	R^2	0.9835	0.9733	0.9634	0.9755

4.4 Chromium (VI) Adsorption Modeling and Model Analysis

The percentage removal of Cr (VI) was carried out using prepared BAC/GO composite using design expert. Optimization of the most significant parameters (pH, adsorbent dosage, initial hexavalent chromium concentration and contact time) for adsorption of Cr (VI) from aqueous solution involved using BBD in Response surface methodology (RSM). To investigate the optimal level and therefore the influence of every parameter in adsorption studies made with batch adsorption experiment. However, only 29 experiments during this study were performed using BBD to determine the maximum hexavalent chromium removal and optimization of those parameters with design-expert 13. The response (Adsorption efficiency Cr (VI)) and therefore the experimental runs generated BBD are presented in Table 4-6.

Table 4-6: Design matrix for Cr (VI) adsorption factors and corresponding response with actual and predicted values from the experiment

Std	Run	Factors				Chromium (VI) Adsorption efficiency (%)	
		A:pH	B:BAC/GO NAC Dosage (mg/L)	C:Cr (VI) Concentration (mg/L)	D:Contact time (min)	Actual	predicted
23	1	4.5	1	17.5	150	49.45	55.09
17	2	2	2.5	5	90	99.34	101.67
26	3	4.5	2.5	17.5	90	90.34	92.41
7	4	4.5	2.5	5	150	85.15	78.83
12	5	7	2.5	17.5	150	48.07	48.64
8	6	4.5	2.5	30	150	84.42	80.32
27	7	4.5	2.5	17.5	90	92.43	92.41
28	8	4.5	2.5	17.5	90	91.98	92.41
21	9	4.5	1	17.5	30	90.58	88.84
22	10	4.5	4	17.5	30	90.59	87.16
10	11	7	2.5	17.5	30	69.63	71.93
16	12	4.5	4	30	90	98.98	101.17
4	13	7	4	17.5	90	71.69	69.21
25	14	4.5	2.5	17.5	90	92.45	92.41
18	15	7	2.5	5	90	67.87	68.44
1	16	2	1	17.5	90	76.44	74.14
2	17	7	1	17.5	90	64.48	63.64
3	18	2	4	17.5	90	99.99	96.05
11	19	2	2.5	17.5	150	71.99	72.26
24	20	4.5	4	17.5	150	80.3	84.25
19	21	2	2.5	30	90	86.68	88.32
6	22	4.5	2.5	30	30	96.85	98.39
9	23	2	2.5	17.5	30	83.63	85.64
20	24	7	2.5	30	90	84.34	84.22
29	25	4.5	2.5	17.5	90	94.85	92.41
13	26	4.5	1	5	90	85.82	86.21
14	27	4.5	4	5	90	98.63	102.35
5	28	4.5	2.5	5	30	98.11	97.43
15	29	4.5	1	30	90	90.97	89.83

4.4.1 Model Selection for Developed Design

The estimate the regression coefficient, a multiple regression analysis was performed on the experimental data. To fit the experimental data were Linear, interactive, quadratic and cubic models to obtain the desired regression equation. Two tests were administered to determine the

adequate model. These included the Sequential model sum square and Model has selected the higher order polynomial where the additional terms were significant and the model was not aliased. Model summary statistics showed that not including a cubic model which was aliased the quadratic model was found to have maximum adjusted R- squared and the predicted R-square values. Therefore, the quadratic model was chosen for developed design. The sequential model and model summary statistics fitting for Adsorption efficiency Cr (VI) of the samples prepared are given in Appendix E 11.

4.4.2 Adequacy Check for the Developed Models

The model adequacy checking is essential to confirm whether the fitted model provides an adequate approximation of actual values or not. The model was tested for adequacy by analysis of variance (ANOVA). The ANOVA summery for Adsorption efficiency Cr (VI) was given in Table 4.8.

To determine the corresponding F value, p value, and sum of square (SS). The larger the F value, the more significant is corresponding term. However, a small p value indicates the rejection of the null hypothesis be checked while considering the significance of particular variable (Montgomery, 2013). As the value of SS increases the significance of variable also increases. It is clear from Appendix 11.1 that the model F value was 26.79 with corresponding p value of < 0.0001 and high SS (5306.40) implied that this model was significant and can appropriately explain the relationship between response and independent variables. There is only a 0.01% chance that a "Model F value" this large could occur because of noise. Values of " prob > F" less than 0.0500 identify model terms are significant. Values greater than 0.1000 identify the model terms aren't significant. In this case, A, B, D, AB, AC, BD, A^2, B^2, C^2, and D^2 factor ware significant model terms whereas C, AD, BC, and CD were insignificant to the response.

Table 4-7: Correlation coefficient (R^2) for the Adsorption efficiency Cr (VI) ion

Std. Dev.	3.76	R²	0.9640
Mean	84.00	Adjusted R²	0.9280
C.V. %	4.48	Predicted R²	0.8007
PRESS	1097.08	Adeq Precision	19.8551

Table 4-8: ANOVA results of the reduced quadratic model Adsorption efficiency Cr (VI) ions

Source	Sum of Squares	df	Mean Square	F-value	p-value	
Model	5306.19	14	379.01	26.79	< 0.0001	significant
A-PH	1045.15	1	1045.15	73.88	< 0.0001	significant
B-BAC/GO NAC Dosage	566.36	1	566.36	40.03	< 0.0001	significant
C-Cr (VI) Concentration	4.47	1	4.47	0.3156	0.5831	Non-significant
D-Contact time	1008.52	1	1008.52	71.29	< 0.0001	Significant
AB	66.75	1	66.75	4.72	0.0475	Significant
AC	212.14	1	212.14	15.00	0.0017	Significant
AD	24.60	1	24.60	1.74	0.2084	Non-significant
BC	5.76	1	5.76	0.4071	0.5337	Non-significant
BD	237.78	1	237.78	16.81	0.0011	significant
CD	0.0702	1	0.0702	0.0050	0.9448	Non-significant
A²	1085.49	1	1085.49	76.73	< 0.0001	Significant
B²	89.52	1	89.52	6.33	0.0247	Significant
C²	248.54	1	248.54	17.57	0.0009	Significant
D²	630.45	1	630.45	44.56	< 0.0001	Significant
Residual	198.06	14	14.15			
Lack of Fit	187.64	10	18.76	7.20	0.0361	not-significant
Pure Error	10.43	4	2.61			
Cor Total	5504.26	28				

The quality of the model developed was evaluated based on coefficient of correlation, R^2 value. The model developed seems to be the most effective at higher R^2 statics which is high predicted value very close to actual value for the response. During this experiment, the R^2 value was 0.9640, this indicated that 96.40% of the total variation within the Cr (VI) adsorption was attributed to the experimental variables studied. For percentage adsorption efficiency of Cr (VI) the "Pred R- squared" of 0.807 in reasonable agreement with the "Adj R- squared" of 0.9280 because the difference is less than 0.2, then the model is fitting the data and can reliably be used to interpolate. "Adeq precision" measures the signal to noise ratio and the ratio greater than 4 is desirable. Thus" Adeq precision" of 19.8551 indicates an adequate signal. This model is often

used to navigate the planning space. A low value of the variation coefficient (C.V. % = 4.48) shows the reliability of the experiments.

4.4.3 Development of Regression Model Equation

Experiments were designed to get a quadratic model containing 2^4 trials plus a star configuration and center point for experimental replicates. Therefore regression model analysis has been developed considering initial pH A), adsorbent dosage B), initial Cr (VI) concentration C), and contact time D). The BBD was used to develop a correlation between the adsorption efficiency of Cr (VI) to carefully chosen operating factors. The final empirical model in terms of coded factors for adsorption efficiency of Cr (VI) can be written in the following form in Equation (4.1).

Adsorption efficiency of hexavalent chromium = $92.41 - 9.33A + 6.87B + 0.6100C - 9.17D - 4.08AB + 7.28AC - 2.48AD - 1.20BC + 7.71BD + 0.135CD - 12.94A^2 - 3.71B^2 + 6.19C^2 - 9.86D^2$ **………** (4.2)

ANOVA technique was applied to the regression model Equation 4.6 and significance of each term is presented in Table 4-8. All terms in the regression models are not equally important, therefore eliminating those insignificant terms from the regression Equation 4.6 and refining the above empirical model equation may be simplified in terms of coded factors to:

Adsorption efficiency of hexavalent chromium= $92.41 - 9.33A + 6.87B - 9.17D - 4.08AB + 7.28AC + 7.71BD - 12.94A^2 - 3.71B^2 + 6.19C^2 - 9.86D^2$ **………………………………………….** (4.3)

4.4.4 Model Diagnosis

Model diagnostic plots are graphical summaries for case statistics. The plots of residual showed how well the model satisfies the residual assumptions of the analysis of variance. Different model diagnostic plots were plotted are the normal probability plot. To compare the distribution of the residual o normal distribution (the straight line) was using the normal probability plot of the studentized residual. As shown in Figure 4-21 a) the data are distributed normally along the center as they le reasonably close to the straight line implies that no response transformation was required which there was no apparent problem with normality. As shown in Figure 4-21 b) shows the predicted values versus the experimental values adsorption. It can be seen that the predicted values obtained from the developed model were quite close to the experimental values

(straight line) which are indicated that the model is well fitted. As shown in Figure 4-21 c) and d) shows that the plot of studentized residuals versus predicted (run number) was tasted to check for consent errors and therefore the residuals were scattered randomly around ±3.00. Although the highlighted run does differ more its predicted value than others, there's no problem for alarm because of its being within the red control limits. This was indication of a stronger fitment of the model with the experimental data
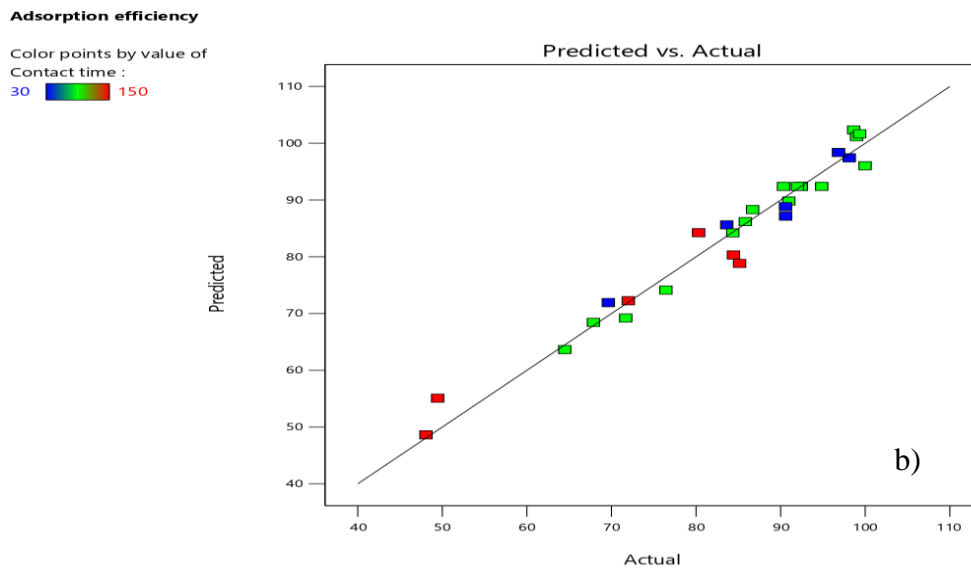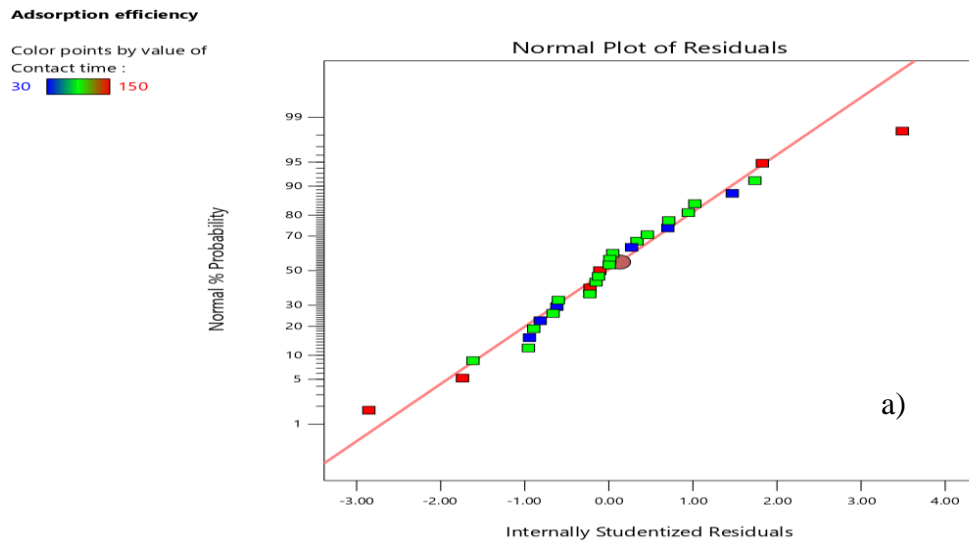
a)

b)
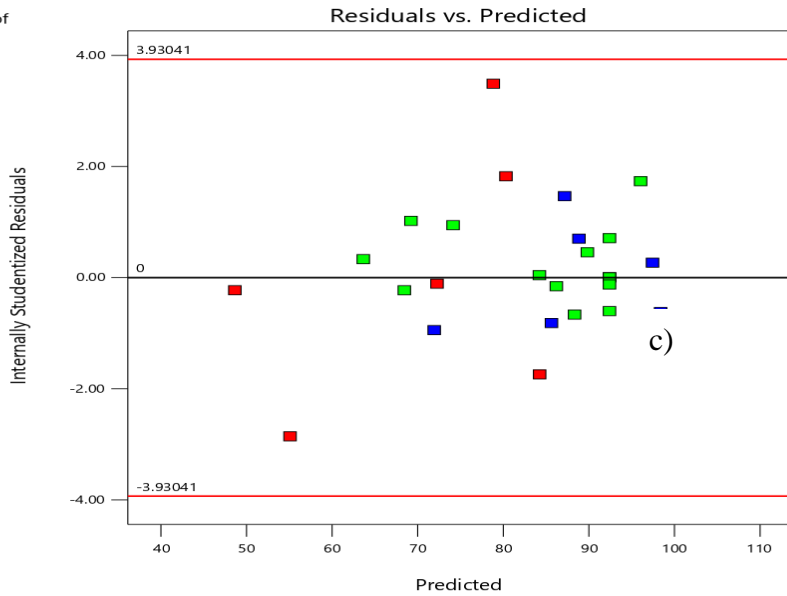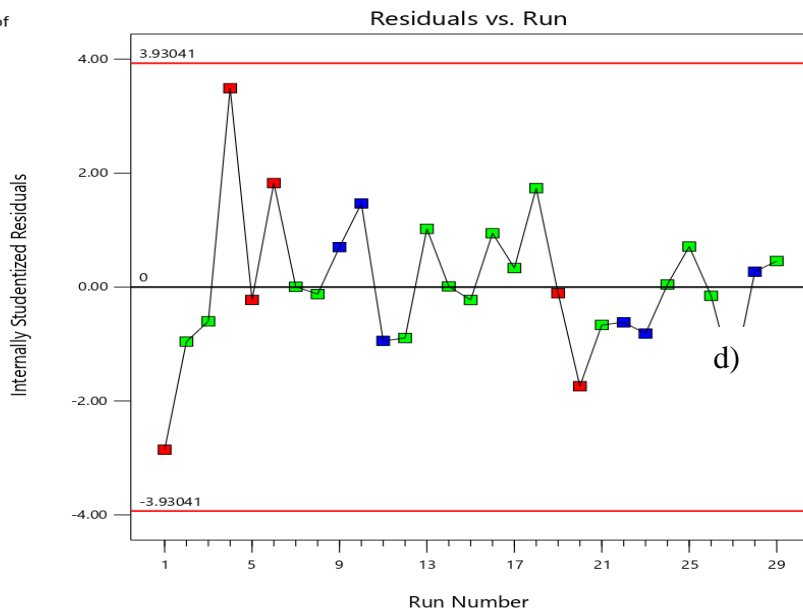
Figure 4-21: Model diagnostic plots of hexavalent chromium adsorption efficiency for the proposed model

4.4.5   Interaction Effect of Process Variables

The residual diagnosis reveals no statistical problem, so now let's generate response surface plots. For the graphical interpretation of the interactions, the use of counter and 3D plots for the regression model is highly recommended for significant effect factors on adsorption efficiency for Cr (VI) removal (Anupam et al., 2011). Such three-dimensional surface can provide useful information about the behavior of the system within the experimental design; facilitate an examination of the effects of the experimental factors on the response and the interaction effect between the independent factors.

4.4.5.1 The Combined Effect of Adsorbent Dosage and Initial pH

The combined effect of adsorbent dosage and pH on adsorption efficiency of Cr (VI) at constant initial Cr (VI) concentration (20 mg/g) and contact time (90 min) as shown in Figure 4-22. It can be seen that the maximum of Cr (VI) adsorption efficiency > 90 % was achieved at a constant initial Cr (VI) concentration (20 mg/g) and contact time (90 min). It had been observed that the adsorption efficiency of Cr (VI) ion was increased with increased adsorbent dosage and reduce the value of initial pH. The rise in percentage adsorption efficiency could also be because of the whole utilization of all active sites within the adsorbent dosage.
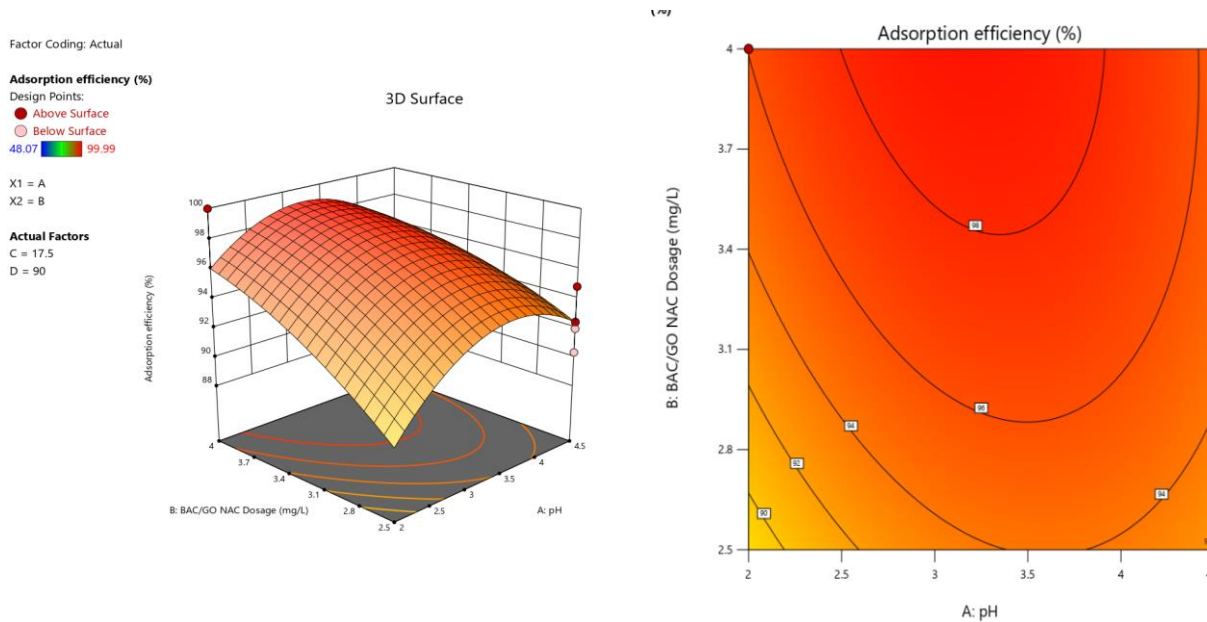
Figure 4-22: 3D response surface and counter plot of Effect of interaction plot between adsorbent dosage and initial pH on desorption efficiency of Cr (VI):

4.4.5.2 The Combined Effect of Initial Cr (VI) Concentration and pH

The interactive effect of initial Cr (VI) concentration and pH adsorption efficiency of Cr (VI) at constant adsorbent dosage (2.5 g/L) and contact time (90 min) as shown in Figure 4-23 Maximum of Cr (VI) adsorption efficiency > 95.0% was achieved at constant adsorbent dosage (2.5 g/L) and contact time (90 min). It had been observed that adsorption efficiency will be decreased due to that the rate adsorption decreased. Also adsorption efficiency will be increases with at lower initial concentration and pH at optimal value in initial stage of adsorption at lower pH and initial concentration the solid surface and the solution is large therefore the adsorption was fast. Lower Cr (VI) concentration adsorption efficiency is high due to the percentage of higher number of active site on adsorbent surface.
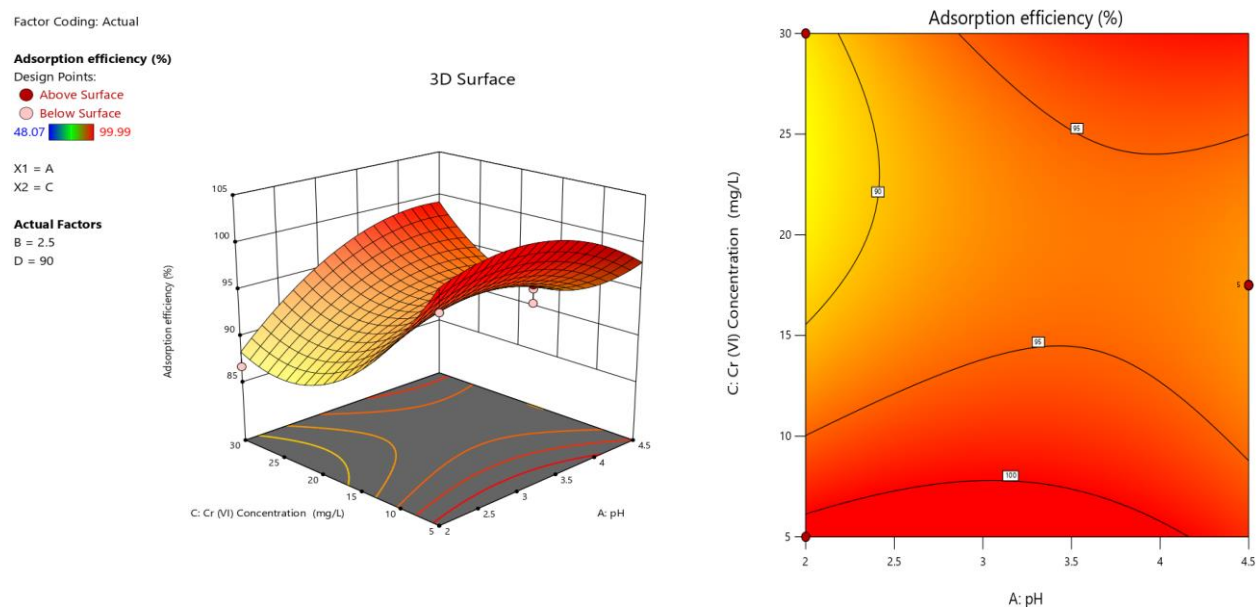
Figure 4-23: 3D response surface and counter plot of Effect of interaction between initial hexavalent chromium concentration and pH on hexavalent chromium adsorption efficiency:

4.4.5.3 The Combined Effect of Contact Time and Adsorbent Dosage

The combined effect of contact time and adsorbent dosage on adsorption efficiency of Cr (VI) at constant initial chromium concentration (20mg/g) and pH=2 as shown in Figure 4-24. The maximum adsorption efficiency of Cr (VI) > 95.0% can be achieved at constant initial pH=2 and initial chromium concentration (20mg/L). It can be seen in the figure that increases in contact time increase adsorption efficiency. According to the obtained 3D and counter model the

adsorption efficiency increased with increasing contact time and BAC/GO composite dosage until it reaches optimal points.
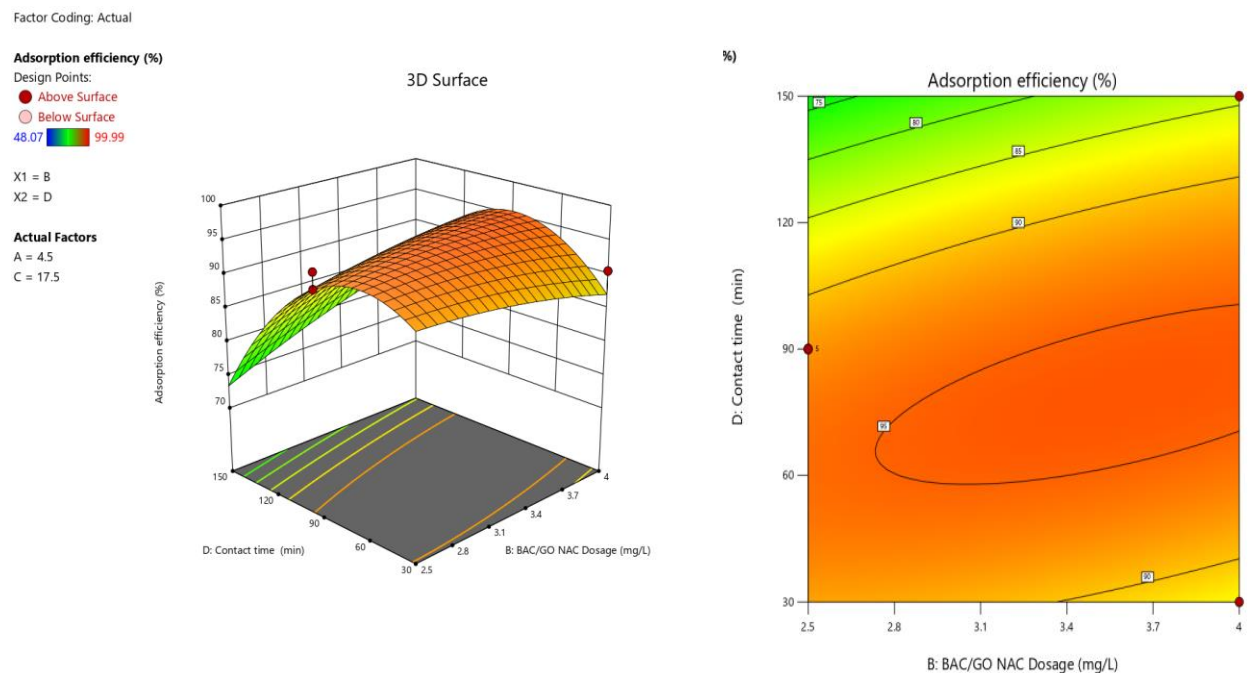
Figure 4-24: 3D response surface and counter plot of Effect of interaction between contact time and adsorbent dosage on efficiency of hexavalent chromium adsorption:

4.4.6   Optimization of Parameters for Hexavalent Chromium Adsorption

In design expert software (DOE) numerical optimization, the possible goals are maximizing, minimize, target, in range, and set to an exact value (factors only)(Fukuda et al., 2018). One of the main aims of this study was to find the optimum process parameters to maximize the adsorption efficiency of Cr (VI) from the developed mathematical model equation. Therefore, in the present study, the desired goal for each factor as well as for the response function was selected from the menu. In the optimization analysis, the quadratic model equation was optimized using quadratic programing to maximize the hexavalent chromium adsorption while the value of the four variables were (pH- minimize, initial Cr (VI) concentration in range, adsorbent dose in range and contact time- within the range) being studied. The goals of maximizing the Cr (VI) adsorption efficiency are then combined to an overall desirability function. The goals are to construct desirability indices. For any given response the desirability

values range from zero to one. A desirability value of one signifies the idea case while a zero specifies that one or more response fall outside the desirable limits.

4.4.6.1 Validation of the Developed Model

Model validation or the experimental confirmation is that the final step within the optimization process using the response surface model. To confirm the optimization results, an experiment was performed under predicted conditions by the developed model. The experimental conditions with the very best desirability (1.000) were selected to be verified. The predicted and experimental result of Cr (VI) adsorption efficiency obtained at optimum conditions are shown in Table 4-9. The optimum adsorption condition was obtained at pH = 2 adsorbent dose 2.5g/L initial Cr (VI) concentration 12.5 mg/L and contact time 90 min. It had observed that the predicted value (101.67%) obtained was good agreement with the value predicted (99.34) from the model with relatively small error between the predicted and the actual value, which was only 2.33% indicating that the regression quadratic model was valid and accurate in predicting the response. The desirability ramp for the optimization of the response and also the variables are shown in Appendix F.

Table 4-9: Optimum conditions and model validation

Process parameters				Chromium (VI) Adsorption efficiency (%)	
A:pH	BAC/GO NAC Dosage (mg/L)	Cr (VI) Concentration (mg/L)	Contact time (min)	Actual	predicted
2	2.5	12.5	90	99.34	101.67

Furthermore, the Cr (VI) adsorption efficiency of CAC, SAC, and BAC at the obtained optimum operating conditions was examined and the obtained result were 90.5%, 94.8%, and 98.95%. It confirms BAC/GO composite has higher adsorption capacity than he left pure AC the detailed callculation show in Appendix F.

Table 4-10: Comparison of the developed Composite with other Composites

No.	Composites	Cr (VI) Ad. Efficiency (%)	Reference
1	ZnO tetrapods and AC based hybrid composite	97%	DOI:10.1016/j.cej.2018.10.031
2	Hexavalent chromium adsorption from aqueous solution using carbon nano-onions (CNOs)	82%	DOI: 10.1016/j.chemosphere.2017.06.094
3	Synthesis of AC/Fe3O4 composite for removal of hexavalent chromium from aqueous solutions	88%	DOI: 10.1016/j.btre.2017.06.094

From the above table we conclude that the composite of BAC/GO which was synthesized on this research was better efficiency than the other literatures which was compared from

4.5 Hexavalent Chromium Analysis in Electroplating Effluent

The electroplating discharged effluent sample was obtained as a pH of 2.26, temperature of 26.6 ^{0}c and therefore the concentration of Cr (VI) was 10.58mg/L, which is lower than the obtained optimum Cr (VI) concentration. The concentration of Cr (VI) with the liquid effluent was above the recommended maximum limit by WHO and EPA which is 0.1 mg/L for inland surface water and 0.05 mg/L for portable water (Onchoke & Sasu, 2016). The increased concentration of Cr (VI) within the waste water sample indicates the possible environmental pollution by electroplating effluents from Armament engineering industries. The amount of Cr (VI) from electroplating effluent must be reduced to a permissible limit because of their high toxic effects before discharging to the environment. Generally, the obtained adsorption efficiency of BAC/GO composite at pH = 2, BAC/GO composite dosage = 2.5mg/L, Cr (VI) concentration = 12.5 mg/L, and contact time = 90min was 99.85%. The detail calculation was given in Appendix F. It confirms the developed composite has high adsorption capacity in both synthetic and real Cr (VI) containing solution.   Therefore, this composite is highly efficient and cost effective to treat Cr (VI) containing real wastewater.

CHAPTER FIVE

5 CONCLUSIONS AND RECOMMENDATIONS

5.2 Conclusions

In this study, the use of corncob AC, sawdust AC, bamboo AC and BAC/GO composite adsorbed for effective removal of Cr (VI) for aqueous Armament electroplating waste water had been investigated based on the batch mode of experiments. Moreover, the activated carbon synthesized from bamboo and graphene oxide composite was found to be a better adsorbent for the removal of Cr (VI) as compared to the corncob, sawdust, and pure bamboo ACs. The prepared BAC/GO composite was characterized by physicochemical analysis (moisture content, ash content, volatile matter, fixed carbon, and bulk density) the prepared of BAC/GO composite shows the great results: 9.9, 2.05, 47.15, 40.82 and 0.96 g/ml respectively. From the Advanced analytical studies (i.e UV-Vis, FTIR, XRD, TGA, BET and SEM-EDX) BAC/GO composite UV-Vis exhibits a peak at 236 nm and 279 nm so it confirms the composite have both AC and GO properties and also the FTIR indicates that the porous carbon surface retained a small number of oxygen-containing functional groups, on the other hand the XRD patterns indicates the two samples are well mixed and the AC was successfully synthesized, also TGA analysis resulted BAC/GO composite has excellent thermal stability in addition to these BET indicates that high adsorption performance of BAC/GO composite, and DLS result of BAC/GO composite shows the faster rate of adsorption kinetics during adsorption process, and finally the SEM image of BAC/GO composite was highly porous these findings suggested that the prepared BAC/GO composite was potentially high performance with better surface modification. The adsorption of Cr (VI) ion was highly influenced by pH, adsorbent dose, contact time, and initial Cr (VI) ion concentration. The maximum percentage removal of Cr (VI) was obtained at pH 2. It had been found from the kinetic studies that the adsorption rate of Cr (VI) is quicker for the initial 30 min then it decreases in the later part of adsorption. The equilibrium time BAC/GO composite for adsorption Cr (VI) was obtained at 90 min. The rise of adsorbent amount, the percentage removal of Cr (VI) increased, and also the adsorption capacity increased due to the availability of more unsaturated adsorption sites. The percentage removal decreases and also the adsorption capacity decrease with a rise in the initial Cr (VI) concentration due to saturated adsorption sites. The kinetics of Cr (VI) adsorption using BAC/GO composite as an adsorbent was explained by the second-order kinetic model which provides the higher correlation coefficient (R=0.9998).

Moreover, the equilibrium adsorption data were satisfactorily fitted with the Freundlich isotherm model which confirms the multilayer adsorption of Cr (VI) over activated carbon. The developed mathematical model for adsorption of Cr (VI) using the statistical design of experiments appears to be a great tool for prediction and understanding of interaction effects between factors. The optimal adsorption of Cr (VI) was obtained as initial pH, adsorbent dose, initial concentration of Cr (VI), and contact time and these were found to be 2, 2.5g/L, 12.5mg/L, and 90 min respectively and therefore reached in 99.63 % of adsorption of Cr (VI).

5.3 Recommendations

Activated carbon adsorbent prepared from corncob, Eucalyptus sawdust, bamboo and BAC/GO composite had been shown to have the potential in removing Cr (VI) ions from aqueous solution. The BAC/GO have high efficiency to adsorb Cr (VI) ions from aqueous solution Thus, in the future, the following works should be explored on ACs and BAC/GO composite for wastewater treatment.

- ❖ An extensive investigation should be carried out for the utilization of prepared BAC/GO composite to treat various other toxic industrial wastes such as dyes and other heavy metals present in wastewater should be undertaken.
- ❖ Based on the current work, pilot studies should be considered for future research through column studies using industrial wastewater containing chromium ions and other metals to investigate the effect of competitive adsorption on chromium and other metals.
- ❖ The saturated adsorbent which contains Cr (VI) is not safe for disposal due to desorption of Cr (VI) and regeneration of spent BAC/GO composite which is essential to evaluate the efficiency of the process which needs immediate attention.
- ❖ The ratio of BAC/GO composite takes into account using ratio optimization method in the future of the study.
- ❖ After adsorption XRD and FTIR analysis should be better to carried out for future study.

REFERENCES

Abas, S. N. A., Ismail, M. H. S., Siajam, S. I., & Kamal, M. L. (2015). Development of novel adsorbent-mangrove-alginate composite bead (MACB) for removal of Pb(II) from aqueous solution. *Journal of the Taiwan Institute of Chemical Engineers*, *50*, 182–189. https://doi.org/10.1016/j.jtice.2014.11.013

Abbas, M. N. (2014). Application of Used Tea Leaves for Multi Functions Mohammed Nsaif Abbas - Application of Used Tea Leaves for Multi Functions. *B+) European Academic Research*, *9*(7), 8660–8690.

Ads-, U. O. P., Sieves, M., Catteruccia, F., Nolan, T., & Blass, C. (2000). should read UOP ADS-34; and (ii) in. *This Paper Was Presented at the National Academy of Sciences Colloquium '"Geology, Mineralogy, and Human Welfare,"' Held November 8–9, 1998 at the Arnold and Mabel Beckman Center in Irvine, CA. Synthetic*, *ii*.

Ahalya, N., Kanamadi, R. D., & Ramachandra, T. V. (2010). Removal of hexavalent chromium using coffee husk. *International Journal of Environment and Pollution*, *43*(1–3), 106–116. https://doi.org/10.1504/IJEP.2010.035917

Al-Degs, Y. S., El-Barghouthi, M. I., El-Sheikh, A. H., & Walker, G. M. (2008). Effect of solution pH, ionic strength, and temperature on adsorption behavior of reactive dyes on activated carbon. *Dyes and Pigments*, *77*(1), 16–23. https://doi.org/10.1016/j.dyepig.2007.03.001

Albadarin, A. B., Mangwandi, C., Al-Muhtaseb, A. H., Walker, G. M., Allen, S. J., & Ahmad, M. N. M. (2012). Kinetic and thermodynamics of chromium ions adsorption onto low-cost dolomite adsorbent. *Chemical Engineering Journal*, *179*, 193–202. https://doi.org/10.1016/j.cej.2011.10.080

ALOthman, Z. A., Naushad, M., & Ali, R. (2013). Kinetic, equilibrium isotherm and thermodynamic studies of Cr(VI) adsorption onto low-cost adsorbent developed from peanut shell activated with phosphoric acid. *Environmental Science and Pollution Research*, *20*(5), 3351–3365. https://doi.org/10.1007/s11356-012-1259-4

Alvarez-galvan, Y., & Minofar, B. (2022). *Adsorption of Hexavalent Chromium Using Activated Carbon Produced from Sargassum ssp .: Comparison between Lab*.

Álvarez, P., Blanco, C., & Granda, M. (2007). The adsorption of chromium (VI) from industrial wastewater by acid and base-activated lignocellulosic residues. *Journal of Hazardous Materials*, *144*(1–2), 400–405. https://doi.org/10.1016/j.jhazmat.2006.10.052

Amendola, V., & Meneghetti, M. (2009). Size evaluation of gold nanoparticles by UV-vis spectroscopy. *Journal of Physical Chemistry C*, *113*(11), 4277–4285. https://doi.org/10.1021/jp8082425

Anah, L., & Astrini, N. (2017). Influence of pH on Cr(VI) ions removal from aqueous solutions using carboxymethyl cellulose-based hydrogel as adsorbent. *IOP Conference Series: Earth and Environmental Science*, *60*(1). https://doi.org/10.1088/1755-1315/60/1/012010

Antony, J., Chou, T., & Ghosh, S. (2003). Training for design of experiments. *Work Study*, *52*(7), 341–346. https://doi.org/10.1108/00438020310502642

Anupam, K., Dutta, S., Bhattacharjee, C., & Datta, S. (2011). Adsorptive removal of chromium (VI) from aqueous solution over powdered activated carbon: Optimisation through response surface methodology. *Chemical Engineering Journal*, *173*(1), 135–143. https://doi.org/10.1016/j.cej.2011.07.049

Aragaw, T. A. (2016). Proximate analysis of cane bagasse and synthesizing activated carbon: emphasis on material balance. *Journal of Environmental Treatment Techniques*, *4*(4), 102–110.

Arora, R. (2019). Adsorption of heavy metals-a review. *Materials Today: Proceedings*, *18*(1), 4745–4750. https://doi.org/10.1016/j.matpr.2019.07.462

Audino, M. J., & Laboratories, U. S. A. R. (2006). *Use of Electroplated Chromium in Gun Barrels*. *May*.

Aurich, A., Hofmann, J., Oltrogge, R., Wecks, M., Gläser, R., Blömer, L., Mauersberger, S., Müller, R. A., Sicker, D., & Giannis, A. (2017). Improved Isolation of Microbiologically

Produced (2R,3S)-Isocitric Acid by Adsorption on Activated Carbon and Recovery with Methanol. *Organic Process Research and Development*, *21*(6), 866–870. https://doi.org/10.1021/acs.oprd.7b00090

Aworanti, A., & Agarry, S. E. (2017). Kinetics, Isothermal and Thermodynamic Modelling Studies of Hexavalent Chromium Ions Adsorption from Simulated Wastewater onto Parkia biglobosa -Sawdust Derived Acid-Steam Activated. *Applied Journal of Environmental Engineering Science*, *3*(1), 58–76.

Ayawei, N., Ebelegi, A. N., & Wankasi, D. (2017). Modelling and Interpretation of Adsorption Isotherms. *Journal of Chemistry*, *2017*. https://doi.org/10.1155/2017/3039817

Ayub, S., Siddique, A. A., Khursheed, M. S., Zarei, A., Alam, I., Asgari, E., & Changani, F. (2020). Removal of heavy metals (Cr, cu, and zn) from electroplating wastewater by electrocoagulation and adsorption processes. *Desalination and Water Treatment*, *179*, 263–271. https://doi.org/10.5004/dwt.2020.25010

Babick, F. (2019). Dynamic light scattering (DLS). In *Characterization of Nanoparticles: Measurement Processes for Nanoparticles*. Elsevier Inc. https://doi.org/10.1016/B978-0-12-814182-3.00010-9

Barbusinski, K., Kalemba, K., Kasperczyk, D., Urbaniec, K., & Kozik, V. (2017). Biological methods for odor treatment – A review. *Journal of Cleaner Production*, *152*, 223–241. https://doi.org/10.1016/j.jclepro.2017.03.093

Battas, A., El Gaidoumi, A., Ksakas, A., & Kherbeche, A. (2019). Adsorption study for the removal of nitrate from water using local clay. *Scientific World Journal*, *2019*. https://doi.org/10.1155/2019/9529618

Bayuo, J., Pelig-Ba, K. B., & Abukari, M. A. (2019). Adsorptive removal of chromium(VI) from aqueous solution unto groundnut shell. *Applied Water Science*, *9*(4), 1–11. https://doi.org/10.1007/s13201-019-0987-8

Belova, L., Vialkova, E. of electroplating wastewatersna, Glushchenko, E., Burdeev, V., & Parfenov, Y. (2020). Treatment of electroplating wastewaters. *E3S Web of Conferences*,

203, 1–7. https://doi.org/10.1051/e3sconf/202020303009

Ben-Mansour, R., Habib, M. A., Bamidele, O. E., Basha, M., Qasem, N. A. A., Peedikakkal, A., Laoui, T., & Ali, M. (2016). Carbon capture by physical adsorption: Materials, experimental investigations and numerical modeling and simulations - A review. *Applied Energy*, *161*, 225–255. https://doi.org/10.1016/j.apenergy.2015.10.011

Bernal, V., Giraldo, L., & Moreno-Piraján, J. (2018). Physicochemical Properties of Activated Carbon: Their Effect on the Adsorption of Pharmaceutical Compounds and Adsorbate–Adsorbent Interactions. *C*, *4*(4), 62. https://doi.org/10.3390/c4040062

BhattacharyyaDesign of an efficient and selective adsorbent of cationic dye through activated carbon - graphene oxide nanocomposite: Study on mechanism and synergy, A., Ghorai, S., Rana, D., Roy, I., Sarkar, G., Saha, N. R., Orasugh, J. T., De, S., Sadhukhan, S., & Chattopadhyay, D. (2021). Design of an efficient and selective adsorbent of cationic dye through activated carbon - graphene oxide nanocomposite: Study on mechanism and synergy. *Materials Chemistry and Physics*, *260*, 124090. https://doi.org/10.1016/j.matchemphys.2020.124090

Buckner, C. A., Lafrenie, R. M., Dénommée, J. A., Caswell, J. M., Want, D. A., Gan, G. G., Leong, Y. C., Bee, P. C., Chin, E., Teh, A. K. H., Picco, S., Villegas, L., Tonelli, F., Merlo, M., Rigau, J., Diaz, D., Masuelli, M., Korrapati, S., Kurra, P., … Mathijssen, R. H. J. (2016). We are IntechOpen , the world ' s leading publisher of Open Access books Built by scientists , for scientists TOP 1 %. *Intech*, *11*(tourism), 13. https://www.intechopen.com/books/advanced-biometric-technologies/liveness-detection-in-biometrics

Chen, J., Hong, X., Zhao, Y., & Zhang, Q. (2014). Removal of hexavalent chromium from aqueous solution using exfoliated polyaniline/montmorillonite composite. *Water Science and Technology*, *70*(4), 678–684. https://doi.org/10.2166/wst.2014.277

Chen, X. (2015). Modeling of experimental adsorption isotherm data. *Information (Switzerland)*, *6*(1), 14–22. https://doi.org/10.3390/info6010014

Ćosović, B., Vojvodić, V., Bošković, N., Plavšić, M., & Lee, C. (2010). substances (melanoidins) by chemical composition and adsorption measurements. Organic Geochemistry, 41(2), 200–205. https://doi.org/10.1016/j.orggeochem.2009.10.002n and adsorption measurementsĆosović, B., Vojvodić, V., Bošković, N., Plavšić, M., & Lee, C. *Substances (Melanoidins) by Chemical Composition and Adsorption Measurements. Organic Geochemistry, 41(2), 200–205. Https://Doi.Org/10.1016/j.Orggeochem.2009.10.002n and Adsorption Measurements*, *41*(2), 200–205. https://doi.org/10.1016/j.orggeochem.2009.10.002

Crini, G., & Lichtfouse, E. (2019). Advantages and disadvantages of techniques used for wastewater treatment. *Environmental Chemistry Letters*, *17*(1), 145–155. https://doi.org/10.1007/s10311-018-0785-9

De Gisi, S., Lofrano, G., Grassi, M., & Notarnicola, M. (2016). Characteristics and adsorption capacities of low-cost sorbents for wastewater treatment: A review. *Sustainable Materials and Technologies*, *9*, 10–40. https://doi.org/10.1016/j.susmat.2016.06.002

Dermentzis, K., Christoforidis, A., Valsamidou, E., Lazaridou, A., & Kokkinos, N. (2011). Removal of hexavalent chromium from electroplating wastewater by electrocoagulation with iron electrodes. *Global Nest Journal*, *13*(4), 412–418. https://doi.org/10.30955/gnj.000770

Dhal, B., Thatoi, H. N., Das, N. N., & Pandey, B. D. (2013). Chemical and microbial remediation of hexavalent chromium from contaminated soil and mining/metallurgical solid waste: A review. *Journal of Hazardous Materials*, *250–251*(Vi), 272–291. https://doi.org/10.1016/j.jhazmat.2013.01.048

Edi, S. F., Ismadji, S., & Ayucitra, A. (2015). *SPRINGER BRIEFS IN MOLECULAR SCIENCE Clay Materials for Environmental Remediation*.

Elystia, S., Edward, H. S., & Putri, A. E. (2020). Removal of Chromium (VI) and Chromium (III) by using Chlorella sp Immobilized at Electroplating Wastewater. *IOP Conference Series: Earth and Environmental Science*, *515*(1). https://doi.org/10.1088/1755-1315/515/1/012078

Feng, M., & Feng, H. (2013). Effect of reducing agent on the chemical reduction of graphene oxides. *Journal of Nanoscience and Nanotechnology*, *13*(2), 937–941. https://doi.org/10.1166/jnn.2013.6005

Fukuda, I. M., Pinto, C. F. F., Moreira, C. D. S., Saviano, A. M., & Lourenço, F. R. (2018). Design of experiments (DoE) applied to pharmaceutical and analytical quality by design (QbD). *Brazilian Journal of Pharmaceutical Sciences*, *54*(Special Issue), 1–16. https://doi.org/10.1590/s2175-97902018000001006

Gadipelli, S., & Guo, Z. X. (2015). Graphene-based materials: Synthesis and gas sorption, storage and separation. *Progress in Materials Science*, *69*, 1–60. https://doi.org/10.1016/j.pmatsci.2014.10.004

Ghorbani-Khosrowshahi, S., & Behnajady, M. A. (2016). Chromium(VI) adsorption from aqueous solution by prepared biochar from Onopordom Heteracanthom. *International Journal of Environmental Science and Technology*, *13*(7), 1803–1814. https://doi.org/10.1007/s13762-016-0978-3

Gin, W. A., Jimoh, A., Abdulkareem, A. S., & Giwa, A. (2014). *Kinetics and Isotherm Study of Heavy Metals Removal from Electroplating Waste Water Usingcassava Peel Activated Carbon*. *3*(1), 25–34.

Gottipati, R. (2012). Preparation and Characterization of Microporous Activated Carbon from Biomass and its Application in the Removal of Chromium (VI) from Aqueous Phase Department of Chemical Engineering. *Department of Chemical Engineering National Institute of Technology, Rourkela Odisha, India*, *January*, 1–242.

Group, F. (2019). Chromium: Metabolism and Toxicity. In *Chromium: Metabolism and Toxicity*. https://doi.org/10.1201/9780429261015

Gunatilake, S. K. (2015). *Methods of Removing Heavy Metals from Industrial Wastewater*. *1*(1), 12–18.

Guo, X., Liu, A., Lu, J., Niu, X., Jiang, M., Ma, Y., Liu, X., & Li, M. (2020). Adsorption mechanism of hexavalent chromium on biochar: Kinetic, thermodynamic, and

characterization studies. *ACS Omega*, *5*(42), 27323–27331. https://doi.org/10.1021/acsomega.0c03652

Gupta, V. K., Ali, I., Saleh, T. A., Siddiqui, M. N., & Agarwal, S. (2013). Chromium removal from water by activated carbon developed from waste rubber tires. *Environmental Science and Pollution Research*, *20*(3), 1261–1268. https://doi.org/10.1007/s11356-012-0950-9

Hua, M., Zhang, S., Pan, B., Zhang, W., Lv, L., & Zhang, Q. (2012). Heavy metal removal from water/wastewater by nanosized metal oxides: A review. *Journal of Hazardous Materials*, *211–212*, 317–331. https://doi.org/10.1016/j.jhazmat.2011.10.016

Iram, M., Guo, C., Guan, Y., Ishfaq, A., & Liu, H. (2010). Adsorption and magnetic removal of neutral red dye from aqueous solution using Fe3O4 hollow nanospheres. *Journal of Hazardous Materials*, *181*(1–3), 1039–1050. https://doi.org/10.1016/j.jhazmat.2010.05.119

Jamiu Mosebolatan Jabar. (2016). Effect of chemical modification on physicochemical properties of coir, empty fruit bunch and palm kernel fibres. *Applied Tropical Agriculture*, *21*(1), 153–158.

Jia, Y. F., Xiao, B., & Thomas, K. M. (2002). Adsorption of metal ions on nitrogen surface functional groups in activated carbons. *Langmuir*, *18*(2), 470–478. https://doi.org/10.1021/la011161z

Kadirvelu, K., Thamaraiselvi, K., & Namasivayam, C. (2001). Removal of heavy metals from industrial wastewaters by adsorption onto activated carbon prepared from an agricultural solid waste. *Bioresource Technology*, *76*(1), 63–65. https://doi.org/10.1016/S0960-8524(00)00072-9

Kajjumba, G. W., Aydın, S., & Güneysu, S. (2018). Adsorption isotherms and kinetics of vanadium by shale and coal waste. *Adsorption Science and Technology*, *36*(3–4), 936–952. https://doi.org/10.1177/0263617417733586

Kalavathy, M. H., Karthikeyan, T., Rajgopal, S., & Miranda, L. R. (2005). Kinetic and isotherm studies of Cu(II) adsorption onto H3PO 4-activated rubber wood sawdust. *Journal of Colloid and Interface Science*, *292*(2), 354–362. https://doi.org/10.1016/j.jcis.2005.05.087

Kerur, S. S., Bandekar, S., Hanagadakar, M. S., Nandi, S. S., Ratnamala, G. M., & Hegde, P. G. (2020). Removal of hexavalent Chromium-Industry treated water and Wastewater: A review. *Materials Today: Proceedings*, *42*, 1112–1121. https://doi.org/10.1016/j.matpr.2020.12.492

Khenblouche, A., Bechki, D., Gouamid, M., Charradi, K., Segni, L., Hadjadj, M., & Boughali, S. (2019). Extraction and characterization of cellulose microfibers from Retama raetam stems. *Polimeros*, *29*(1), 1–8. https://doi.org/10.1590/0104-1428.05218

Khorasgani, F. C. (2013). Removal of Cd (II) and Cr (VI) from Electroplating Wastewater by Coconut Shell. *International Journal of Environmental Engineering and Management*, *4*(4), 273–280. http://www.ripublication.com/ijeem.htm

Konstantinos, D., Achilleas, C., & Evgenia, V. (2011). Removal of nickel, copper, zinc and chromium from synthetic and industrial wastewater by electrocoagulation. *International Journal of Environmental Sciences*, *1*(5), 697–710. http://www.ipublishing.co.in/jesvol1no12010/EIJES2026.pdf

Koo, W. K., Gani, N. A., Shamsuddin, M. S., Subki, N. S., & Sulaiman, M. A. (2015). Comparison of wastewater treatment using activated carbon from bamboo and oil palm: an overview. *Journal of Tropical Resources and Sustainable Science*, *3*(1), 54–60. https://doi.org/10.47253/jtrss.v3i1.689

Kortlever, R., Shen, J., Schouten, K. J. P., Calle-Vallejo, F., & Koper, M. T. M. (2015). Catalysts and Reaction Pathways for the Electrochemical Reduction of Carbon Dioxide. *Journal of Physical Chemistry Letters*, *6*(20), 4073–4082. https://doi.org/10.1021/acs.jpclett.5b01559

Kyotani, T. (2003). Porous Carbon. *Carbon Alloys: Novel Concepts to Develop Carbon Science and Technology*, *28*(April), 109–127. https://doi.org/10.1016/B978-008044163-4/50007-3

Labied, R., Benturki, O., Eddine Hamitouche, A. Y., & Donnot, A. (2018). Adsorption of hexavalent chromium by activated carbon obtained from a waste lignocellulosic material (Ziziphus jujuba cores): Kinetic, equilibrium, and thermodynamic study. *Adsorption Science and Technology*, *36*(3–4), 1066–1099. https://doi.org/10.1177/0263617417750739

Lazic, V., Fantoni, R., Colao, F., Santagata, A., Morone, A., & Spizzichino, V. (2004). Quantitative laser induced breakdown spectroscopy analysis of ancient marbles and corrections for the variability of plasma parameters and of ablation rate. *Journal of Analytical Atomic Spectrometry*, *19*(4), 429–436. https://doi.org/10.1039/b315606k

Li, S., Hu, Z., Xie, S., Liu, H., & Liu, J. (2018). Removal of Cr(VI) from electroplating industry effluent via electrochemical reduction. *International Journal of Electrochemical Science*, *13*(1), 655–663. https://doi.org/10.20964/2018.01.83

Li, X. (2004). Physical, chemical, and mechanical properties of bamboo and its utilization potential for fiberboard manufacturing. *Agriculture and Mechanical College*, *Master of*, 76.

Liu, F., Wang, C., Sui, X., Riaz, M. A., Xu, M., Wei, L., & Chen, Y. (2019). Synthesis of graphene materials by electrochemical exfoliation: Recent progress and future potential. *Carbon Energy*, *1*(2), 173–199. https://doi.org/10.1002/cey2.14

Liu, Q. S., Zheng, T., Wang, P., & Guo, L. (2010). Preparation and characterization of activated carbon from bamboo by microwave-induced phosphoric acid activation. *Industrial Crops and Products*, *31*(2), 233–238. https://doi.org/10.1016/j.indcrop.2009.10.011

Liu, Q., Zhou, Y., Lu, J., & Zhou, Y. (2020). Novel cyclodextrin-based adsorbents for removing pollutants from wastewater: A critical review. *Chemosphere*, *241*. https://doi.org/10.1016/j.chemosphere.2019.125043

M. Gopala Krishnamurthy, D. Dinakar, I. M. Chhabra, P. Kishore, N. V. N. R. P. and K. C. Das. (2019). *Engineering Vibration, Communication and Information Processing* (Vol. 478). Springer Singapore. https://doi.org/10.1007/978-981-13-1642-5

Macedo, J. de S., da Costa Júnior, N. B., Almeida, L. E., Vieira, E. F. da S., Cestari, A. R., Gimenez, I. de F., Villarreal Carreño, N. L., & Barreto, L. S. (2006). Kinetic and calorimetric study of the adsorption of dyes on mesoporous activated carbon prepared from coconut coir dust. *Journal of Colloid and Interface Science*, *298*(2), 515–522. https://doi.org/10.1016/j.jcis.2006.01.021

Mahanim, S. M. A., Wan Asma, I., Rafidah, J., Puad, E., & Shaharuddin, H. (2011). Production

of activated carbon from industrial bamboo wastes. *Journal of Tropical Forest Science*, *23*(4), 417–424.

Malik, D. S., Jain, C. K., Yadav, A. K., Vishwavidyalaya, G. K., Division, E. H., & Vishwavidyalaya, G. K. (2015). Preparation and Characterization of Plant Based Low Cost. *Journal of Global Biosciences*, *4*(1), 1824–1829.

Mazumder, D., Ghosh, D., & Bandyopadhyay, P. (2011). Treatment of Electroplating Wastewater by Adsorption Technique. *International Journal of Civil and Environmental Engineering*, *3*(2), 101–110.

Mekonnen, E., Yitbarek, M., & Soreta, T. R. (2015). Kinetic and thermodynamic studies of the adsorption of Cr(VI) onto some selected local adsorbents. *South African Journal of Chemistry*, *68*, 45–52. https://doi.org/10.17159/0379-4350/2015/v68a7

Menkiti, M. C., Ejikeme, P. M., Onukwuli, O. D., Aneke, M. C., Ugonabo, V. I., & Menkiti, N. U. (2015). Adsorptive treatment of brewery waste water using activated carbon prepared from Afzelia africana wood sawdust . *Journal of the Chinese Advanced Materials Society*, *3*(3), 231–255. https://doi.org/10.1080/22243682.2015.1017607

Mohan, D., & Pittman, C. U. (2006). Activated carbons and low cost adsorbents for remediation of tri- and hexavalent chromium from water. *Journal of Hazardous Materials*, *137*(2), 762–811. https://doi.org/10.1016/j.jhazmat.2006.06.060

Montgomery, D. C. (2013). Design and Analysis of Experiments Eighth Edition. Arizona State University. In *Copyright* (Vol. 2009, Issue 2005).

Mopoung, S., & Dejang, N. (2021). Activated carbon preparation from eucalyptus wood chips using continuous carbonization–steam activation process in a batch intermittent rotary kiln. *Scientific Reports*, *11*(1), 1–9. https://doi.org/10.1038/s41598-021-93249-x

Nadler, G. (2004). R Eflections on. *Journal of Management*, *13*(Fall 2008), 239–246.

Nagar, V. V. (2019). *REMOVAL OF CHROMIUM (VI) FROM ELECTROPLATING WASTEWATER USING TEA WASTE*. *6*(4), 559–564.

Natrayan, L., Kumar, P. V. A., Dhanraj, J. A., Kaliappan, S., Sivakumar, N. S., Patil, P. P., Sekar, S., & Paramasivam, P. (2022). *Synthesis and Analysis of Impregnation on Activated Carbon in Multiwalled Carbon Nanotube for Cu Adsorption from Wastewater*. *2022*.

Njoku, V. O., & Hameed, B. H. (2011). Preparation and characterization of activated carbon from corncob by chemical activation with H3PO4 for 2,4-dichlorophenoxyacetic acid adsorption. *Chemical Engineering Journal*, *173*(2), 391–399. https://doi.org/10.1016/j.cej.2011.07.075

Nourbakhsh, M., Saǧ, Y., Özer, D., Aksu, Z., Kutsal, T., & Çaǧlar, A. (1994). A comparative study of various biosorbents for removal of chromium(VI) ions from industrial waste waters. *Process Biochemistry*, *29*(1), 1–5. https://doi.org/10.1016/0032-9592(94)80052-9

Olak-Kucharczyk, M., Szczepańska, G., Kudzin, M. H., & Pisarek, M. (2020). The photocatalytical properties of RgO/TiO2 coated fabrics. *Coatings*, *10*(11), 1–15. https://doi.org/10.3390/coatings10111041

Olatunji, M. A., Khandaker, M. U., Mahmud, H. N. M. E., & Amin, Y. M. (2015). Influence of adsorption parameters on cesium uptake from aqueous solutions- a brief review. *RSC Advances*, *5*(88), 71658–71683. https://doi.org/10.1039/c5ra10598f

Onchoke, K. K., & Sasu, S. A. (2016). Determination of Hexavalent Chromium (Cr(VI)) Concentrations via Ion Chromatography and UV-Vis Spectrophotometry in Samples Collected from Nacogdoches Wastewater Treatment Plant, East Texas (USA). *Advances in Environmental Chemistry*, *2016*(Iii), 1–10. https://doi.org/10.1155/2016/3468635

Patnukao, P., Kongsuwan, A., & Pavasant, P. (2008). Batch studies of adsorption of copper and lead on activated carbon from Eucalyptus camaldulensis Dehn. bark. *Journal of Environmental Sciences*, *20*(9), 1028–1034. https://doi.org/10.1016/S1001-0742(08)62145-2

Qiu, H., Lv, L., Pan, B. C., Zhang, Q. J., Zhang, W. M., & Zhang, Q. X. (2009). Critical review in adsorption kinetic models. *Journal of Zhejiang University: Science A*, *10*(5), 716–724. https://doi.org/10.1631/jzus.A0820524

Rahman, M. L., Wong, Z. J., Sarjadi, M. S., Soloi, S., Arshad, S. E., Bidin, K., & Musta, B. (2021). Heavy metals removal from electroplating wastewater by waste fiber-based poly(Amidoxime) ligand. *Water (Switzerland)*, *13*(9), 1–20. https://doi.org/10.3390/w13091260

Rahman, M. M., Muttakin, M., Pal, A., Shafiullah, A. Z., & Saha, B. B. (2019). A statistical approach to determine optimal models for IUPAC-classified adsorption isotherms. *Energies*, *12*(23). https://doi.org/10.3390/en12234565

Rashid, R., Shafiq, I., Akhter, P., Iqbal, M. J., & Hussain, M. (2021). A state-of-the-art review on wastewater treatment techniques: the effectiveness of adsorption method. *Environmental Science and Pollution Research*, *28*(8), 9050–9066. https://doi.org/10.1007/s11356-021-12395-x

Rodrigo Garcia Motta, Angélica Link, Viviane Aparecida Bussolaro, G. de N. J., Palmeira, G., Riet-Correa, F., Moojen, V., Roehe, P. M., Weiblen, R., Batista, J. S., Bezerra, F. S. B., Lira, R. A., Carvalho, J. R. G., Neto, A. M. R., Petri, A. A., Teixeira, M. M. G., Molossi, F. A., de Cecco, B. S., Henker, L. C., Vargas, T. P., Lorenzett, M. P., Bianchi, M. V., … Alfieri, A. A. (2021). No 主観的健康感を中心とした在宅高齢者における 健康関連指標に関する共分散構造分析Title. *Pesquisa Veterinaria Brasileira*, *26*(2), 173–180. http://www.ufrgs.br/actavet/31-1/artigo552.pdf

Sanchez-Hachair, A., & Hofmann, A. (2018). Hexavalent chromium quantification in solution: Comparing direct UV–visible spectrometry with 1,5-diphenylcarbazide colorimetry. *Comptes Rendus Chimie*, *21*(9), 890–896. https://doi.org/10.1016/j.crci.2018.05.002

Sessarego, S. (2017). *Phosphonium-Enhanced Chitosan for Hexavalent Chromium Adsorption in Wastewater Treatment*. https://doi.org/10.11575/PRISM/27336

Seyoum, A., & Asso, L. (2015). *ADDIS ABABA UNIVERSITY SCHOOL OF GRADUATE STUDIES CENTER FOR ENVIRONMENTAL SCIENCE Heavy Metals Removal from Electroplating Waste Water Using Activated Carbon of Coffee Husk By : Temesgen Aragaw A thesis Submitted to Center for Environmental Science Prese*.

Sharma, P., Vyas, S., & Patel, A. (2004). Heteropolyacid supported onto neutral alumina: Characterization and esterification of 1° and 2° alcohol. *Journal of Molecular Catalysis A: Chemical*, *214*(2), 281–286. https://doi.org/10.1016/j.molcata.2003.12.038

Shojaeiarani, J., Bajwa, D. S., & Chanda, S. (2021). Cellulose nanocrystal based composites: A review. *Composites Part C: Open Access*, *5*(May), 100164. https://doi.org/10.1016/j.jcomc.2021.100164

Shrestha, D., Gyawali, G., & Rajbhandari, A. (2018). Preparation and Characterization of Activated Carbon from Waste Sawdust from Saw Mill. *Journal of Institute of Science and Technology*, *22*(2), 103–108. https://doi.org/10.3126/jist.v22i2.19600

Simate, G. S., Iyuke, S. E., Ndlovu, S., & Heydenrych, M. (2012). The heterogeneous coagulation and flocculation of brewery wastewater using carbon nanotubes. *Water Research*, *46*(4), 1185–1197. https://doi.org/10.1016/j.watres.2011.12.023

Sivasangari, S., Suseendhar, S., Suresh Kumar, K., Vijayaprasath, N., & Thirumurugan, M. (2007). luenCharacteristic Study of Electroplating and Dye Industrial Effts. *International Journal of Innovative Research in Science, Engineering and Technology (An ISO*, *3297*, 20810–20816. https://doi.org/10.15680/IJIRSET.2016.0512122

Sun, Y., & Webley, P. A. (2010). Preparation of activated carbons from corncob with large specific surface area by a variety of chemical activators and their application in gas storage. *Chemical Engineering Journal*, *162*(3), 883–892. https://doi.org/10.1016/j.cej.2010.06.031

Tan, I. A. W., Ahmad, A. L., & Hameed, B. H. (2009). Adsorption isotherms, kinetics, thermodynamics and desorption studies of 2,4,6-trichlorophenol on oil palm empty fruit bunch-based activated carbon. *Journal of Hazardous Materials*, *164*(2–3), 473–482. https://doi.org/10.1016/j.jhazmat.2008.08.025

Technological trends in heavy metals removal from industrial wastewater: A reviewShrestha, R., Ban, S., Devkota, S., Sharma, S., Joshi, R., Tiwari, A. P., Kim, H. Y., & Joshi, M. K. (2021). Technological trends in heavy metals removal from industrial wastewater: A review. *Journal of Environmental Chemical Engineering*, *9*(4).

https://doi.org/10.1016/j.jece.2021.105688

Theydan, S. K. (2018). Effect of process variables, adsorption kinetics and equilibrium studies of hexavalent chromium removal from aqueous solution by date seeds and its activated carbon by ZnCl2. *Iraqi Journal of Chemical and Petroleum Engineering*, *19*(1), 1–12.

Thommes, M., Kaneko, K., Neimark, A. V., Olivier, J. P., Rodriguez-Reinoso, F., Rouquerol, J., & Sing, K. S. W. (2015). Physisorption of gases, with special reference to the evaluation of surface area and pore size distribution (IUPAC Technical Report). *Pure and Applied Chemistry*, *87*(9–10), 1051–1069. https://doi.org/10.1515/pac-2014-1117

Tomczyk, A., Sokołowska, Z., & Boguta, P. (2020). Biochar physicochemical properties: pyrolysis temperature and feedstock kind effects. *Reviews in Environmental Science and Biotechnology*, *19*(1), 191–215. https://doi.org/10.1007/s11157-020-09523-3

Villabona-ortíz, Á., Tejada-tovar, C., & Gonzalez-delgado, Á. D. (2021). Adsorption of cd2+ ions from aqueous solution using biomasses of theobroma cacao, zea mays, manihot esculenta, dioscorea rotundata and elaeis guineensis. *Applied Sciences (Switzerland)*, *11*(6). https://doi.org/10.3390/app11062657

Wagner, N. J., & Jula, R. J. (2018). Activated carbon adsorption. In *Activated Carbon Adsorption For Wastewater Treatment*. https://doi.org/10.1201/9781351069465-3

Webb, P. a. (2003). Introduction to Chemical Adsorption Analytical Techniques and their Applications to Catalysis. *MIC Technical Publications*, *13*(January), 1–4.

Wu, S. H., & Pendleton, P. (2001). Adsorption of anionic surfactant by activated carbon: Effect of surface chemistry, ionic strength, and hydrophobicity. *Journal of Colloid and Interface Science*, *243*(2), 306–315. https://doi.org/10.1006/jcis.2001.7905

Yahya, M. D., Aliyu, A. S., Obayomi, K. S., Olugbenga, A. G., & Abdullahi, U. B. (2020). Column adsorption study for the removal of chromium and manganese ions from electroplating wastewater using cashew nutshell adsorbent. *Cogent Engineering*, *7*(1). https://doi.org/10.1080/23311916.2020.1748470

Yang, X., Wan, Y., Zheng, Y., He, F., Yu, Z., Huang, J., Wang, H., Ok, Y. S., Jiang, Y., & Gao, B. (2019). Surface functional groups of carbon-based adsorbents and their roles in the removal of heavy metals from aqueous solutions: A critical review. *Chemical Engineering Journal*, *366*(352), 608–621. https://doi.org/10.1016/j.cej.2019.02.119

Yoro, K. O., Amosa, M. K., Sekoai, P. T., Mulopo, J., & Daramola, M. O. (2020). Diffusion mechanism and effect of mass transfer limitation during the adsorption of CO2 by polyaspartamide in a packed-bed unit. *International Journal of Sustainable Engineering*, *13*(1), 54–67. https://doi.org/10.1080/19397038.2019.1592261

Zhang, Y., Wang, Y., Zhang, H., Li, Y., Zhang, Z., & Zhang, W. (2020). Zhang, Y., Wang, Y., Zhang, H., Li, Y., Zhang, Z., & Zhang, W. (2020). Recycling spent lithium-ion battery as adsorbents to remove aqueous heavy metals: Adsorption kinetics, isotherms, and regeneration assessment. Resources, Conservation and Recycling, 15. *Resources, Conservation and Recycling*, *156*(October 2019), 104688. https://doi.org/10.1016/j.resconrec.2020.104688

Zheng, C., Zhou, X., Cao, H., Wang, G., & Liu, Z. (2014). Synthesis of porous graphene/activated carbon composite with high packing density and large specific surface area for supercapacitor electrode material. *Journal of Power Sources*, *258*, 290–296. https://doi.org/10.1016/j.jpowsour.2014.01.056

APPENDICES

Appendix A: **Evaluate proximate analysis of bamboo activated carbon**

Moisture content determination

$$\text{Moisture content (\%) bamboo} = \frac{B2 - B3}{B2 - B1} \times 100$$

B1= mass of crucible with bamboo (air dried)

B2= bamboo mass after dried

B3= crucible mass

Initial mass of bamboo = 10gr (air dried)

After dried = 5.298gr

Mass of crucible = 54.2gr

$$\text{Moisture content (\%)} = \frac{63.5 - 61.902}{64.2 - 54.2} \times 100$$

$$\text{Moister content (\%) bamboo} = 15.98\%$$

$$\text{Moisture content (\%) saw dust} = \frac{S2 - S3}{S2 - S1} \times 100$$

$$= \frac{63.9 - 61,902}{10} \times 100$$

Moisture content (%) saw dust =19.98

$$\text{Moisture content (\%) corn cob} = \frac{C2 - C3}{C2 - C1} \times 100$$

$$= \frac{64.2 - 61.902}{10} \times 100$$

Moisture content (%) corn cob =24.04%

$$\text{Moisture content (\%) BAC/GO} = \frac{BA2 - BA3}{BA2 - BA1} \times 100$$

$$\text{Moisture content (\%) BAC/GO} = \frac{62.9 - 61.902}{10} \times 100$$

$$\text{Moisture content (\%) BAC/GO} = 9.98\%$$

Ash content determination

$$\text{Ash content (\%) bamboo} = \frac{B3 - B1}{B2 - B1} \times 100$$

$$= \frac{2 - 1.956}{2} \times 100$$

Ash content (%) bamboo =2.2%

$$\text{Ash content (\%) sawdust} = \frac{S3 - S1}{S2 - S1} \times 100$$

$$= \frac{2 - 1.8746}{2} \times 100$$

Ash content (%) sawdust = 6.27%

Ash content (%) corn cob = $\frac{C3-C1}{C2-C1} \times 100$

$$= \frac{2-1.776}{2} \times 100$$

Ash content (%) corn cob= 11.2%

Ash content (%) BAC/GO = $\frac{BA3-BA1}{BA2-BA1} \times 100$

Ash content (%) BAC/GO = $\frac{2-1.959}{2} \times 100$

Ash content (%) BAC/GO = 2.05%

Volatile content determination

Volatile content (%) bamboo = $\frac{B2-B3}{B2-B1} \times 100$

$$= \frac{3-1.5654}{3} \times 100$$

Volatile content (%) bamboo = 47.82%

Volatile content (%) sawdust = $\frac{S2-S3}{S2-S1} \times 100$

$$= \frac{3-1.5006}{3} \times 100$$

Volatile content (%) sawdust= 49.98%

Volatile content (%) corn cob = $\frac{C2-C3}{C2-C1} \times 100$

$$= \frac{3-1.4262}{3} \times 100$$

Volatile content (%) corn cob = 52.46%

Volatile content (%) BAC/GO = $\frac{BA2-BA3}{BA2-BA1} \times 100$

Fixed carbon determination = $\frac{3-1.5854}{3} \times 100$

$$= 47.15\%$$

Fixed carbon (%) bamboo = 100-(moisture + ash + volatile)

$$= 100\text{-}(15.89\%+2.2\%+47.82)$$

$$= 34.09\%$$

Fixed carbon (%) saw dust = 100-(moisture + ash + volatile)

$$= 100\text{-}(19.98\%+6.27\%+49.98)$$

$$= 23.77\%$$

Fixed carbon (%) corn cob = 100-(moisture + ash + volatile)

$$= 100\text{-}(24.04\%+11.2\%+52.40)$$

$$= 12.36\%$$

Fixed carbon (%) BAC/GO = 100-(moisture + ash + volatile)

$$= 100\text{-}(9.98\%+2.05\%+47.15)$$

$$= 40.82\%$$

Appendix B: Evaluation of other characteristics of activated carbons

B.1 Yield

Yield (%) bamboo = $\frac{BC}{BO} \times 100$

$$\frac{5.987}{10} \times 100$$

Yield (%) bamboo = 59.87%

Yield (%) saw dust = $\frac{SC}{SO} \times 100$

$$= \frac{5.297}{10} \times 100$$

Yield (%) saw dust = 52.97%

Yield (%) corn cob = $\frac{CC}{CO} \times 100$

$$= \frac{3.44}{10} \times 100$$

Yield (%) corn cob = 34.4%

Yield (%) BAC/GO = $\frac{BAC}{BAO} \times 100$

Yield (%) BAC/GO = $\frac{6.267}{10} \times 100$

$$= 62.67\%$$

Where BC= the yield weight activated carbon from bamboo

BO = the air dried of bamboo

SC = the yield weight activated carbon from saw dust

SO = the air dried of saw dust

CC = the yield weight activated carbon from corn cob

CO = the air dried of corn cob

BAC = the yield weight of composite of BAC/GO

BAC = the air dried of composite of BAC/GO

B.2 Bulk density

Bamboo

Weight of AC (MAC) = 5gr

Cylinder with sample weight (M1) =60.38gr

Total weight of cylinder (mH_2O) = 100.74gr

Total volume of cylinder (V) = 50 ml

Weight of added water = m H_2O − m

$$100.74–60.38 \text{ gr}$$

$$40.36 \text{ gr}$$

Volume added water (V H_2O) = $\frac{mH_2O}{H_2O}$

$$= 40.36\text{ml}$$

Volume of added AC (VAC) = V − V H_2O

$$= 9.64 \text{ ml}$$

Density of AC (ρ AC) = $\frac{m\ AC}{V\ AC}$

$$= 0.52\text{g/ml}$$

Sawdust

 Weight of AC (MAC) = 5gr

Cylinder with sample weight (M1) =61.8gr

Total weight of cylinder (mH_2O) = 98.9gr

Total volume of cylinder (V) = 50 ml

Weight of added water = m H_2O − m_1

$$= 98.9 \text{ gr} − 61.8 \text{ gr}$$

$$=37.1 \text{ gr}$$

Volume added water (V H_2O) = $\frac{mH_2O}{H_2O}$

$$= 37.1\text{ml}$$

Volume of added AC (VAC) = V − V H_2O

$$= 12.9 \text{ ml}$$

Density of AC (ρ AC) = $\frac{m\ AC}{V\ AC}$

$$= 0.388\text{g/ml}$$

Corncob

Weight of AC (MAC) = 5gr

Cylinder with sample weight (M1) =62.2gr

Total weight of cylinder (mH_2O) = 96.5gr

Total volume of cylinder (V) = 50 ml

Weight of added water = m H_2O − m

$\qquad$ 96.5gr −62.2 gr

$\qquad$ 33.9 gr

Volume added water (V H_2O) = $\frac{mH_2O}{dH_2O}$

$\qquad$ = 33.9ml

Volume of added AC (VAC) = V − V H_2O

$\qquad$ = 16.1 ml

Density of AC (ρ AC) = $\frac{m\ AC}{V\ AC}$

$\qquad$ = 0.311 g/ml

BAC/GO composite

Weight of AC (MAC) = 5gr

Cylinder with sample weight (M1) =59.8gr

Total weight of cylinder (mH_2O) = 104.62gr

Total volume of cylinder (V) = 50 ml

Weight of added water = m H_2O − m

$\qquad$ =104.62 − 59.8 gr

$\qquad$ =44.82 gr

Volume added water (V H_2O) = $\frac{mH_2O}{H_2O}$

$\qquad$ = 44.82ml

Volume of added AC (VAC) = V − V H_2O

$\qquad$ = 5.18 ml

Density of AC (ρ AC) = $\frac{m\ AC}{V\ AC}$

$\qquad$ = 0.96 g/ml

Appendix C: Experimental data and statistical result

Table .1: Point of zero charge determination values

Change in pH for corncob

Initial pH	2	4	6	8	10	12
Final pH	2.41	6.05	6.88	6.23	5.47	10.49
ΔpH	0.41	2.05	0.88	-1.77	-4.53	-1.51

Change in pH for sawdust

Initial pH	2	4	6	8	10	12
Final pH	2.91	6.25	6.93	5.164	6.28	10.77
ΔpH	0.91	2.25	0.93	-2.836	-3.72	-1.23

Change in pH for bamboo

Initial pH	2	4	6	8	10	12
Final pH	0.31	5.76	5.84	5.55	6.33	11.04
ΔpH	0.31	1.76	-0.16	-2.45	-3.67	-0.96

Change in pH for bamboo

Initial pH	2	4	6	8	10	12
Final pH	2.32	6.15	5.73	5.34	6.15	11.9
ΔpH	0.32	2.15	-0.27	-2.66	-3.85	-0.1

Appendix D .1 BET data

Quantachrome NovaWin - Data Acquisition and Reduction

for NOVA instruments

©1994-2010, Quantachrome Instruments
Version 11.0

Analysis   Report
Operator: Alex   Date: 2022/08/03   Operator: Alex   Date:8/3/2022
Sample ID: BA F111 2222   Filename: C:\QCdata\Physisorb\BA F111.qps
Sample Desc: Comment:
Sample weight: 0.04 g   Sample Volume: 0.010256 cc   Sample Density:3.9 g/cc
Outgas Time: 8.0 hours   OutgasTemp: 300.0 C
Analysis gas: Nitrogen   Bath Temp: 77.3 K

Press. Tolerance:0.100/0.100 (ads/des)Equil time: 60/60 sec (ads/des) Equil timeout: 240/240 sec (ads/des)

Analysis Time: 145.9 min   End of run: 2022/08/03 17:03:44 Instrument: Nova Station C

Cell ID: 2   F/W version: 0.00

Adsorbate   Nitrogen   Temperature   77.350K

          Mole c. Wt.: 28.013 g   Cross Section: 16.200 Å²   Liquid Density: 0.808 g/cc

Relative Pressure P/Po	Volume @ STP cc/g	$1 / [W((Po/P) - 1)]$
5.26550e-02	176.4099	2.5209e-01
1.11611e-01	226.1121	4.4456e-01
1.74937e-01	272.3347	6.2293e-01
2.37826e-01	317.8202	7.8555e-01
3.01554e-01	363.8651	9.4938e-01

BET summary

Slope =   2.779

Intercept =   1.225e-01

Correlation coefficient, r =   0.998749

C constant=   23.688

Surface Area =   1200.058 m²/g

For NOVA instruments

©1994-2010, Quantachrome Instruments

Version 11.0

Analysis   Report

Operator: Alex   Date: 2022/08/03   Operator: Alex   Date: 8/3/2022

Sample ID: GO AC 2222   Filename: C:\QCdata\Physisorb\GO ACC 22.qps

Sample Desc: Comment:

Sample weight: 0.04 g   Sample Volume: 0.010256 cc   Sample Density: 3.9 g/cc

Outgas Time: 8.0 hours   OutgasTemp: 300.0 C

Analysis gas: Nitrogen   Bath Temp: 77.3 K

Press. Tolerance:0.100/0.100 (ads/des)Equil time: 60/60 sec (ads/des) Equil timeout: 240/240 sec (ads/des)

Analysis Time: 136.7 min   End of run: 2022/08/03 16:54:34 Instrument: Nova Station B

Cell ID: 2   F/W version: 0.00

Adsorbate   Nitrogen   Temperature   77.350K

Mole c. Wt.: 28.013 g   Cross Section: 16.200 Å²   Liquid Density: 0.808 g/cc

Relative Pressure P/Po	Volume @ STP cc/g	$1 / [\ W((Po/P) - 1) \ ]$
4.85210e-02	278.6171	1.4644e-01
1.15955e-01	353.0992	2.9721e-01
1.71686e-01	404.1309	4.1036e-01
2.43839e-01	464.0033	5.5606e-01
3.00374e-01	509.4771	6.7425e-01

BET summary

Slope =   2.081

Intercept =   5.040e-02

Correlation coefficient, r =   0.999808

C constant=   42.298

Surface Area =   1633.667 m²/g

Quantachrome NovaWin - Data Acquisition and Reduction
for NOVA instruments
©1994-2010, Quantachrome Instruments
Version 11.0

Analysis   Report

Operator: Alex   Date: 2022/08/03   Operator: Alex   Date:8/3/2022

Sample ID: BA F111 2222   Filename: C:\QCdata\Physisorb\BA F111.qps

Sample Desc: Comment:

Sample weight: 0.04 g   Sample Volume: 0.010256 cc   Sample Density:3.9 g/cc

Outgas Time: 8.0 hours   OutgasTemp: 300.0 C

Analysis gas: Nitrogen   Bath Temp: 77.3 K

Press. Tolerance:0.100/0.100 (ads/des)Equil time: 60/60 sec (ads/des) Equil timeout: 240/240 sec (ads/des)

Analysis Time: 145.9 min   End of run: 2022/08/03 17:03:44 Instrument: Nova Station C

Cell ID: 2   F/W version: 0.00

Adsorbate   Nitrogen   Temperature   77.350K

          Mole c. Wt.: 28.013 g   Cross Section: 16.200 Å²   Liquid Density: 0.808 g/cc

                 Surface Area Data

MultiPoint BET   1.200e+03 m²/g

NLDFT cumulative surface area   6.107e+02 m²/g

                 Pore Volume Data

HK method cumulative pore volume   3.958e-01 cc/g

SF method cumulative pore volume   4.126e-01 cc/g

NLDFT method cumulative pore volume   5.220e-01 cc/g

                 Pore Size Data

HK method pore Radius (Mode)   1.838e+00 Å

SF method pore Radius (Mode)   2.261e+00 Å

NLDFT pore Radius (Mode)   1.324e+01 Å

Quantachrome NovaWin - Data Acquisition and Reduction

             for NOVA instruments

          ©1994-2010, Quantachrome Instruments

               version 11.0

Analysis   Report

Operator:alex   Date:2022/08/03   Operator:alex   Date:8/3/2022

Sample ID: GO AC 2222   Filename: C:\QCdata\Physisorb\GO ACC 22.qps

Sample Desc: Comment:

Sample weight: 0.04 g   Sample Volume: 0.010256 cc   Sample Density:3.9 g/cc

Outgas Time: 8.0 hrs   OutgasTemp: 300.0 C

Analysis gas: Nitrogen   Bath Temp: 77.3 K

Press. Tolerance:0.100/0.100 (ads/des)Equil time: 60/60 sec (ads/des) Equil timeout: 240/240 sec (ads/des)

Analysis Time: 136.7 min   End of run: 2022/08/03 16:54:34 Instrument: Nova Station B

Cell ID: 2   F/W version: 0.00

Adsorbate   Nitrogen   Temperature   77.350K

          Molec. Wt.: 28.013 g   Cross Section: 16.200 Å²   Liquid Density: 0.808 g/cc

Surface Area Data

Multi Point BET   1.634e+03 m²/g
NLDFT cumulative surface area   9.408e+02 m²/g

Pore Volume Data

HK method cumulative pore volume   5.978e-01 cc/g
SF method cumulative pore volume   6.187e-01 cc/g
NLDFT method cumulative pore volume   7.325e-01 cc/g

Pore Size Data

HK method pore Radius (Mode)   1.838e+00 Å
SF method pore Radius (Mode)   2.261e+00 Å
NLDFT pore Radius (Mode)   1.324e+01 Å

Appendix D.2: Particle size distribution a) BAC, and b) BAC/GO composite

Size Distribution by Intensity

a)

Size Distribution by Intensity

b)
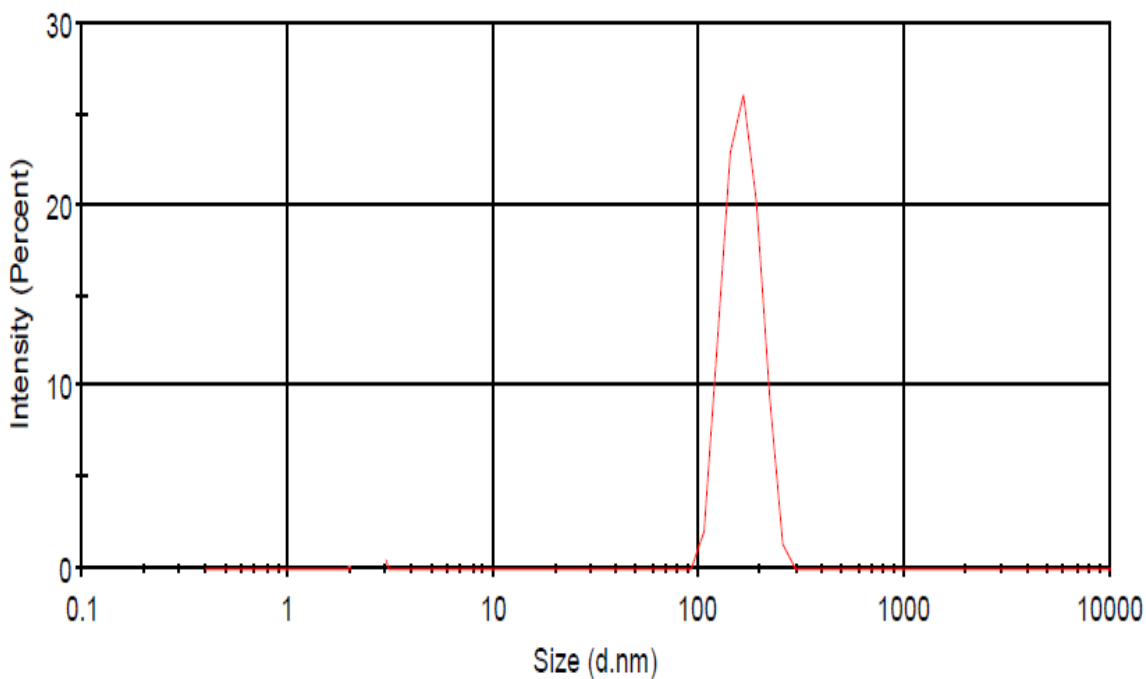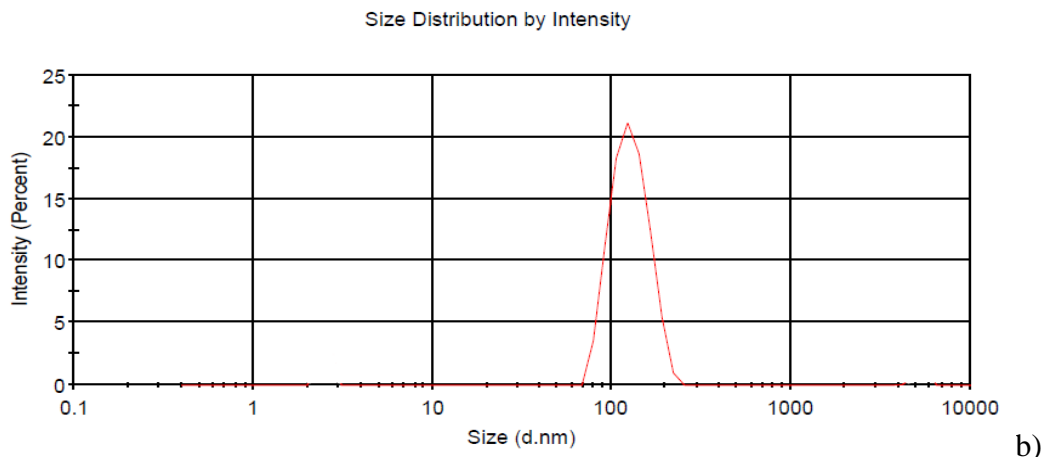
Appendix E.1: Experimental data statistical result for PH effect, initial concentration of Cr (VI), dosage and contact time

For pH effect

Where: initial con. of Cr(VI) = 5mg/L, time = 180 min, volume= 100ml, dose of AC= 0.1g/L and initial absorbance = 0.173 and e = 0.03984

Table E 3.1: Effects of solution pH on the adsorption of Cr (IV) using corn cob AC

PH	Absorbance	Final conc (c_e mg/L)	Adsorption capacity q_e (mg/g)	Adsorption efficency (%)
2	0.0032	0.080	4.92	98.12
4	0.0088	0.221	4.78	94.9
6	0.0123	0.308	4.69	92.91
8	0.0181	0.454	4.55	89.56
10	0.0200	0.502	4.49	88.43
12	0.0258	0.647	4.34	85.1

Table E 3.2: Effects of solution pH on the adsorption of Cr (IV) using sawdust AC

PH	Absorbance	Final conc (c_e mg/L)	Adsorption capacity q_e (mg/g)	Adsorption efficency (%)
2	0.0029	0.073	4.93	98.32
4	0.0030	0.075	4.92	98.02
6	0.0069	0.173	4.83	96.26
8	0.0086	0.216	4.78	95
10	0.0169	0.424	4.58	90.25
12	0.0174	0.437	4.56	89.92

Table E 3.3: Effects of solution pH on the adsorption of Cr (IV) using bamboo AC

PH	Absorbance	Final conc (c$_e$ mg/L)	Adsorption capacity q$_e$ (mg/g)	Adsorption efficency (%)
2	0.0014	0.035	4.96	99.18
4	0.0022	0.055	4.94	98.75
6	0.0047	0.118	4.88	97.28
8	0.0063	0.158	4.84	96.36
10	0.0131	0.329	4.67	92.45
12	0.0158	0.397	4.60	90.85

Table E 3.4: Effects of solution pH on the adsorption of Cr(IV) using BAC/GO composite

PH	Absorbance	Final conc (c$_e$ mg/L)	Adsorption capacity q$_e$ (mg/g)	Adsorption efficency (%)
2	0.0001	0.003	5.00	99.98
4	0.0016	0.040	4.96	99.07
6	0.0026	0.065	4.93	98.5
8	0.0038	0.095	4.91	97.81
10	0.0106	0.266	4.73	93.9
12	0.0157	0.394	4.61	90.9

For Dasage

Where: initial con. Of Cr(VI) = 5mg/L, pH= 2, time = 180 min, volume = 100ml and initial absorbance = 0.173, e = 0.03984

Table E 4.1: Effect of adsorbent Dose on the adsorption of Cr (VI) using corncob AC

Dosage (g/L)	Absorbance	Final conc (c$_e$ mg/L)	Adsorption capacity q$_e$ (mg/g)	Adsorbance efficency cr(IV)
0.1	0.0188	0.472	4.53	89.12
0.15	0.0094	0.236	3.18	94.55
0.2	0.0041	0.103	2.45	97.65
0.25	0.0024	0.060	1.98	98.74
0.3	0.0022	0.055	1.65	98.76
0.35	0.0021	0.053	1.41	98.78
0.4	0.0020	0.050	1.24	98.79

Table E 4.2: Effect of adsorbent Dose on the adsorption of Cr (VI) using sawdust AC

Dosage (mg/L)	Absorbance	Final conc (c_e mg/L)	Adsorption capacity q_e (mg/g)	Adsorbance efficency cr(IV)
0.1	0.0158	0.397	4.60	90.85
0.15	0.0085	0.213	3.19	95.1
0.2	0.0034	0.085	2.46	98.01
0.25	0.0009	0.022	1.99	99.45
0.3	0.0008	0.020	1.49	99.48
0.35	0.0008	0.020	1.42	99.49
0.4	0.0008	0.020	1.25	99.5

Table E 4.3: Effect of adsorbent Dose on the adsorption of Cr (VI) using bamboo AC

Dosage	Absorbance	Final conc (c_e mg/L)	Adsorption capacity q_e (mg/g)	Adsorbance efficency cr(IV)
0.1	0.0139	0.349	4.65	91.92
0.15	0.0118	0.296	3.14	93.14
0.2	0.0053	0.133	2.43	96.92
0.25	0.0007	0.018	1.99	99.6
0.3	0.0006	0.015	1.66	99.63
0.35	0.0005	0.014	1.64	99.65
0.4	0.0003	0.012	1.25	99.68

Table E 4.4: Effect of adsorbent Dose on the adsorption of Cr (VI) using BAC/GO composite

Dosage	Absorbance	Final conc (c_e mg/L)	Adsorption capacity q_e (mg/g)	Adsorbance efficency cr(IV)
0.1	0.0083	0.208	4.79	95.2
0.15	0.0049	0.123	3.25	97.11
0.2	0.0003	0.008	2.49	99.85
0.25	0.0002	0.005	1.99	99.98
0.3	0.0001	0.003	1.66	99.99
0.35	0.0001	0.003	1.66	99.99
0.4	0.0001	0.003	1.66	99.99

For con. Of Cr(VI)

Where: pH=10, dose = 0.25g/L, volume of solution = 100ml and time = 180 min , e = 0.03984

Table E 5.1: Effect of initial Cr(VI) concentration on the adsorption of Cr (VI) using corncob AC

Initial Cr(VI) conc. (mg//L)	Initial Absorbance	Final Absorbance	Final conc (c_e mg/L)	Adsorption capacity q_e (mg/g)	Adsorbance efficency cr(IV)
5	0.1730	0.0022	0.055	1.98	98.74
7.5	0.2595	0.0192	0.482	2.81	92.6
10	0.3990	0.0498	1.250	3.50	87.5
12.5	0.4980	0.0997	2.502	3.99	79.98
15	0.5440	0.1485	3.727	4.51	72.7
17.5	0.6350	0.2172	5.452	4.82	65.8
20	0.7520	0.3843	9.646	4.80	48.9

Table E 5.2: Effect of initial Cr (VI) concentration on the adsorption of Cr (VI) using sawdust AC

Initial Cr(VI) conc. (mg//L)	Initial Absorbance	Final Absorbance	Final conc (c_e mg/L)	Adsorption capacity q_e (mg/g)	Adsorbance efficency cr(IV)
5	0.1730	0.0009	0.023	1.99	99.45
7.5	0.2595	0.0140	0.351	2.86	94.6
10	0.3990	0.0419	1.052	3.58	89.5
12.5	0.4980	0.0866	2.174	4.13	82.6
15	0.5440	0.1164	2.922	4.83	78.6
17.5	0.6350	0.2000	5.020	4.99	68.5
20	0.7520	0.3038	7.625	4.95	59.6

Table E 5.3: Effect of initial Cr(VI) concentration on the adsorption of Cr (VI) using bamboo AC

Initial Cr(VI) conc. (mg//L)	Initial Absorbance	Final Absorbance	Final conc (c_e mg/L)	Adsorption capacity q_e (mg/g)	Adsorbance efficency cr(IV)
5	0.1730	0.0007	0.018	1.99	99.6
7.5	0.2595	0.0026	0.065	2.97	99
10	0.3990	0.0299	0.751	3.69	92.5
12.5	0.4980	0.0508	1.275	4.49	89.8
15	0.5440	0.1072	2.691	4.93	80.3
17.5	0.6350	0.1428	3.584	5.57	77.5
20	0.7520	0.2376	5.963	5.49	68.4

Table E. 5.4: Effect of initial Cr (VI) concentration on the adsorption of Cr (VI) using BAC/GO composite

Initial Cr(VI) conc. (mg//L)	Initial Absorbance	Final Absorbance	Final conc (c_e mg/L)	Adsorption capacity q_e (mg/g)	Adsorbance efficency cr(IV)
5	0.1730	0.0003	0.008	1.99	99.98
7.5	0.2595	0.0013	0.033	2.99	99.5
10	0.3990	0.0120	0.301	3.88	96.98
12.5	0.4980	0.0268	0.673	4.73	94.6
15	0.5440	0.0571	1.433	5.43	89.5
17.5	0.6350	0.0793	1.990	6.26	87.5
20	0.7520	0.1737	4.359	6.20	76.9

For Contact Time

Where: pH=10, dose = 0.25g/L, con. of Cr(VI)=12.5mg/L and initial absorbance = 0.498,

e = 0.03984

Table E.6.1: Effect of contact time on the adsorption of Cr (VI) using corncob AC

Contact time (min)	Absorbance	Final conc (c_t mg/L)	Adsorption capacity Q_t (mg/g)	Adsorbance efficency cr(IV)
30	0.1523	3.823	3.47	69.45
60	0.1265	3.175	3.73	74.6
90	0.1021	2.563	3.97	79.5
120	0.0834	2.093	4.16	83.25
150	0.0833	2.091	4.18	83.26
180	0.0832	2.088	4.18	83.28

Table E.6.2: Effect of contact time on the adsorption of Cr VI) using sawdust AC

Contact time (min)	Absorbance	Final conc (c_t mg/L)	Adsorption capacity Q_t (mg/g)	Adsorbance efficency cr(IV)
30	0.1269	3.185	3.73	74.5
60	0.1026	2.575	3.97	79.4
90	0.0798	2.003	4.19	83.98
120	0.0576	1.435	4.43	88.42
150	0.0572	1.436	4.43	88.5
180	0.0580	1.437	4.43	88.59

Table E.6.3: Effect of contact time on the adsorption of Cr (VI) using bambooAC

Contact time (min)	Absorbance	Final conc (c_t mg/L)	Adsorption capacity Q_t (mg/g)	Adsorbance efficency cr(IV)
30	0.1116	2.801	3.88	77.6
60	0.0866	2.174	4.13	82.6
90	0.0657	1.649	4.34	86.8
120	0.0523	1.313	4.46	89.5
150	0.0514	1.129	4.47	89.68
180	0.0513	1.287	4.47	89.7

Table E.6.4: Effect of contact time on the adsorption of Cr (VI) using BAC/GO composite

Contact time (min)	Absorbance	Final conc (c_t mg/L)	Adsorption capacity Q_t (mg/g)	Adsorbance efficency cr(IV)
30	0.1018	2.563	3.97	79.56
60	0.0722	1.812	4.28	85.5
90	0.0508	1.275	4.49	89.8
120	0.0399	1.002	4.59	91.98
150	0.0399	1.002	4.59	91.99
180	0.0399	1.002	4.59	91.99

Pseudo-First-Order Model

Table E.7. 1: Pseudo-first-order model parameters for Corncob AC

Time (min)	Absorbance	Final conc (c_t mg/L)	Adsorption capacity Q_t (mg/g)	q_e	q_e-q_t	Log(q_e-q_t)
30	0.1523	3.823	3.47	4.18	0.71	-0.149
60	0.1265	3.175	3.73	4.18	0.45	-0.347
90	0.1021	2.563	3.97	4.18	0.21	-0.678
120	0.0834	2.093	4.16	4.18	0.02	-1.699
150	0.0833	2.091	4.18	4.18	-	-
180	0.0832	2.088	4.18	4.18	-	-

Table E.7. 2: Pseudo-first-order model parameters for Sawdust AC

Time (min)	Absorbance	Final conc (c_t mg/L)	Adsorption capacity Q_t (mg/g)	q_e	q_e-q_t	Log(q_e-q_t)
30	0.1269	3.185	3.73	4.43	0.7	-1.155
60	0.1026	2.575	3.97	4.43	0.46	-0.337
90	0.0798	2.003	4.19	4.43	0.24	-0.619
120	0.0576	1.435	4.41	4.43	0.02	-1.699
150	0.0572	1.436	4.43	4.43	-	-
180	0.0580	1.437	4.43	4.43	-	-

Table E.7. 3: Pseudo-first-order model parameters for Bamboo AC

Time (min)	Absorbance	Final conc (c_t mg/L)	Adsorption capacity Q_t (mg/g)	q_e	q_e-q_t	Log(q_e-q_t)
30	0.1116	2.801	3.88	4.47	0.59	-0.229
60	0.0866	2.174	4.13	4.47	0.34	-0.469
90	0.0657	1.649	4.34	4.47	0.13	-0.886
120	0.0523	1.313	4.46	4.47	0.01	-2
150	0.0514	1.129	4.47	4.47	-	-
180	0.0513	1.287	4.47	4.47	-	-

Table E.7. 4: Pseudo-first-order model parameters for Corncob AC BAC/GO composite

Time (min)	Absorbance	Final conc (c_t mg/L)	Adsorption capacity Q_t (mg/g)	q_e	q_e-q_t	Log(q_e-q_t)
30	0.1018	2.563	3.97	4.59	0.62	-0.207
60	0.0722	1.812	4.28	4.59	0.31	-0.509
90	0.0508	1.275	4.49	4.59	0.1	-1
120	0.0399	1.002	4.59	4.59	-	-
150	0.0399	1.002	4.59	4.59	-	-
180	0.0399	1.002	4.59	4.59	-	-

According to Figure 4-17, a) the equation of the linerized first-order kinatic model for corncob AC was follows:

$$y= 0.0166x + 0.527$$

according to Equation 4.1 the equation obtained is:

$$\log(q_e\text{-}q_t) = 0.0166t + 0.527$$

from the above Equation 4.1, slope $= -\dfrac{k1}{2.303} = 0.0166$ $\qquad$ Intercept $= \log q_e = 0.527$

Rate constant $K_1 = -0.038$ min^{-1}

q_t calculated from graph $q_{ecal} = 3.365$ mg/g

According to Figure 4-17, b) the equation of the linerized first-order kinatic model for sawdust AC was follows:

$$y = -0.01638x + 0.526$$

according to Equation 4.1 the equation obtained is:

$$\log(q_e\text{-}q_t) = -0.01638x + 0.526$$

from the above equation, slope $= -\dfrac{k1}{2.303} = 0.01638$ $\qquad$ Intercept $= \log q_e = 0.526$

Rate constant $K_1 = 0.038$ min^{-1}

q_t calculated from graph $q_{ecal} = 3.357$ mg/g

According to Figure 4-17, c) the equation of the linerized first-order kinatic model for bamboo AC was follows:

$$y = -0.0191x + 0.5365$$

according to Equation 4.1 the equation obtained is:

$$\log(q_e\text{-}q_t) = -0.0191x + 0.5365$$

from the above equation, slope $= -\dfrac{k1}{2.303} = = -0.0191$ $\qquad$ Intercept $= \log q_e = 0.5365$

Rate constant $K_1 = 0.044$ min^{-1}

q_t calculated from graph $q_{ecal} = 3.439$ mg/g

According to Figure 4-17, d) the equation of the linerized first-order kinatic model for BAC/GO composite was follows:

$$y = -0.0132x + 0.221$$

according to Equation 4.1 the equation obtained is:

$$\log(q_e\text{-}q_t) = -0.0132x + 0.221$$

from the above equation, slope $= -\dfrac{k1}{2.303} = -0.0132$ $\qquad$ Intercept $= \log q_e = 0.221$

Rate constant $K_1 = 0.029$ min $^{-1}$

q_t calculated from graph $q_{ecal} = 1.663$ mg/g

Psedoo-Second-Order Model

Table E.8.1: Psedoo-second-order model parameters for Corncob AC

Time (min)	Absorbance	Final conc (c_t mg/L)	Adsorption capacity q_t (mg/g)	q_e mg/g	t/q_t min/(mg/g)
30	0.1523	3.823	3.47	4.18	8.646
60	0.1265	3.175	3.73	4.18	16.086
90	0.1021	2.563	3.97	4.18	22.670
120	0.0834	2.093	4.16	4.18	28.846
150	0.0833	2.091	4.18	4.18	35.885
180	0.0832	2.088	4.18	4.18	43.062

Table E.8.2: Psedoo-second-order model parameters for Sawdust AC

Time (min)	Absorbance	Final conc (c_t mg/L)	Adsorption capacity q_t (mg/g)	q_e	t/q_t min/(mg/g)
30	0.1269	3.185	3.73	4.43	8.043
60	0.1026	2.575	3.97	4.43	15.113
90	0.0798	2.003	4.19	4.43	21.47
120	0.0576	1.435	4.41	4.43	27.211
150	0.0572	1.436	4.43	4.43	33.860
180	0.0580	1.437	4.43	4.43	40.632

Table E.8.3: Psedoo-second-order model parameters for Bamboo AC

Time (min)	Absorbance	Final conc (c_t mg/L)	Adsorption capacity q_t (mg/g)	q_e	t/q_t min/(mg/g)
30	0.1116	2.801	3.88	4.47	7.732
60	0.0866	2.174	4.13	4.47	14.528
90	0.0657	1.649	4.34	4.47	20.737
120	0.0523	1.313	4.46	4.47	26.906
150	0.0514	1.129	4.47	4.47	33.557
180	0.0513	1.287	4.47	4.47	40.268

Table E.8.1: Psedoo-second-order model parameters for BAC/GO composite

Time (min)	Absorbance	Final conc (c_t mg/L)	Adsorption capacity q_t (mg/g)	q_e	t/q_t min/(mg/g)
30	0.1018	2.563	3.97	4.59	7.556
60	0.0722	1.812	4.28	4.59	14.019
90	0.0508	1.275	4.49	4.59	20.045
120	0.0399	1.002	4.59	4.59	26.144
150	0.0399	1.002	4.59	4.59	32.679
180	0.0399	1.002	4.59	4.59	39.216

According to Figure 4-18, a) the equation of linerized scond-order kinetic model for corncob AC was as follows:

y= 0.2263x + 2.1005

According to Equation 4.2 the equation obtained is:

$$\frac{t}{qt} = 0.2263t + 2.1005$$

From the above Equation 4.2, intercept = $\frac{1}{K_1 q_e 2} = 2.1005$ slope = $\frac{1}{q_e} = 0.2263$

Rate constant $k_2 = 0.0244$ g/ (mg min)

q_e calculated from graph $q_{ecal} = 0.0218$

According to Figure 4-18, b)the equation of linerized scond-order kinetic model for saw dust AC was as follows:

y= 0.2142x + 1.8955

According to Equation 4.2 the equation obtained is:

$$\frac{t}{qt} = 0.2142t + 1.8955$$

From the above equation, intercept = $\frac{1}{K_1 q_e 2} = 1.8955$ slope = $\frac{1}{q_e} = 0.2142$

Rate constant $k_2 = 0.0242$ g/ (mg min)

q_e calculated from graph $q_{ecal} = 0.0258$

According to Figure 4-18, c) the equation of linerized scond-order kinetic model for bamboo AC was as follows:

y= 0.2152x + 1.3611

According to Equation 4.2 the equation obtained is:

$$\frac{t}{qt} = 0.2152t + 1.3611$$

From the above equation, intercept = $\dfrac{1}{K_1 q_e 2}$ = 1.3611   slope = $\dfrac{1}{q_e}$ = 0.2152

Rate constant k_2 = 0.0340 g/ (mg min)

q_e calculated from graph q_{ecal} =0.1274

According to Figure 4-18, d) the equation of linerized scond-order kinetic model for BAC/GO composite was as follows:

y= 0.2099x + 1.2386

According to Equation 4.2 the equation obtained is:

$$\frac{t}{qt} = 0.2099t + 1.2386$$

From the above equation, intercept = $\dfrac{1}{K_1 q_e 2}$ =1.2386   slope = $\dfrac{1}{q_e}$ = 0.2099

Rate constant k_2 = 0.0356 g/ (mg min)

q_e calculated from graph q_{ecal} =0.1567

Lengumer isotherm model

Table E.9.1: Lengumer isotherm model parameters for corncob AC

Initial Cr(VI) conc. (mg//L)	Initial Absorbance	Final Absorbance	Final conc (c_e mg/L)	Adsorption capacity q_e (mg/g)	$1/c_e$ (mg/L) [-1]	$1/q_e$ (mg/g) [-1]
5	0.1730	0.0022	0.055	1.98	18.182	0.505
7.5	0.2595	0.0192	0.482	2.81	7.75	0.256
10	0.3990	0.0498	1.250	3.50	4.8	0.186
12.5	0.4980	0.0997	2.502	3.99	2.399	0.051
15	0.5440	0.1485	3.727	4.51	0.268	0.008
17.5	0.6350	0.2172	5.452	4.82	0.183	0.007
20	0.7520	0.3843	9.646	4.80	0.104	0.002

Table E.9.2: Lengumer isotherm model parameters For sawdust AC

Initial Cr(VI) conc. (mg//L)	Initial Absorbance	Final Absorbance	Final conc (c_e mg/L)	Adsorption capacity q_e (mg/g)	$1/c_e$ (mg/L)$^{-1}$	$1/q_e$ (mg/g)$^{-1}$
5	0.1730	0.0009	0.023	1.99	43.478	0.503
7.5	0.2595	0.0140	0.351	2.86	32.849	0.349
10	0.3990	0.0419	1.052	3.58	20.951	0.279
12.5	0.4980	0.0866	2.174	4.13	3.459	0.242
15	0.5440	0.1164	2.922	4.83	1.342	0.207
17.5	0.6350	0.2000	5.020	4.99	0.199	0.2
20	0.7520	0.3038	7.625	4.95	0.031	0.202

Table E.9.3: Lengumer isotherm model parameters For bamboo AC

Initial Cr(VI) conc. (mg//L)	Initial Absorbance	Final Absorbance	Final conc (c_e mg/L)	Adsorption capacity q_e (mg/g)	$1/c_e$ (mg/L)$^{-1}$	$1/q_e$ (mg/g)$^{-1}$
5	0.1730	0.0007	0.018	1.99	55.556	0.503
7.5	0.2595	0.0026	0.065	2.97	35.384	0.337
10	0.3990	0.0299	0.751	3.69	21.332	0.271
12.5	0.4980	0.0508	1.275	4.49	8.784	0.223
15	0.5440	0.1072	2.691	4.93	6.372	0.203
17.5	0.6350	0.1428	3.584	5.57	0.279	0.179
20	0.7520	0.2376	5.963	5.49	0.168	0.182

Table E.9.4: Lengumer isotherm model parameters for BAC/GO comosite

Initial Cr(VI) conc. (mg//L)	Initial Absorbance	Final Absorbance	Final conc (c_e mg/L)	Adsorption capacity q_e (mg/g)	$1/c_e$ (mg/L)$^{-1}$	$1/q_e$ (mg/g)$^{-1}$
5	0.1730	0.0003	0.008	1.99	95	0.503
7.5	0.2595	0.0013	0.033	2.99	30.303	0.3
10	0.3990	0.0120	0.301	3.88	23.322	0.258
12.5	0.4980	0.0268	0.673	4.73	11.486	0.211
15	0.5440	0.0571	1.433	5.43	4.697	0.184
17.5	0.6350	0.0793	1.990	6.26	0.503	0.159
20	0.7520	0.1737	4.359	6.20	0.229	0.161

According to Figure 4-19, a)the equation of the linerized lengmuir model for corncob AC was as follows:

y= 0.0284x + 0.00854

According to Equation 4.3 the equation obtaied is:

$$\frac{1}{q_e} = 0.0284 \quad \frac{1}{C_e} + 0.00854$$

From the above equation,

$$\text{Intercept} = \frac{1}{q_m} = 0.00854, \text{ and } q_m = 117.09 \text{ mg/g}$$

$$\text{Slope} = \frac{1}{q_m \, K_L} = 0.0284 \text{ , and } K_L = 0.0301 \text{ L/g}$$

According to Figure 4-19, b) the equation of the linerized lengmuir model for sawdust AC was as follows:

y= 0.006x + 0.1969

According to Equation 4.3 the equation obtaied is:

$$\frac{1}{q_e} = 0.006 \frac{1}{C_e} + 0.1969$$

From the above equation,

$$\text{Intercept} = \frac{1}{q_m} = 0.1969 \text{ and } q_m = 5.08 \text{mg/g}$$

$$\text{Slope} = \frac{1}{q_m \, K_L} = 0.006 \text{ , and } K_L = 32.817 \text{ L/g}$$

According to Figure 4-19, c) the equation of the linerized lengmuir model for bamboo AC was as follows:

y= 0.0056x + 0.1696

According to Equation 4.3 the equation obtaied is:

$$\frac{1}{q_e} = 0.0056 \frac{1}{C_e} + 0.1696$$

From the above equation,

$$\text{Intercept} = \frac{1}{q_m} = 0.1696, \text{ and } q_m = 5.89 \text{mg/g}$$

$$\text{Slope} = \frac{1}{q_m \, K_L} = 0.0056 \text{ , and } K_L = 30.318 \text{ L/g}$$

According to Figure 4-19, d)the equation of the linerized lengmuir model for BAC/GO composite was as follows:

y= 0.0036x + 0.1629

According to Equation 4.3 the equation obtaied is:

$$\frac{1}{q_e} = 0.0036 \frac{1}{C_e} + 0.1629$$

From the above equation,

$$\text{Intercept} = \frac{1}{q_m} = 0.1629, \text{ and } q_m = 6.14 \text{mg/g}$$

$$\text{Slope} = \frac{1}{q_m K_L} = 0.0036 \text{ , and } K_L = 45.250 \text{ L/g}$$

Freundlich Isotherm Model

Table E.10.1:Freundlich isotherm model parameters for corncob AC

Initial Cr(VI) conc. (mg//L)	Initial Absorbance	Final Absorbance	Final conc (c_e mg/L)	Adsorption capacity q_e (mg/g)	Log C_e (mg/L)	Log q_e (mg/L)
5	0.1730	0.0022	0.055	1.98	-1.259	0.297
7.5	0.2595	0.0192	0.482	2.81	-0.317	0.449
10	0.3990	0.0498	1.250	3.50	0.097	0.544
12.5	0.4980	0.0997	2.502	3.99	0.398	0.601
15	0.5440	0.1485	3.727	4.51	0.571	0.654
17.5	0.6350	0.2172	5.452	4.82	0.737	0.683
20	0.7520	0.3843	9.646	4.80	0.984	0.681

Table E 10.2:Freundlich isotherm model parameters For sawdust AC

Initial Cr(VI) conc. (mg//L)	Initial Absorbance	Final Absorbance	Final conc (c_e mg/L)	Adsorption capacity q_e (mg/g)	Log C_e (mg/L)	Log q_e (mg/L)
5	0.1730	0.0009	0.023	1.99	-1.638	0.299
7.5	0.2595	0.0140	0.351	2.86	-0.455	0.456
10	0.3990	0.0419	1.052	3.58	0.022	0.554
12.5	0.4980	0.0866	2.174	4.13	0.337	0.616
15	0.5440	0.1164	2.922	4.83	0.466	0.684
17.5	0.6350	0.2000	5.020	4.99	0.701	0.698
20	0.7520	0.3038	7.625	4.95	0.882	0.695

Table E 10.3:Freundlich isotherm model parameters For bamboo AC

Initial Cr(VI) conc. (mg//L)	Initial Absorbance	Final Absorbance	Final conc (c_e mg/L)	Adsorption capacity q_e (mg/g)	Log C_e (mg/L)	Log q_e (mg/L)
5	0.1730	0.0007	0.018	1.99	-1.745	0.299
7.5	0.2595	0.0026	0.065	2.97	-1.187	0.473
10	0.3990	0.0299	0.751	3.69	-0.124	0.567
12.5	0.4980	0.0508	1.275	4.49	0.106	0.652
15	0.5440	0.1072	2.691	4.93	0.429	0.693
17.5	0.6350	0.1428	3.584	5.57	0.554	0.746
20	0.7520	0.2376	5.963	5.49	0.775	0.739

Table E 10.4:Freundlich isotherm model parameters For BAC/GO composite

Initial Cr(VI) conc. (mg//L)	Initial Absorbance	Final Absorbance	Final conc (c_e mg/L)	Adsorption capacity q_e (mg/g)	Log C_e (mg/L)	Log q_e (mg/L)
5	0.1730	0.0003	0.008	1.99	-2.097	0.299
7.5	0.2595	0.0013	0.033	2.99	-1.481	0.476
10	0.3990	0.0120	0.301	3.88	-0.521	0.589
12.5	0.4980	0.0268	0.673	4.73	-0.172	0.675
15	0.5440	0.0571	1.433	5.43	0.156	0.735
17.5	0.6350	0.0793	1.990	6.26	0.299	0.797
20	0.7520	0.1737	4.359	6.20	0.639	0.792

According to Figure 4-20, a)the equation of linerized freundlich model for corncb AC was as follows:

$$y= 0.1857x + 0.5263$$

According to the Equation 4.5, the equation obtained is :

$$\log q_e = 0.1857 \ \log C_e + 0.5263$$

From above equation ,

$$\text{Slope} = \frac{1}{n} = 0.1857 \text{ , and } n = 5.39$$

$$\text{Intercept} = \log k_f = 0.5263$$

Freundlich cofficent, $k_f = 3.359$ (mg/g) (L/mg)$^{1/n}$

According to Figure 4-20, b)the equation of linerized freundlich model for sawdust AC was as follows:

$$y= 0.1706x + 0.5640$$

According to the Equation 4.5, the equation obtained is :

$$\log q_e = 0.1706 \ \log C_e + 0.5640$$

From above equation ,

$$\text{Slope} = \frac{1}{n} = 0.5640 \quad \text{and } n = 1.77$$

$$\text{Intercept} = \log k_f = 0.5640$$

Freundlich cofficent, $k_f = 3.664$ (mg/g) (L/mg)$^{1/n}$

According to Figure 4-20, c)the equation of linerized freundlich model for bamboo AC was as follows:

y= 0.1693x + 0.6244

According to the Equation 4.5,the equation obtained is :

$\log q_e = 0.1693 \quad \log C_e + 0.6244$

From above equation ,

$$\text{Slope} = \frac{1}{n} = 0.1957 \qquad \text{and} \quad n = 5.11$$

$$\text{Intercept} = \log k_f = 0.6244$$

Freundlich cofficent, $k_f = 4.211 (\text{mg/g}) \, (\text{L/mg})^{1/n}$

According to Figure 4-20, d) the equation of linerized freundlich model for BAC/GO composite was as follows:

y= 0.1816x + 0.7057

According to the Equation 4.5, the equation obtained is :

$\log q_e = 0.1816 \quad \log C_e + 0.7057$

From above equation ,

$$\text{Slope} = \frac{1}{n} = 0.1816 \qquad \text{and} \quad n = 5.51$$

$$\text{Intercept} = \log k_f = 0.7057$$

Freundlich cofficent, $k_f = 5.078 \, (\text{mg/g}) \, (\text{L/mg})^{1/n}$

Appendix E 11: Sequential model and model summery statistics for percentage adsorption of Cr (VI) ions using BAC/GO

E.11.1 Sequential Model Sum of Squares

Source	Sum of Squares	df	Mean Square	F-value	p-value	
Mean vs Total	2.046E+05	1	2.046E+05			
Linear vs Mean	2624.49	4	656.12	5.47	0.0028	
2FI vs Linear	547.10	6	91.18	0.7036	0.6507	
Quadratic vs 2FI	2134.61	4	533.65	37.72	< 0.0001	Suggested
Cubic vs Quadratic	118.89	8	14.86	1.13	0.4551	Aliased
Residual	79.17	6	13.20			
Total	2.101E+05	29	7246.09			

E.11.2 Model summary stastics

Source	Std. Dev.	R²	Adjusted R²	Predicted R²	PRESS	
Linear	10.95	0.4768	0.3896	0.2128	4332.71	
2FI	11.38	0.5762	0.3408	-0.2583	6925.92	
Quadratic	3.76	0.9640	0.9280	0.8007	1097.08	Suggested
Cubic	3.63	0.9856	0.9329	-0.8014	9915.53	Aliased

Appendix F: Desirability Ramp for the Optimization of Response and the Variables
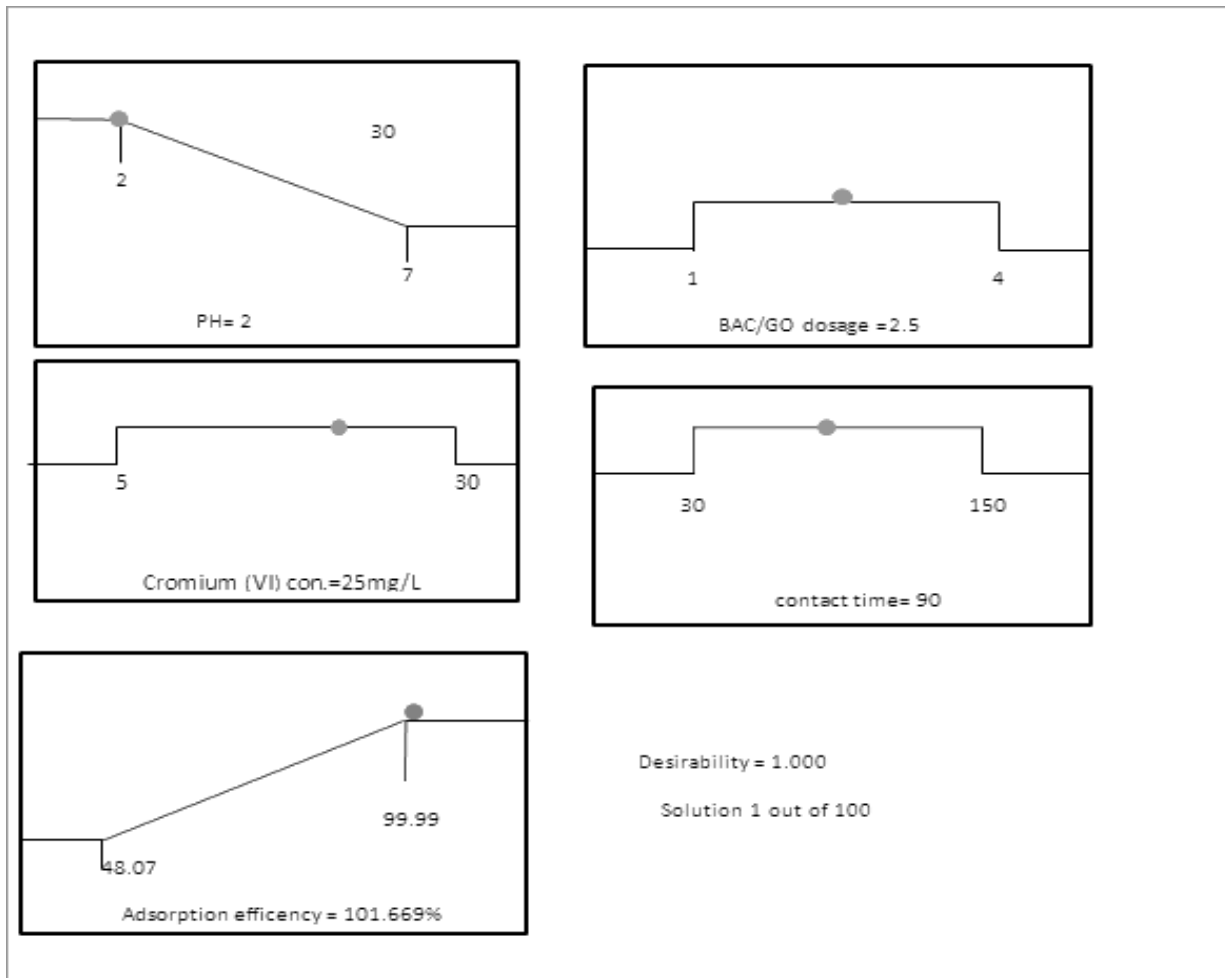
Appendix G: standard solution and measured absorbance for the calibration curve

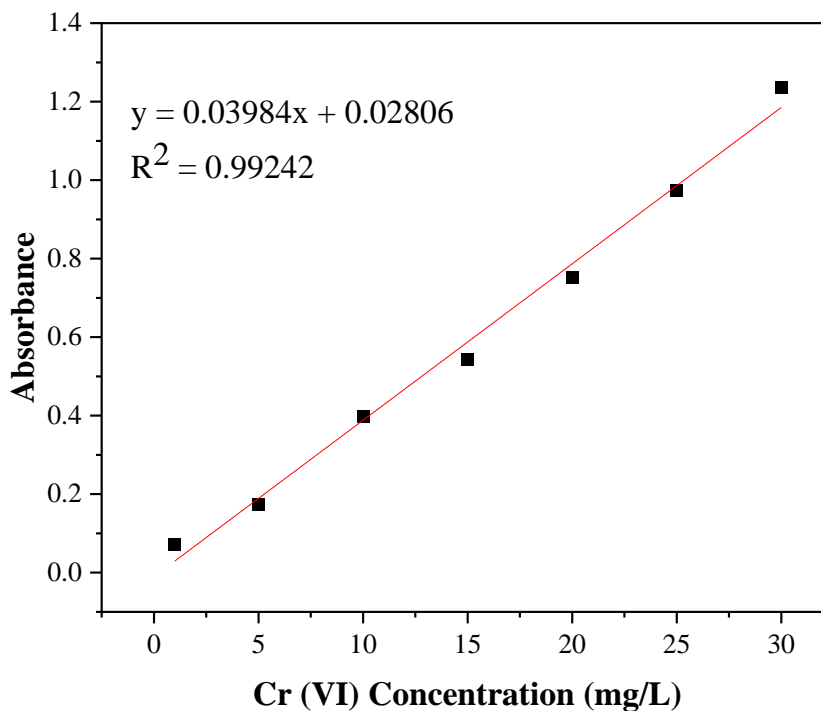| Concentration	Absorbance
Blank	0
1	0.5
5	0.193
10	0.398
15	0.584
20	0.792
25	0.995
30	1.237

Calibration Curve

Figure G 1: Calibration curve for Cr (VI) analysis (Abs. Versus concentration, at ʎmax 350 nm)

Wastewater absorbance = 0.765, based on Beer's law equation we can obtain the unknown concentration of wastewater

A = εbc

0.465 = ε (of Cr(VI) * 1 cm *concentration

Rearenge the formula and you can obtain the concentration C =10.58

A= 0.03984×1cm×10.58

= 0.4215

The adsorbtion efficiency using BAC/GO NAC using real sample = 98.95%

The optimum Cr (VI) adsorption efficiency of CAC, SAC, and BAC

Percentage Adsorption $= \frac{A_O - A_O}{A_O} \times 100$

% adsorption of corncob $= \frac{0.469 - 0.0471}{0.496} \times 100\%$

$= 90.05\%$

% adsorption of sawdust $= \frac{0.469 - 0.0258}{0.496} \times 100\%$

$=94.8\%$

% adsorption of bamboo $= \frac{0.469 - 0.0055}{0.496} \times 100\%$

$=98.95\%$

% adsorption of bamboo $= \frac{0.469 - 0.0015}{0.496} \times 100\%$

$=99.85\%$

Appendix H: Some Pictures Taken during this Reserch Work and Instruments

Sample prepartion

Muffel furnace

Centrifuge

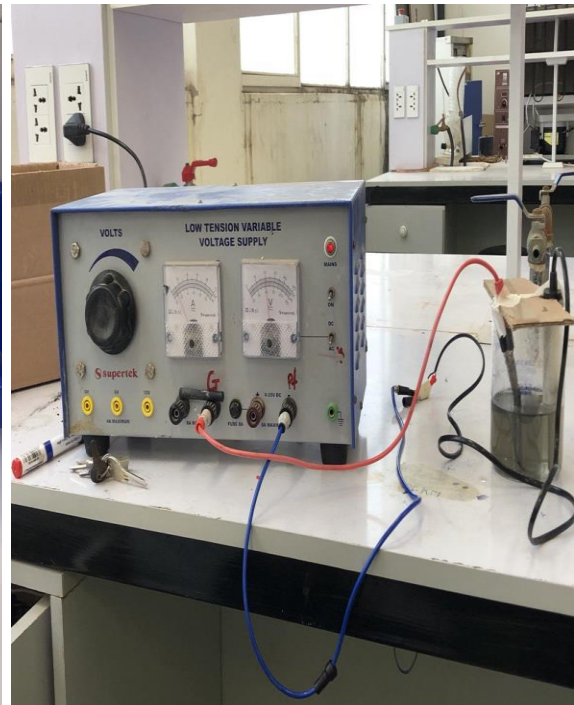Impregnation process

For pH effect sample prepartion

UV-Vis spectrometer

Experimental design results of 29 runs

GO exfoliation

pH meter   electroplating waste water